

PRECISE: PRivacy-loss-Efficient and Consistent Inference based on poSterior quantilEs

Ruyu Zhou, Fang Liu*

Department of Applied and Computational Mathematics and Statistics,

University of Notre Dame, IN 46556, USA

Abstract

Differential privacy (DP) is a mathematical framework for releasing information with formal privacy guarantees. Despite the existence of various DP procedures for performing a wide range of statistical analysis and machine learning tasks, methods of good utility are still lacking for obtaining valid statistical inference with DP guarantees. We address this gap by introducing the notion of valid Privacy-Preserving Interval Estimation (PPIE) and proposing PRivacy-loss-Efficient and Consistent Inference based on poSterior quantilEs (PRECISE). PRECISE is a general-purpose Bayesian approach for constructing privacy-preserving posterior intervals. We establish the Mean-Squared-Error (MSE) consistency for our proposed private posterior quantiles converging to the population posterior quantile as sample size or privacy loss increases. We conduct extensive experiments to compare the utilities of PRECISE with common existing privacy-preserving inferential approaches in various inferential tasks, data types and sizes, privacy loss levels. The results demonstrated a significant advantage of PRECISE with its nominal coverage and substantially narrower intervals than the existing methods, which are prone to either under-coverage or impractically wide intervals.

keywords: Bayesian, differential privacy, MSE consistency, privacy-preserving inference, privacy loss, quantiles.

* Correspondence author: fliu2@nd.edu

1 Introduction

1.1 Background

The unprecedented availability of data containing sensitive information has heightened concerns about the potential privacy risks associated with the direct release of such data and the outputs of statistical analyses and machine learning tasks. Providing a rigorous framework for privacy guarantees, Differential privacy (DP) has been widely adopted for performing privacy-preserving analysis since its debut in 2006 (Dwork et al., 2006b,a) and gained enormous popularity among privacy researchers and in practice (e.g., Apple (Apple, 2020), Google (Erlingsson et al., 2014), the U.S. Census (Abowd, 2018)). Many DP procedures have been developed for various statistical problems, including sample statistics (e.g. mean (Smith, 2011), median (Dwork and Lei, 2009), variance or covariance (Amin et al., 2019; Biswas et al., 2020)), linear regression (Alabi et al., 2020; Wang, 2018), empirical risk minimization (ERM) (Chaudhuri et al., 2011), and so on.

Most existing DP methods to date focus on releasing privatized or sanitized statistics without uncertainty quantification, limiting their usefulness for robust decision-making. Though there exists work on DP statistical inference, including both hypothesis testing and interval estimation, this line of research is still in its early stages and is largely focused on relatively simple inference tasks, such as DP χ^2 -test (Gaboardi et al., 2016), uniformly most powerful tests for Bernoulli data (Awan and Slavković, 2018), F -test in linear regression (Alabi and Vadhan, 2022), and privacy-preserving interval estimation for Gaussian means or regression coefficient. Our work contributes to this field by introducing a novel procedure for valid *privacy-preserving interval estimation (PPIE)*.

1.2 Related work

Most of the existing works on PPIE can be loosely grouped into two broad categories. The first group obtains PPIE through the derivation of the asymptotic distribution of privacy-

preserving (PP) estimator, where either asymptotic Gaussian distributions (e.g., inferring univariate Gaussian mean (Du et al., 2020; Evans et al., 2023; D’Orazio et al., 2015; Karwa and Vadhan, 2017), multivariate sub-Gaussian mean (Biswas et al., 2020), proportion (Lin et al., 2024), and complicated problems like M-estimators (Avella-Medina et al., 2023) and ERM (Wang et al., 2019)), or asymptotic t -distributions (e.g., inferring linear regression coefficient (Sheffet, 2017) and the general-purpose multiple sanitization (MS) procedure (Liu, 2022)) are assumed. The second group employs a quantile-based approach. The frequentist methods in this category primarily rely on the bootstrap technique to build PPIE, such as the simulation approach (Du et al., 2020) and the parametric bootstrap method (Ferrando et al., 2022). The BLBquant method (Chadha et al., 2024) and the GVDP (General Valid DP) method (Covington et al., 2021) employ the Bag of Little Bootstraps (BLB) technique (Kleiner et al., 2014) to obtain private quantiles. BLBquant provides quantitative error bounds and outperforms GVDP empirically. Wang et al. (2022) leverages deconvolution (a technique that deals with contaminated data) to analyze DP bootstrap estimates and obtain PPIE. In the Bayesian framework, the existing methods focus on incorporating DP noise in PP posterior inference and computation, such as PP regression coefficient estimation through sufficient statistics perturbation (Bernstein and Sheldon, 2019; Kulkarni et al., 2021) and data augmentation MCMC sampler (Ju et al., 2022). Outside these two categories, other PPIE approaches include non-parametric methods for population medians (Drechsler et al., 2022), synthetic data-based methods (Bojkovic and Loh, 2024; Räisä et al., 2023; Liu, 2022), and simulation-based methods (Awan and Wang, 2023), among others.

While research on PPIE has been growing, notable limitations remain in current techniques from methodological, computational, and application perspectives. *First*, most methods are designed for specific basic inferential tasks (e.g., Gaussian means), creating a need for more general PPIE procedures that can accommodate a wide range of statistical inference problems. *Second*, some existing methods are compatible only with certain types of DP guarantees (e.g., ϵ -DP), limiting their applicability. *Third*, even for basic PPIE tasks,

there is considerable room to improve existing methods in achieving an optimal trade-off between privacy and utility, particularly in practically meaningful privacy loss settings with better computational efficiency, as some existing sampling-based methods tend to be computationally intensive. *Fourth*, there is a lack of comprehensive comparisons on the practical feasibility and utility of existing PP inferential methods across common statistical problems, which is essential for guiding their practical applications.

1.3 Our work and contributions

In this work, we address several research and application gaps in PPIE mentioned in Section 1.2. To that end, we introduce a formal definition on valid PPIE, propose a general-purpose PPIE approach with theoretically proved statistical validity and DP guarantees, and conduct a comparative study on the privacy-utility trade-offs of various PPIE methods. Our main contributions are summarized below.

- We propose PRECISE, a novel Bayesian approach for PPIE based on consistent PP posterior quantile estimation. PRECISE is broadly applicable whenever Bayesian posterior samples are obtainable. PRECISE exhibits low sensitivity to global bound specifications – an issue that consistently challenges the preservation of utility in private inference, resulting in a superior privacy-utility tradeoff compared to existing PPIE methods whose performance is significantly impacted by global bound specifications.
- Theoretically, we establish the Mean-Squared-Error (MSE) consistency of the quantiles obtained by PRECISE for their corresponding non-private population posterior quantiles, and derive the convergence rate in sample size and privacy loss parameter.
- Our empirical results in various experiment settings show that PRECISE achieves nominal coverage with significantly narrower intervals, whereas other PPIE methods may either under-cover or produce unacceptably wide intervals at low privacy loss, providing strong evidence of PRECISE’ superior performance in the privacy-utility trade-offs.
- We introduce an exponential-mechanism-based PP posterior quantile estimator as an-

other PPIE approach and examine its theoretical properties and practical limitations.

2 Preliminaries

In this section, we provide a brief overview of the basic concepts in differential privacy (DP). For the definitions below, we refer two datasets \mathbf{x} and \mathbf{x}' as neighbors (denoted by $d(\mathbf{x}, \mathbf{x}') = 1$) if \mathbf{x} differs from \mathbf{x}' by exactly one record by either removal or substitution.

Definition 1 ((ε, δ) -DP (Dwork et al., 2006a,b)). *A randomized algorithm \mathcal{M} is of (ε, δ) -DP if for all pairs of neighboring datasets $(\mathbf{x}, \mathbf{x}')$ and for any subset $\mathcal{S} \subset \text{Image}(\mathcal{M})$,*

$$\Pr(\mathcal{M}(\mathbf{x}) \in \mathcal{S}) \leq e^\varepsilon \cdot \Pr(\mathcal{M}(\mathbf{x}') \in \mathcal{S}) + \delta. \quad (1)$$

$\varepsilon > 0$ and $\delta \geq 0$ are privacy loss parameters. When $\delta = 0$, (ε, δ) -DP reduces to pure ε -DP. Smaller values of ε and δ imply stronger privacy guarantees for the individuals in a dataset as the outputs based on \mathbf{x} and \mathbf{x}' are more similar.

Laplace mechanism (Dwork et al., 2006b) is a widely-used mechanism to achieve ε -DP. Let $\mathbf{s} = (s_1, \dots, s_r)$ denote the statistics calculated from a dataset; and its sanitized version via the Laplace mechanism is $\mathbf{s}^* = \mathbf{s} + \mathbf{e}$, where $\mathbf{e} = \{e_j\}_{j=1}^r$ with $e_j \sim \text{Laplace}(0, \Delta_1/\varepsilon)$, and $\Delta_1 = \max_{\mathbf{x}, \mathbf{x}', d(\mathbf{x}, \mathbf{x}')=1} \|\mathbf{s}(\mathbf{x}) - \mathbf{s}(\mathbf{x}')\|_1$ is the ℓ_1 *global sensitivity* of \mathbf{s} , representing the maximum change in \mathbf{s} between two neighboring datasets in ℓ_1 norm. Higher sensitivity requires more noise to achieve the pre-set privacy guarantee. **Exponential mechanism** (McSherry and Talwar, 2007) is a general mechanism of ε -DP and releases sanitized s^* with probability $\propto \exp(\varepsilon \cdot u(s^*|\mathbf{x})/2\Delta_u)$, where u is a utility function that assigns a score to every possible output s^* and Δ_u is the ℓ_1 global sensitivity of u .

Definition 2 (μ -GDP (Dong et al., 2022)). *Let \mathcal{M} be a randomized algorithm and \mathcal{S} be any subset of $\text{Image}(\mathcal{M})$. Consider the hypothesis test $H_0 : S \sim \mathcal{M}(\mathbf{x})$ versus $H_1 : S \sim \mathcal{M}(\mathbf{x}')$, where $d(\mathbf{x}, \mathbf{x}') = 1$. \mathcal{M} is of μ -Gaussian DP if it satisfies*

$$T(\mathcal{M}(\mathbf{x}), \mathcal{M}(\mathbf{x}'))(\alpha) \geq \Phi(\Phi^{-1}(1 - \alpha) - \mu), \quad (2)$$

where $T(\cdot, \cdot)(\alpha)$ is the minimum type II error among all such tests at significance level α and $\Phi(\cdot)$ is the CDF of the standard normal distribution.

In less technical terms, Def. 2 states that \mathcal{M} is of μ -GDP if distinguishing any two neighboring datasets based on the information sanitized via \mathcal{M} is at least as difficult as distinguishing $\mathcal{N}(0, 1)$ and $\mathcal{N}(\mu, 1)$. (ε, δ) -GDP relates to μ -GDP, with one μ corresponding to infinite pairs of (ε, δ) .

Lemma 1 (Conversion between (ε, δ) -DP and μ -GDP (Dong et al., 2022)). *A mechanism is of μ -GDP if and only if it is of $(\varepsilon, \delta(\varepsilon))$ -DP for all $\varepsilon \geq 0$, where $\delta(\varepsilon) = \Phi(-\varepsilon/\mu + \mu/2) - e^\varepsilon \Phi(-\varepsilon/\mu - \mu/2)$.*

Gaussian mechanism can be used achieve both (ε, δ) -GDP and μ -GDP. In this work, we use the Gaussian mechanism of μ -GDP. Specifically, sanitized $\mathbf{s}^* = \mathbf{s} + \mathbf{e}$, where $\mathbf{e} = \{e_j\}_{j=1}^r$ and $e_j \sim \mathcal{N}(0, \Delta_2^2/\mu^2)$, and $\Delta_2 = \max_{\mathbf{x}, \mathbf{x}', d(\mathbf{x}, \mathbf{x}')=1} \|\mathbf{s}(\mathbf{x}) - \mathbf{s}(\mathbf{x}')\|_2$ is the ℓ_2 global sensitivity of \mathbf{s} , the maximum change in \mathbf{s} between two neighboring datasets in ℓ_2 norm.

DP and many of its variants, μ -GDP included, have several attractive properties for both research and practical applications. For example, they are *immune to post-processing*; that is, any further processing on the differentially private output without accessing the original data maintains the same privacy guarantees. Furthermore, the *composition* property of DP allows privacy loss tracking and accounting over repeatedly accessing and releasing information from a dataset. The basic composition principle states that if \mathcal{M}_1 is of $(\varepsilon_1, \delta_1)$ -DP (or μ_1 -GDP) and \mathcal{M}_2 is of $(\varepsilon_2, \delta_2)$ -DP (or μ_2 -GDP), then $\mathcal{M}_1 \circ \mathcal{M}_2$ is of $(\varepsilon_1 + \varepsilon_2, \delta_1 + \delta_2)$ -DP (or $\sqrt{\mu_1^2 + \mu_2^2}$ -GDP) if \mathcal{M}_1 and \mathcal{M}_2 operate on the same dataset. The privacy loss composition bound in μ -GDP is tighter than that of the (ε, δ) -DP.

3 Privacy-Preserving Interval Estimation (PPIE)

Before introducing PRECISE as a PPIE procedure, we provide a formal definition on PPIE in Def. 3. The definition is applicable to PP intervals constructed in both the Bayesian and frequentist frameworks.

Definition 3 (privacy-preserving interval estimate (PPIE)). *Let \mathbf{x} be a sensitive dataset of n records that is a random sample from probability distribution $f(\mathbf{x}|\boldsymbol{\theta}_0)$ with unknown parameters $\boldsymbol{\theta}_0$. Denote the non-private interval estimator for $\boldsymbol{\theta}_0$ at confidence level $1 - \alpha$ by $(l(\mathbf{x}), u(\mathbf{x}))$ and the DP mechanism by \mathcal{M} . The PPIE at privacy loss $\boldsymbol{\eta}$ for $\boldsymbol{\theta}_0$, denoted by interval $(\mathcal{M}(l(\mathbf{x})), \mathcal{M}(u(\mathbf{x})))$, satisfies*

$$\Pr_{\mathcal{M}, \mathbf{x}}(\mathcal{M}(l(\mathbf{x})) < \boldsymbol{\theta}_0 < \mathcal{M}(u(\mathbf{x}))) \geq 1 - \alpha \text{ for every } \boldsymbol{\theta}_0, \boldsymbol{\eta}. \quad (3)$$

The DP mechanism \mathcal{M} in Def. 3 can be based on (ε, δ) -DP ($\boldsymbol{\eta} = (\varepsilon, \delta)$) and any of its variants, such as μ -GDP ($\boldsymbol{\eta} = \mu$). Def. 3 is not exact – that is, instead of requiring $\Pr(\mathcal{M}(l(\mathbf{x})) < \boldsymbol{\theta}_0 < \mathcal{M}(u(\mathbf{x}))) = 1 - \alpha$, it only requires the probability $\geq 1 - \alpha$ – for a couple of reasons. First, intervals with exact coverage may be difficult to construct; second, Def. 3 is more useful when dealing with discrete distributions. That said, the interval width $|\mathcal{M}(u(\mathbf{x})) - \mathcal{M}(l(\mathbf{x}))|$ should be as short as possible while satisfying $\geq 1 - \alpha$; otherwise, the PPIE would be imprecise and meaningless.¹

3.1 Overview of the PRECISE procedure

Let $\{\mathbf{x}_i\}_{i=1}^n \stackrel{\text{i.i.d.}}{\sim} f(\mathbf{x}|\boldsymbol{\theta}_0)$ denote a sensitive dataset containing data points from n individuals, where $\mathbf{x}_i \in \mathbb{R}^q$ and $\boldsymbol{\theta}_0 = (\theta_0^{(1)}, \theta_0^{(2)}, \dots, \theta_0^{(p)})^\top \in \Theta$ represents the p -dimensional true parameter vector. The PRECISE procedure constructs a pointwise interval estimation for $\boldsymbol{\theta}_0$ in a Bayesian framework, with the steps outlined as follows.

First, it draws m posterior samples $\{\theta_j^{(k)}\}_{j=1}^m$ from the marginal posterior distribution $f(\theta^{(k)}|\{\mathbf{x}_i\}_{i=1}^n)$ for $k = 1, \dots, p$ and constructs a histogram $H^{(k)}$ based on these m samples. *Second*, it perturbs the bin counts in $H^{(k)}$ using a DP mechanism \mathcal{M} at a pre-specified privacy loss $\boldsymbol{\eta}$, resulting in a P³ (Privacy-Preserving Posterior) histogram $H^{(k)*}$. *Third*, at a specified confidence coefficient $1 - \alpha \in (0, 1)$ for PPIE, identify two bins in $H^{(k)*}$ where the cumulative probability up to each is the closest to $\frac{\alpha}{2}$ and $1 - \frac{\alpha}{2}$ respectively. *Finally*,

¹For completeness, Def. 3 can be extended to scenarios where there exist other parameters that are not of immediate inferential interest. That is, $\mathbf{x} \sim f(X|\boldsymbol{\theta}_0, \boldsymbol{\beta}_0)$ and Eq. (3) holds for every $\boldsymbol{\theta}_0, \boldsymbol{\beta}_0$ and $\boldsymbol{\eta}$.

release a random sample from each of these two identified intervals as the PP estimate of the population posterior quantiles $F_{\theta^{(k)}|\{\mathbf{x}_i\}_{i=1}^n}^{-1}(\frac{\alpha}{2})$ and $F_{\theta^{(k)}|\{\mathbf{x}_i\}_{i=1}^n}^{-1}(1 - \frac{\alpha}{2})$.

3.2 Global sensitivity of posterior histogram

A key step in the PRECISE procedure is the construction of the *Privacy-Preserving Posterior* (P³) histogram with a set of posterior samples for the parameter of interest. To achieve this, we will first determine the sensitivity of the histogram constructed from the posterior samples and then design a proper randomized mechanism to ensure its privacy. It is important to note that *sanitizing a histogram constructed from a set of posterior samples of $\theta^{(k)}$ given sensitive data \mathbf{x} is fundamentally different and more complex than sanitizing a histogram $H(\mathbf{x})$ of the sensitive data \mathbf{x} itself*. Specifically, the DP definition pertains to changing one record in the sensitive dataset \mathbf{x} . Removing a record from \mathbf{x} only affects one bin in $H(\mathbf{x})$ and thus the global sensitivity of $H(\mathbf{x})$, represented in the count, is 1 if the neighboring relation is removal and 2 if the neighboring relation is substitution. In contrast, our goal is to sanitize the histogram of a parameter $H(\theta|\mathbf{x})$ given a set of posterior samples from $f(\theta|\mathbf{x})$. Changing one record in \mathbf{x} will alter the whole posterior distribution from $f(\theta|\mathbf{x})$ to $f(\theta|\mathbf{x}')$ and the influence is indirect and more complex compared to how it affects $H(\mathbf{x})$, eventually complicating the calculation of the sensitivity of $H(\theta|\mathbf{x})$. Figure 1 illustrates how the sensitivities of $H(\mathbf{x})$ and $H(\theta|\mathbf{x})$ differ using a toy example.

With this clarified, we can proceed to derive $G(n)$, the supremum of the absolute difference between two posterior distributions given two neighboring datasets, where n is the sample size of dataset \mathbf{x} . $G(n)$ is a critical quantity for constructing the P³ histogram. For a single parameter, Theorem 2 suggests that $G(n)$ converges to a constant G_0 as n increases.

Theorem 2 ($G(n)$ is asymptotically constant). *Define*

$$G(n) \triangleq \sup_{\theta \in \Theta, d(\mathbf{x}, \mathbf{x}')=1} |f_{\theta|\mathbf{x}}(\theta) - f_{\theta|\mathbf{x}'}(\theta)| \quad (4)$$

for scalar θ . Assume that the prior $f(\theta)$ is non-informative relative to the amount of data, let $\hat{\theta}_n$ and $\hat{\theta}'_n$ be the maximum a posteriori (MAP) estimates evaluated on two neighboring

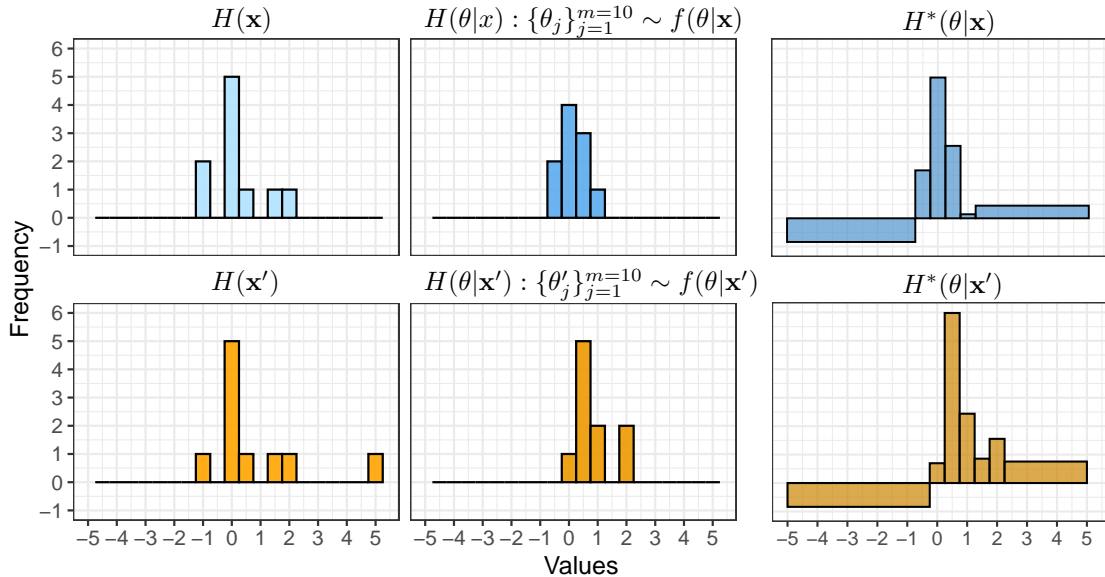


Figure 1: A toy example to illustrate the difference in how alternating one individual in dataset \mathbf{x} affects the histogram of data \mathbf{x} (first column) and the histogram of posterior samples drawn from $f(\theta|\mathbf{x})$ (second column). $\mathbf{x} = \{x_i\}_{i=1}^{10} \sim \mathcal{N}(0, 1)$; $L_{\mathbf{x}} = L = -5$, $U_{\mathbf{x}} = U = 5$; the neighboring dataset \mathbf{x}' is constructed by substituting the $\min(\mathbf{x})$ with $U_{\mathbf{x}}$. P³ histogram (third column) is obtained via the Laplace mechanism at $\varepsilon = 1$.

datasets \mathbf{x} and \mathbf{x}' with substitution relation, respectively. If $\hat{\theta}'_n - \hat{\theta}_n \approx \mathcal{O}(n^{-1})$, then

$$G(n) \approx \left(\frac{CI_{\theta_0}}{\sqrt{2\pi}} \right) e^{-\frac{1}{2} + \mathcal{O}(n^{-\frac{1}{2}})} + \mathcal{O}(n^{-\frac{1}{2}}) \rightarrow G_0 = \frac{CI_{\theta_0}}{\sqrt{2e\pi}} \text{ as } n \rightarrow \infty, \quad (5)$$

where C is a constant and I_{θ_0} is the Fisher information at the true parameter θ_0 given a single data point x .

The detailed proof of Theorem 2 is provided in Appendix A.1.1. Briefly, per the Bernstein-von Mises theorem, we assume the two posteriors given two neighboring datasets are approximately Gaussian, approximate their difference with a third-order Taylor expansion, then leverage the symmetry to identify the maximizer of the absolute difference.

The Fisher information I_{θ_0} in Eq. (5) may not always have an analytically closed form, especially for uncommon likelihoods, high-dimensional data, and data with complex dependency structures. In such cases, numerical methods such as Monte Carlo approaches can be used. As for the constant C , its value depends on the specific problem. For example, consider mean μ and variance σ^2 of a Gaussian likelihood, their MAP estimates are the sample mean

and variance of data \mathbf{x} with non-informative prior $p(\mu, \sigma^2) \propto (\sigma^2)^{-3/2}$. Suppose $\mathbf{x} = \{x_i\}_{i=1}^n$, and \mathbf{x}' differ from \mathbf{x} in the last observation. WLOG, that is, replacing x_n with x'_n . Then

$$C \triangleq |x'_n - x_n| \text{ for } \hat{\theta}_n^{(1)} = \bar{x};$$

$$C \triangleq |(x_n - \bar{x}_{n-1})^2 - (x'_n - \bar{x}_{n-1})^2| \text{ for } \hat{\theta}_n^{(2)} = n^{-1} \left(\sum_{i=1}^n (x_i - \bar{x})^2 \right).$$

Eq. (5) suggests that $G(n)$ decreases at a rate of $\mathcal{O}(n^{-1/2})$ as n increases. When n is relatively large, $G(n)$ can be replaced with constant $G_0 = CI_{\theta_0}/\sqrt{2e\pi}$ in practical applications. To ensure DP guarantees while maintaining utility on sanitized results that are based on $G(n)$, we recommend using a tight upper bound on CI_{θ_0} , leveraging the global bounds (L, U) for θ_0 and the global bounds $(L_{\mathbf{x}}, U_{\mathbf{x}})$ for \mathbf{x} and derive as tight an upper bound for G_0 as possible.

With $G(n)$ determined, we can calculate the global sensitivity of a posterior histogram for a parameter, as stated in Theorem 3.

Theorem 3 (global sensitivity of posterior histogram). *Let n be the sample size of data \mathbf{x} , m be the number of posterior samples on parameter θ from $f(\theta|\mathbf{x})$, and H be the histogram based on the m posterior samples with bin width h . The global sensitivity of H is*

$$\Delta_H = 2mhG(n). \tag{6}$$

The detailed proof of Theorem 3 is provided in Appendix A.2. The main idea is to relate the ℓ_1 distance between two posterior histograms given two neighboring datasets to the total variation distance (TVD) between discretized distributions. The TVD is then upper-bounded using the mean value theorem for integrals.

Δ_H increases linearly with m , which is intuitive as releasing more posterior samples implies more information in the original data \mathbf{x} is leaked, requiring a higher scale parameter in the randomized mechanism to ensure privacy at a preset level. In this case, m is a user-specified hyper-parameter. A more user-friendly way of using Eq. (6) is to fix Δ_H at a constant – a convenient choice is 1 – and back-calculate m . That is,

$$\Delta_H = 1 = 2mhG(n) \quad \Rightarrow \quad m = \lceil (2G(n)h)^{-1} \rceil. \tag{7}$$

Given the sensitivity of H in Eqs. (6) or (7), one can sanitize the bin counts in H to obtain a P^3 histogram H^* by plugging in the sensitivity into a randomized mechanism. Specifically, denote the vector of B bin counts by $\mathbf{c} = \{c_1, \dots, c_B\}$, where $\sum_{b=1}^B c_b = m$; then,

$$H^* = \mathcal{M}(H) = \mathbf{c} + \mathbf{e}, \text{ where } \mathbf{e} = \{e_1, \dots, e_B\} \text{ and } e_j \sim \begin{cases} \text{Laplace}(0, \Delta_H/\epsilon) \text{ if the Laplace mechanism of } \epsilon\text{-DP is used} \\ \mathcal{N}(0, \Delta_H^2/\mu^2) \text{ if the Gaussian mechanism of } \mu\text{-GDP is used.} \end{cases} \quad (8)$$

Remark 1. *Theorem 2 can be extended to the multidimensional case $\boldsymbol{\theta} = (\theta^{(1)}, \dots, \theta^{(p)})^\top \in \Theta$ for $p > 1$. We show that $G(n) \asymp n^{\frac{p-1}{2}}$ (see Appendix A.1.3 for the proof), implying that $G(n)$ does not converge to a constant as $n \rightarrow \infty$ when $p > 1$.*

3.3 Construction of P^3 Histogram with DP guarantees

Alg. 1 lists the steps for constructing a univariate P^3 histogram. Based on some mild regularity conditions listed in Assumption 4, which are readily satisfied for not too-small h , we show Alg. 1 adheres to DP guarantees in Theorem 5.

Algorithm 1: Construction of P^3 Histogram

- input** : posterior distribution $f(\theta|\mathbf{x})$ (up to a constant), global bounds (L, U) for θ , bin width h , DP mechanism \mathcal{M} , privacy loss $\boldsymbol{\eta}$, P^3 histogram version, $G(n)$ (Eq. (5)).
- output**: P^3 histogram H^* .
- 1 Calculate the number of posterior sample $m \leftarrow \lceil (2G(n)h)^{-1} \rceil$ (Eq. (7)) ;
 - 2 Draw posterior samples $\{\theta_j\}_{j=1}^m \stackrel{\text{iid}}{\sim} f(\theta|\mathbf{x})$;
 - 3 Form a histogram H with bin width h (number of bins $B = (U - L)/h$) based on the m samples. Denote the bins by $\Lambda_b = [L + (b - 1)h, L + b \cdot h)$ and the bin frequencies by $c_b = \sum_{j=1}^m \mathbb{1}(\theta_j \in \Lambda_b)$ for $b = 1, \dots, B$;
 - 4 Set $b_L \leftarrow \arg \min_{b \in \{1, \dots, B\}} \{c_b > 0\}$ and $b_U \leftarrow \arg \max_{b \in \{1, \dots, B\}} \{c_b > 0\}$;
 - 5 Set $\Lambda_0 \leftarrow \cup_{b < b_L} \{\Lambda_b\}$ and $\Lambda_{B'+1} \leftarrow \cup_{b > b_U} \{\Lambda_b\}$, where $B' = b_U - b_L + 1$;
 - 6 Re-index uncollapsed bins using new indices from 1 to B' ;
 - 7 **for** $b = 0, \dots, B'+1$ **do**
 - 8 **if** P^3 histogram version == “+”, **then** $c_b^* \leftarrow \max\{0, \mathcal{M}(c_b, \boldsymbol{\eta})\}$ (Eq. (8)) ;
 - 9 **if** P^3 histogram version == “-”, **then** $c_b^* \leftarrow \mathcal{M}(c_b, \boldsymbol{\eta})$ (Eq. (8));
 - 10 **end**
 - 11 Return H^* with sanitized bin counts $\{c_b^*\}_{b=0}^{B'+1}$ for bins $\{\Lambda_b\}_{b=0}^{B'+1}$.
-

Assumption 4. Let $F_{\theta|\mathbf{x}}^{-1}(q) = \inf\{\theta : F(\theta|\mathbf{x}) \geq q\}$ for $0 < q < 1$. Assume

(a) $f(\theta|\mathbf{x}) \geq 0$ in its support Θ and the corresponding cumulative distribution function (CDF) $F(\theta|\mathbf{x})$ is continuous on any closed interval Λ_b for $b \in \{1, \dots, B\}$.

(b) $\sum_{b=1}^{b_L} f(\xi_b|\mathbf{x}) \leq G(n)$, where $\xi_b \in \Lambda_b$ for $b \in \{1, \dots, b_L\}$, and $\sum_{b=b_U}^B f(\xi_b|\mathbf{x}) \leq G(n)$, where $\xi_b \in \Lambda_b$ for $b \in \{b_U, \dots, B\}$.

Theorem 5 (DP guarantees of P³ Histogram). *Under Assumption 4, the P³ Histogram in Alg. 1 satisfies η -DP.*

3.3.1 Choice of bin width h

A key hyperparameter that users need to specify in Alg. 1 is the histogram bin width h . A large h would result in a coarse histogram estimate of $f(\theta|\mathbf{x})$, leading to inaccurate quantile estimates of $F_{\theta|\mathbf{x}}^{-1}(q)$ from the subsequent histogram-based PRECISE procedure (even in the absence of DP). Conversely, a small h , while reducing the global sensitivity Δ_H , would result in a large number of bins and thus a sparse histogram with numerous empty or low-count bins, which would also compromise the utility of the histogram.² Furthermore, the choice of h is also critical in establishing the MSE consistency of the PP quantiles estimates based on the P³ histogram (see Section 3.4.3 and Theorem 6). Finally, Assumption 4 is more readily satisfied when h is not too small.

3.3.2 Two versions of P³ histogram

We provide two versions of P³ histogram in Alg. 1, depending on whether non-negativity correction is applied to the bin counts of the sanitized posterior histogram (+ representing Yes vs. – for No; lines 7 to 10). Since counts are inherently non-negative, the correction (+ versions) is more intuitive but overestimates the original bin counts.

²A similar narrative exists for m when it is not back-calculated by fixing Δ_H as the above: a smaller m implies lower Δ_H thus less DP noise but it also leads to worse quantile estimation due to the data sparsity issue; and a higher m implies richer data for more accurate quantile estimation but higher Δ_H and thus more DP noise, which counteracts the accuracy gains from the larger m .

3.3.3 Effects of bounds (L, U) on P^3 utility

Unknown parameters in a statistical model can be bounded, such as proportions $\in [0, 1]$; or unbounded such as Gaussian mean $\in (-\infty, \infty)$, or bounded on one end, such as variance $\in (0, \infty)$. In the DP framework, bounds on numeric quantities to be sanitized, whether statistics or parameters, are necessary to design or apply a mechanism to achieve DP guarantees. Though this may be regarded as a strong assumption from the perspective of statistical theory, real-life data and scenarios often support bounding on data or parameters, justifying bounding for practical applications.

The global bounds (L, U) for θ affect the performance of the subsequent PRECISE PP quantile estimates derived from the P^3 histogram, as they are associated with the amount of noise required to reach the preset DP guarantee level – wider bounds often imply more noise. On the other hand, it is important not to impose unreasonably tight bounds to the extent that they cause significant bias or information loss. As a result, in practice, (L, U) are often wide to be safe and conservative, regardless of n . However, as n increases, $f(\theta|\mathbf{x})$ becomes increasingly concentrated around the underlying “population” parameter θ_0 ; static bounds (L, U) invariant to n can become overly conservative, negatively impacting the privacy-utility trade-off. More concretely, the posterior histogram H naturally becomes more concentrated around θ_0 as n increases, suggesting that tighter bounds on θ can be used as n grows without sacrificing information or introducing bias in the PP inference of θ . While the rate at which the difference $U(n) - L(n)$ decreases with increasing n can be theoretically derived, this information alone is insufficient for the application of a DP mechanism that requires explicit values for $L(n)$ and $U(n)$ individually, which would depend on the unknown θ_0 , posing a practical challenge to proposing analytical $(L(n), U(n))$.

To address this, we incorporate a subroutine in Alg. 1 (lines 4 to 6) to allow it self-adjusting in the case of overly conservative global bounds (L, U) by collapsing empty bins at the two tails of the posterior histogram before adding DP noise. This collapsing effectively reduces excessive noise addition without affecting global sensitivity Δ_H under Assumption 4,

preserving DP guarantees.

3.4 PRECISE based on P³ Histogram

After obtaining the P³ histogram H^* for the parameter of interest θ , we can derive the PP quantile estimates for θ from H^* via the PRECISE procedure with the same privacy guarantees per the immunity to post-processing of DP. The steps for the PRECISE algorithm are provided in Alg. 2.

3.4.1 Four versions of PRECISE

PRECISE has four versions $\{+m, +m^*, -m, -m^*\}$. $+$ and $-$ are inherited from the P³ histogram procedure in Alg. 1. The choice between m and m^* depends on whether the CDF based on H^* is normalized by the pre-specified total m of posterior samples of θ , or by the sum of sanitized bin counts $m^* = \sum_{i=0}^{B'+1} c_i^*$. While using m leverages its being a known constant and enhances the stability of the output from Alg. 2, it introduces inconsistency for normalized H^* as the individual bin counts in H^* are sanitized and their sum is highly unlikely to be equal to m in actual implementations. In fact, the sum equals to m only in expectation for the $-$ version of P* and is biased upward for the $+$ version. The simulation studies in Section 4.1 compares the performance of the four version of PRECISE.

3.4.2 Rationale for PRECISE

The key to any valid PP inference, PPIE included, is to acknowledge and account for the additional source of variability introduced by DP sanitation on top of the sampling variability of the data. Ignoring the former would lead to invalid inference, and in the case of a PPIE method, potential under-coverage and failing to satisfy Def. 3. PRECISE accounts for both sources of variability in an implicit manner. Rather than explicitly quantifying the uncertainty for a PP estimate of θ and then calculating the half width for its PP interval estimate based on the quantified uncertainty, PRECISE converts the interval estimation for θ to a point estimation problem, leveraging the Bayesian concept.

Specifically, the central posterior interval of $(1-\alpha)\times 100\%$ is formulated as $(F_{\theta|\mathbf{x}}^{-1}(\frac{\alpha}{2}), F_{\theta|\mathbf{x}}^{-1}(1-$

Algorithm 2: PRECISE

input : \mathbb{P}^3 histogram H^* from Alg. 1 with bins $\{\Lambda_b\}_{b=0}^{B'+1}$ and corresponding sanitized bin counts $\{c_b^*\}_{b=0}^{B'+1}$, confidence level $1 - \alpha \in (0, 1)$, PRECISE version

output: PPIE at level $1 - \alpha$ for θ_0 : $(\theta_{\alpha/2}^*, \theta_{1-\alpha/2}^*)$.

1 **if** PRECISE version == $+m^*$ or $-m^*$, **then** set the indices

$$b_{\alpha/2}^* = \min \left\{ \arg \min_{b \in \{0, \dots, B'+1\}} \left| \sum_{i=0}^b c_i^* - \frac{\alpha}{2} \sum_{i=0}^{B'+1} c_i^* \right| \right\}, \quad b_{1-\alpha/2}^* = \min \left\{ \arg \min_{b \in \{0, \dots, B'+1\}} \left| \sum_{i=b}^{B'+1} c_i^* - \frac{\alpha}{2} \sum_{i=0}^{B'+1} c_i^* \right| \right\}.$$

2 **if** PRECISE version == $+m$ or $-m$, **then** set the indices

$$b_{\alpha/2}^* = \min \left\{ \arg \min_{b \in \{0, \dots, B'+1\}} \left| \sum_{i=0}^b c_i^* - \frac{\alpha}{2} m \right| \right\}, \quad b_{1-\alpha/2}^* = \min \left\{ \arg \min_{b \in \{0, \dots, B'+1\}} \left| \sum_{i=b}^{B'+1} c_i^* - \frac{\alpha}{2} m \right| \right\}.$$

3 Draw $\theta_{\alpha/2}^*$ uniformly from $I_{b_{\alpha/2}^*}$, and $\theta_{1-\alpha/2}^*$ uniformly from $I_{b_{1-\alpha/2}^*}$.

$\frac{\alpha}{2}$)) per definition. PRECISE first identifies an index b^* (lines 1 and 2 in Alg. 2) by minimizing the absolute difference between the “empirical” cumulative counts of samples at $\alpha/2$ vs. the expected cumulative counts out of a total of m^* (or m) from both ends of the distribution; that is, $\sum_{i \leq b} c_i^*$ and $\alpha m^*/2$ (or $\alpha m/2$), and $\sum_{i \geq b} c_i^*$ and $\alpha m^*/2$ (or $\alpha m/2$). A random sample of θ is then drawn from the identified bin I_{b^*} as the $\alpha/2 \times 100\%$ PP quantile estimate; similarly for the $(1 - \alpha/2) \times 100\%$ PP quantile estimate. After the PP point estimates are attained, they can be plugged in directly to form the PPIE for θ , which is $(\theta_{\alpha/2}^*, \theta_{1-\alpha/2}^*)$.

As shown in the following Section 3.4.3, PP quantile outputs from PRECISE are consistent estimators for the population posterior quantiles as the sensitive data size or privacy loss approaches ∞ .

3.4.3 MSE consistency of PRECISE

We establish the MSE consistency for the pointwise PPIE from PRECISE ($+m^*$) in Theorem 6 with ε -DP. Results for the other three PRECISE variants ($+m$, $-m^*$, $-m$) and other DP notation variants (e.g., μ -GDP) can be proved in a similar manner.

Theorem 6 (MSE consistency of PRECISE (+ m^*)). *Given i.i.d. data $\mathbf{x} = \{x_i\}_{i=1}^n \sim f(X|\theta)$ and a non-informative prior $f(\theta)$ relative to the amount of data; let $\{\theta_j\}_{j=1}^m$ denote the set of samples drawn from the posterior distribution $f(\theta|\mathbf{x})$. Under Assumption 4, the PP q^{th} sample quantile $\theta_{(q)}^*$ from \mathcal{M} : PRECISE (+ m^*) of ε -DP satisfies*

$$\mathbb{E}_{\theta} \mathbb{E}_{\mathcal{M}|\{\theta_j\}_{j=1}^m} (\theta_{(q)}^* - F_{\theta|\mathbf{x}}^{-1}(q))^2 = \mathcal{O}(h), \text{ where } h = \Omega(n^{-1/2} \exp(-n^{1/2}\varepsilon)). \quad (9)$$

The detailed proof is provided in Appendix A.3. Briefly, the proof first applies the Cauchy-Schwarz inequality to decompose the MSE between $\theta_{(q)}^*$ and $F_{\theta|\mathbf{x}}^{-1}(q)$ into the MSE between $\theta_{(q)}^*$ and $\theta_{(q)}$ due to DP sanitization error (term T_1) and the MSE between $\theta_{(q)}$ and $F_{\theta|\mathbf{x}}^{-1}(q)$ (term T_2) and then upper bounds each of them. Under the assumption on h and given $m = \lceil (2G(n)h)^{-1} \rceil$, as n increases, h decreases, m increases, and $T_1 \rightarrow 0$ at rate $\mathcal{O}(m^{-2})$ and $T_2 \rightarrow 0$ at rate $\mathcal{O}(m^{-1})$. Not only does this prove Eq. (9), but it also implies the limiting factor in the convergence is the data sampling error (the T_2 term) rather than the sanitization error (accounted for by T_1).

Based on Theorem 6, we show the PPIE from PRECISE asymptotically achieves the nominal coverage as n or ε increases in the proposition below, satisfying Defn 3.

Proposition 7 (asymptotical nominal coverage of PRECISE). *Under the conditions of Theorem 6, as $n \rightarrow \infty$ or $\varepsilon \rightarrow \infty$, the PPIE via PRECISE for the true parameter θ_0 at level $(1 - \alpha)$ satisfies $\Pr(\theta_{\alpha/2}^* \leq \theta_0 \leq \theta_{1-\alpha/2}^* | \mathbf{x}) \rightarrow 1 - \alpha$.*

3.4.4 Other usage and Extensions of the PRECISE Procedure

Though we propose PRECISE primarily for constructing PP interval estimates in this work, this procedure is general for releasing a PP quantile estimate³ for $F_{\theta|\mathbf{x}}^{-1}(q)$ based on the PP posterior distribution of θ given sensitive data \mathbf{x} for any given $q \in (0, 1)$ (e.g., median, Q1, Q3, etc). Due to the empty bin collapsing on the tails, PRECISE may not perform optimally for q values very close to 0 or 1, including minimum and maximum.

³PRECISE should not be used to sanitize sample quantiles of the sensitive data \mathbf{x} itself, which is well-studied problem; for that, users may use existing procedures like PrivateQuantile (Smith, 2011) and JointExp (Gillenwater et al., 2021).

In the multivariate case of $\boldsymbol{\theta} = (\theta^{(1)}, \dots, \theta^{(p)})^\top$, both the P³ histogram procedure in Alg. 1 and PRECISE in Alg. 2 can be utilized to generate pointwise PPIE for each dimension $\theta^{(k)}$ where $1 \leq k \leq p$. This can be achieved by drawing posterior samples from the marginal posterior distribution of $\theta^{(k)}$, while allocating the privacy budget $\boldsymbol{\eta}$ across all p dimension according to the privacy loss composition principle of the specific DP notion being employed.

3.4.5 An alternative to PRECISE

We also explore the exponential mechanism for privately estimating the posterior quantile and provide an alternative approach – *Private Posterior quantile estimator (PPquantile)* in Alg. 3 – to PRECISE, motivated by the PrivateQuantile procedure (Alg. S.1 in the appendix) for releasing private sample quantiles of data \mathbf{x} (Smith, 2011). The procedure and the theoretical results are presented to achieve ε -DP guarantees.

Algorithm 3: PPquantile

- input** : posterior distribution $f(\theta|\mathbf{x})$, quantile $q \in (0,1)$, privacy loss ε , global bounds (L, U) for θ , number of posterior samples m .
- output**: PP estimate $\theta_{(q)}^*$ of the population posterior quantile $F_{\theta|\mathbf{x}}^{-1}(q)$.
- 1 Generate posterior samples $\{\theta_j\}_{j=1}^m \stackrel{\text{iid}}{\sim} f(\theta|\mathbf{x})$;
 - 2 Replace $\theta_j < L$ with L and $\theta_j > U$ with U ;
 - 3 Sort θ_i in ascending order as $L = \theta_{(0)} \leq \theta_{(1)} \leq \dots \leq \theta_{(m)} \leq \theta_{(m+1)} = U$;
 - 4 Set $k = \arg \min_{j \in \{0,1,\dots,m+1\}} |\theta_{(j)} - F_{\theta|\mathbf{x}}^{-1}(q)|$;
 - 5 For $j = 0, 1, \dots, m$, set $y_j = (\theta_{(j+1)} - \theta_{(j)}) \cdot \exp\left(-\frac{\varepsilon|j-k|}{2(m+1)}\right)$;
 - 6 Sample an integer $j^* \in \{0, 1, 2, \dots, m\}$ with probability $y_{j^*} / \sum_{j=0}^m y_j$;
 - 7 Draw $\theta_{(q)}^* \sim \text{Uniform}(\theta_{(j^*)}, \theta_{(j^*+1)})$.
-

PrivateQuantile and PPquantile are fundamentally different, despite that the latter is inspired by the former. PrivateQuantile outputs a sanitized sample quantile directly from the sensitive data \mathbf{x} , whereas PPquantile, similar to the P³ histogram in Alg. 1, outputs sanitized posterior quantiles for parameter θ . It is more complex to design a DP randomized mechanism in the latter case since, as mentioned in Sec 3.2, alternating one individual in \mathbf{x} influences the entire posterior distribution $f(\theta|\mathbf{x})$ instead of a single bin as in the former.

Prior to the utility analysis on PPquantile, we first establish the MSE consistency of PrivateQuantile in Theorem 8. To our knowledge, this is the first theoretical result demonstrat-

ing MSE consistency of PrivateQuantile to population quantiles, despite being well-known.

Theorem 8 (MSE consistency of PrivateQuantile). *Denote the sensitive dataset by $\mathbf{x} = \{x_i\}_{i=1}^n$. Let $x_{([qn])}^*$ be the private q -th sample quantile of \mathbf{x} from \mathcal{M} : PrivateQuantile of ε -DP (Smith, 2011). Under Assumption S.1, and assume \exists constant $C \geq 0$ such that global bounds $(L_{\mathbf{x}}, U_{\mathbf{x}})$ for \mathbf{x} satisfy $\lim_{n \rightarrow \infty} (U_{\mathbf{x}} - x_{(n)}) = \lim_{n \rightarrow \infty} (x_{(1)} - L_{\mathbf{x}}) = C$, then*

$$\mathbb{E}_{\mathbf{x}} \mathbb{E}_{\mathcal{M}|\mathbf{x}} \left(x_{([qn])}^* - F_{\mathbf{x}}^{-1}(q) \right)^2 = \mathcal{O}(n^{-1}) + \mathcal{O} \left(e^{-\mathcal{O}(n\varepsilon)} n^{-3/2} \right). \quad (10)$$

The detailed proof is provided in Appendix A.5. Eq. (10) suggests that the MSE between $x_{([qn])}^*$ and $F_{\mathbf{x}}^{-1}(q)$ can be decomposed into two components: (1) the MSE between $x_{([qn])}^*$ and $x_{([qn])}$ introduced by DP sanitization noise that converges at rate $\mathcal{O}(e^{-\mathcal{O}(n\varepsilon)} n^{-3/2})$ and (2) the MSE between $x_{([qn])}$ and $F_{\mathbf{x}}^{-1}(q)$ due to the sampling error that converges at rate $\mathcal{O}(n^{-1})$. The faster convergence rate of the former implies that the sampling error, rather than the sanitization error, is the limiting factor in the convergence of $x_{([qn])}^*$ to $F_{\mathbf{x}}^{-1}(q)$.

Theorem 9 (Utility guarantees for PPquantile in Alg. 3). *Assume $f(\theta|\mathbf{x})$ is continuous at $F_{\theta|\mathbf{x}}^{-1}(q)$ for $q \in (0, 1)$. Let m be the number of posterior samples on θ from its posterior distribution $f(\theta|\mathbf{x})$, (U, L) be the global bounds on θ , $\xi = e^{-\frac{\varepsilon}{2(m+1)}}$, $s = \min_{j \in \{0, 1, \dots, m\}} (\theta_{(j+1)} - \theta_{(j)})$, and $p_{\min} = \inf_{|\tau - F_{\theta|\mathbf{x}}^{-1}(q)| \leq 2\eta} f_{\theta|\mathbf{x}}(\tau)$ for $\eta > 0$. The PP q^{th} quantile $\theta_{(q)}^*$ from \mathcal{M} : PPquantile of ε -DP in Alg. 3 satisfies*

$$\Pr \left(\left| \theta_{(q)}^* - \theta_{(k)} \right| > 2u \right) \leq \frac{U - L - 4u}{s} \cdot \frac{1 - \xi}{1 + \xi - \xi^{k+1} - \xi^{m-k+1}} \cdot \exp \left(-\frac{\varepsilon u p_{\min}}{4} \right) \quad (11)$$

$$+ \frac{2\eta}{u} \exp \left(-\frac{(m+1)u p_{\min}}{8} \right) + 2 \exp \left(-\frac{m\eta^2 p_{\min}^2}{12(1-q)} \right) \text{ for } 0 \leq u \leq \eta.$$

The detailed proof is in Appendix A.6. In brief, per the Bernstein-von Mises theorem, $\theta_{(m)} - \theta_{(1)} \asymp n^{-1/2}$ as $n \rightarrow \infty$, implying $s = \mathcal{O}(n^{-1/2} m^{-1})$. Under regularity condition that p_{\min} is constant for $\eta \asymp n^{-1/2}$, we let $\{\varepsilon \asymp m, m \asymp n^2, u \asymp n^{-1}\}$ and set $U - L \asymp n^{-5/2}$, then the right hand side of Eq. (11) $\rightarrow 1$ and $\theta_{(q)}^* \xrightarrow{p} \theta_{([qm])}$ asymptotically.

Theorem 9 suggests that PPquantile can return an asymptotically accurate posterior quantile estimate with a high probability. The probability depends on multiple hyperparam-

eters $(U, L, u, \eta, p_{\min})$ and their relationship (e.g. how L, U individually shrink with n) that can be challenging to verify, making it difficult for practical implementation and also leading to potential under-performance in finite-sample scenarios (e.g., if overly conservative bounds L, U are used). We will continue to explore ways to enhance the practical application of the PPquantile procedure, given that it is theoretically sound.

4 Experiments

We evaluate our method (4 versions of PRECISE) for generating PPIE through both extensive simulation studies (Section 4.1), where we also compare it to existing PPIE procedures, and two real-world data applications (Section 4.2).

4.1 Simulation studies

In this section, we use simulated data to examine several common data and inferential scenarios – Gaussian mean and variance, Bernoulli proportion, Poisson mean, and simple linear regression. We choose these inferential tasks because they are commonly studied by existing PPIE methods (see Section 1.2); focusing on these tasks enables a more comprehensive and fair comparison between PRECISE and these methods.

The goals of the simulation studies are 1) to validate that PRECISE achieves nominal coverage across various inferential tasks in data of different sample sizes at varying privacy loss; 2) to showcase the improved performance of PRECISE over the existing PPIE methods with narrower intervals while maintaining correct coverage. The performance of PRECISE in comparison with some existing PPIE methods is summarized in Table 1. *The experiment results suggest that both goals stated above have been attained.*

4.1.1 Simulation settings

We examine a wide range of sample size $n \in (100, 500, 1000, 5000, 10000, 50000)$ and privacy loss $\varepsilon \in (0.1, 0.5, 1, 2, 5, 10, 50)$ for the Laplace mechanism of ε -DP and $\mu \in (0.1, 0.5, 1, 5)$ for the Gaussian mechanism of μ -GDP. Large values for ε or μ are used to demonstrate whether

Table 1: PPIE methods examined in the experiments and performance summary

Method	Experiments	Applicable DP	(nominal CP achieved ?) Performance summary
PRECISE (+)	all	all	(✓) $+m^*$ is the best, $+m$ is worse than $+m^*$, $-m^*$, $-m$
PRECISE (-)	all	all	(×) $-m^*$, $-m$ similar, under-coverage when $n\varepsilon \leq 100$
MS (Liu, 2022)	all	all	(✓) fast and flexible, wide intervals
PB (Ferrando et al., 2022)	all	all	(✓) fast and flexible, wide intervals
deconv (Wang et al., 2022)	Gaus.	μ -GDP	(✓) the widest intervals
repro (Awan and Wang, 2023)	Gaus.	μ -GDP	(✓) slow computation for large n , wide intervals
BLBquant (Chadha et al., 2024)	Gaus., Bern., Pois.	ε -DP	(×) slow for large n , under-coverage due to narrow width
Aug.MCMC (Ju et al., 2022)	linear regression	ε -DP	(✓) slow computation & convergence, sensitive to prior

[†] There are PPIE methods (Karwa and Vadhan, 2017; Covington et al., 2021; Evans et al., 2023; D’Orazio et al., 2015) designed specifically for Gaussian means, they are not evaluated in this work as previous studies (Du et al., 2020; Ferrando et al., 2022) have demonstrated that they are inferior to those listed in the table.

We opt to exclude the approaches in Avella-Medina et al. (2023) and Wang et al. (2019). Both are procedurally complicated and would be excessive for the inferential tasks in our experiments with closed-form estimators.

the PPIE methods converge to the original as the privacy loss increases.

We simulated Gaussian data $\mathbf{x} \sim \mathcal{N}(\mu = 0, \sigma^2 = 1)$, Poisson data $\mathbf{x} \sim \text{Pois}(\lambda = 10)$, and Bernoulli data $\mathbf{x} \sim \text{Bern}(p = 0.3)$. For PRECISE, we used prior $f(\mu, \sigma^2) \propto (\sigma^2)^{-1}$ for the Gaussian data, the corresponding marginal posteriors are $f(\mu|\mathbf{x}) = t_{n-1}(\bar{x}, s^2/n)$ and $f(\sigma^2|\mathbf{x}) = \text{IG}((n-1)/2, (n-1)s^2/2)$ respectively, where s^2 is the sample variance and $\text{IG}(\alpha, \beta)$ is the inverse-gamma distribution with shape parameter α and scale parameter β . For the Poisson data, we set $f(\lambda) = \text{Gamma}(\alpha = 0.1, \beta = 0.1)$; the corresponding posterior is $f(\lambda|\mathbf{x}) = \text{Gamma}(\alpha + \sum_{i=1}^n x_i, \beta + n)$. For the Bernoulli data, we set $f(p) = \text{beta}(\alpha = 1, \beta = 1)$; the corresponding posterior is $f(p|\mathbf{x}) = \text{beta}(\alpha + \sum_{i=1}^n x_i, \beta + n - \sum_{i=1}^n x_i)$. For the linear model $\mathbf{x} = \beta_0 + \beta_1 \mathbf{z} + \mathcal{N}(0, \sigma^2 = 0.25^2)$, where $\beta_0 = 1, \beta_1 = 0.5$ and $\mathbf{z} \sim \mathcal{N}(0, 1)$, we used prior $f(\beta_0, \beta_1, \sigma^2) \propto \sigma^{-2}$; and the corresponding marginal posterior for β_1 is $\beta_1|\mathbf{z}, \mathbf{x} \sim t_{n-2}(\hat{\beta}_1, \frac{\hat{\sigma}^2}{\sum_{i=1}^n (z_i - \bar{z})^2})$, where $\hat{\sigma}^2 = \frac{\sum_{i=1}^n (x_i - \mathbf{z}_i \hat{\beta})^2}{n-2}$ and $\hat{\beta} = (\mathbf{z}^\top \mathbf{z})^{-1} \mathbf{z}^\top \mathbf{x}$ ⁴. Other implementation details for PRECISE, including the hyper-parameters for the P³ and PRECISE algorithms, are provided in Appendix B.1, along with the implementation details for all the comparison methods in Table 1.

⁴Though conjugate priors are employed in all the experiments that have closed-form posterior distributions are easy to sample from, this is not a requirement for PRECISE, which can be coupled with all posterior sampling methods such as MCMC to construct PPIE.

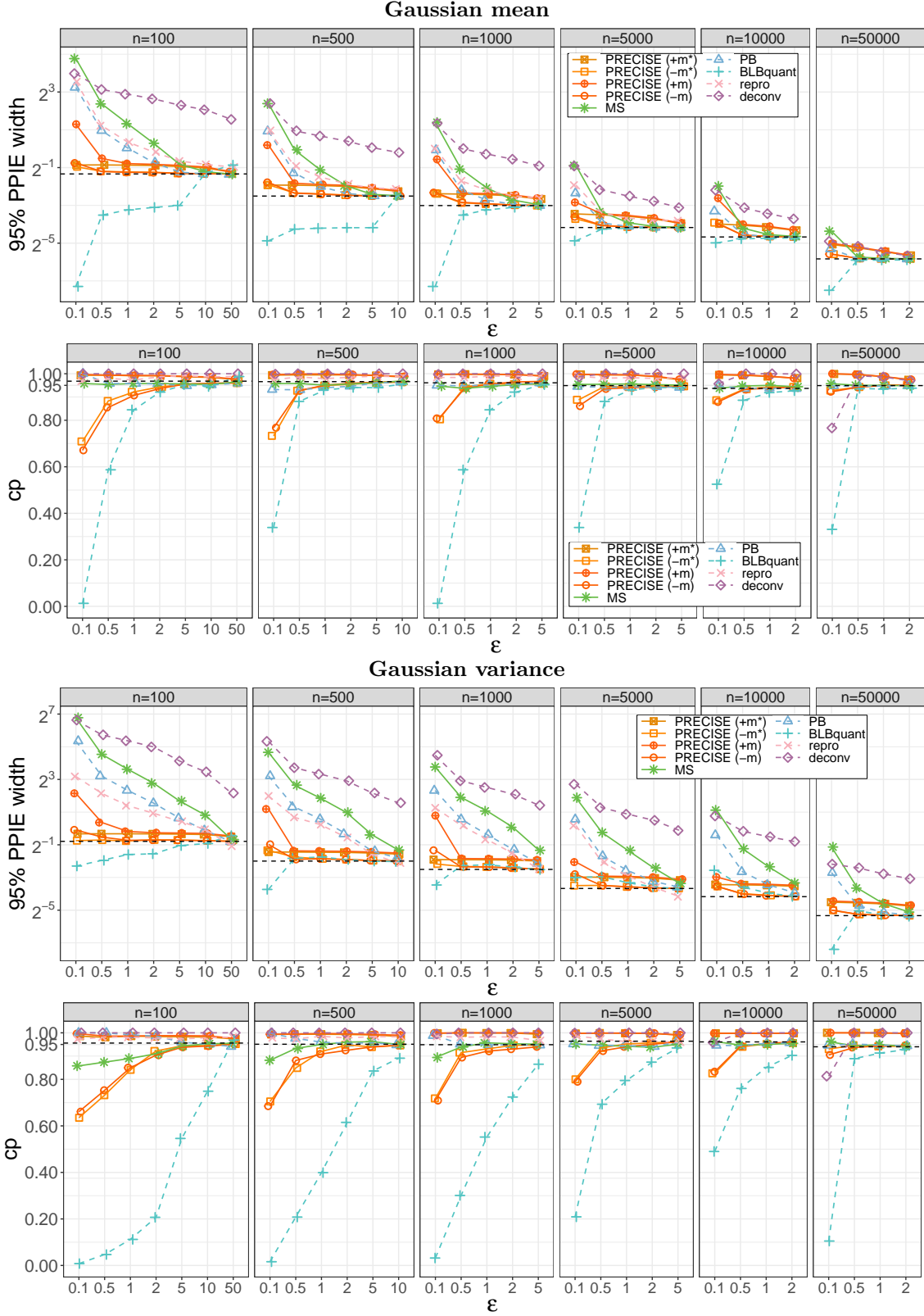


Figure 2: Comparisons of PPIE width and CP for Gaussian mean and variance. All methods use the Laplace mechanism of ϵ -DP except for deconv and repro that are designed for μ -GDP; μ is calculated given ϵ and $\delta=1/n$ per Lemma 1. Black dashed lines represent the original non-private results. The results on μ -GDP are in the appendix.

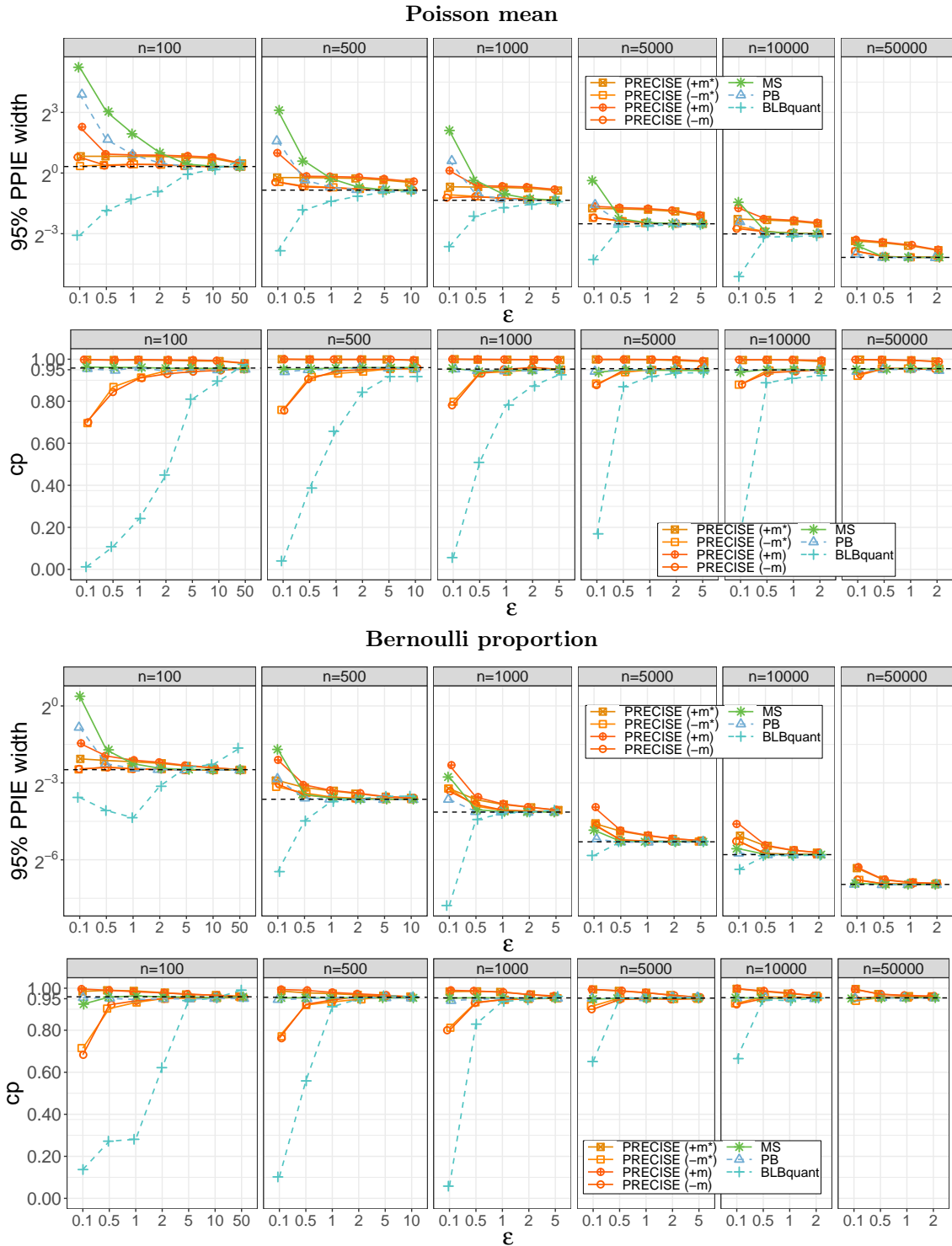


Figure 3: Comparisons of PPIE width and CP for Bernoulli proportion and Poisson mean PPIE with ϵ -DP. Black dashed lines represent the original non-private results. The results on μ -GDP are in the appendix.

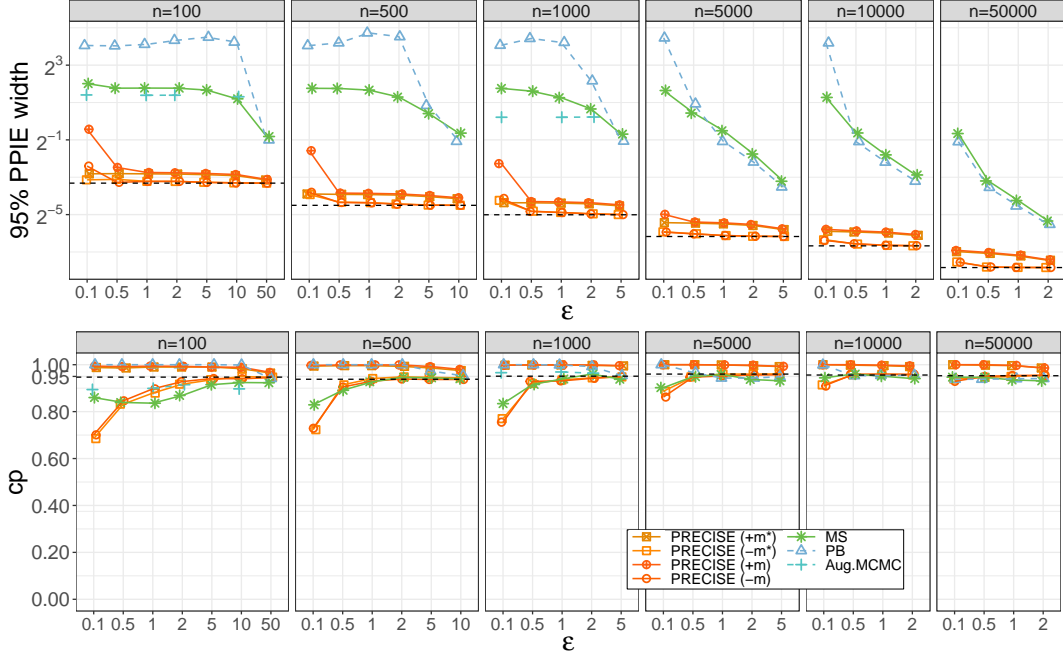


Figure 4: Comparisons of PPIE width and CP for the linear regression slope with ε -DP. Black dashed lines represent the original non-private results. The results on μ -DP are in the appendix.

4.1.2 Results on PPIE width and Inference validity.

The inferential results are summarized by coverage probability (CP) and widths of 95% interval estimates over 1,000 repeats in each simulation setting. Due to space limitations, we present the results on the population mean and variance with ε -DP guarantees in Figures 2 and 3 (the results on μ -DP are available in Appendix C, the findings from which on the relative performance of the methods are consistent with those with ε -DP).

In summary, *PRECISE (+m*) outperformed all competing methods examined in the experiments, offering nominal coverage and notably narrower interval estimates in all n scenarios, data types, inferential tasks, and for both DP types.*

Specifically, among the four versions of PRECISE, the two with non-negativity correction (+m* and +m) achieve the nominal coverage for all ε and n . While +m generates the widest PPIE intervals among the four variants of PRECISE for low privacy loss, they are still the *narrowest* compared to the existing methods. PRECISE without non-negativity correction (-m* and -m) exhibit similar performances. Though both have notable under-coverage

when $n\varepsilon \leq 500$, they converge quickly to the original as ε increases. The differences in the results among the four PRECISE versions imply that non-negativity correction have a stronger and more lasting impact on the performance than the intra-consistency correction, but both are important for robust PP inference.

The CP and interval width for all the examined PPIE methods in Figures 2 and 3 converge toward the original metrics as ε or n increases. MS and PB capture the extra variability from the DP sanitization – as reflected by their nominal coverage, but they also output wide intervals especially for small ε . BLBquant suffers from under-coverage when n or ε is small for every inference task due to not accounting for the sanitization variability in addition to the sampling variability, leading to invalid PPIE. For the Gaussian mean and variance estimation, the interval widths follow the order of $\text{PRECISE}(-) < \text{PRECISE}(+m^*) < \text{PRECISE}(+m) < \text{repro} < \text{PB} < \text{MS} < \text{deconv}$. For Bernoulli proportion, PB and PRECISE $(-)$ are the best performers when $\varepsilon \geq 0.05$ and $n \geq 1000$ and converge to the original faster than PRECISE $(+)$ as ε or n increases. For the linear regression in Figure S.6, the hybrid PB method (Ferrando et al., 2022) designed for OLS estimation achieves the nominal coverage at the cost of wide intervals. The Aug.MCMC method is sensitive to hyperparameter specification and is also computationally extensive (one MCMC chain of 10,000 iterations took about 1.5 mins for $n=100$ and 16 mins for $n=1000$). Even with carefully tuned hyperparameters to mitigate the under-coverage issue with a reasonable width, Aug.MCMC still converges to the original much slower than other methods.

4.1.3 Asymptotic G_0 as a proxy for $G(n)$

The value of $G(n)$ is critical in the implementation of PRECISE to determine the posterior sample size $m = \lceil 2G(n)h \rceil^{-1}$ (Eq. 7) for ensuring privacy guarantees. In simulation studies where the true distributions $f(x|\theta)$ are specified, one may simulate all possible $d(\mathbf{x}, \mathbf{x}') = 1$ and perform a grid search over $\theta \in \Theta$ to numerically approximate $G(n) = \sup_{\theta \in \Theta, d(\mathbf{x}, \mathbf{x}')=1} |f_{\theta|\mathbf{x}}(\theta) - f_{\theta|\mathbf{x}'}(\theta)|$ for a given n . Since it is infeasible or impossible to exhaust the search space of $d(\mathbf{x}, \mathbf{x}') = 1$ especially when \mathbf{x} is high dimensional or con-

tinuous, the numerical $G(n)$ is approximate at best. In addition, this numerical approach becomes inapplicable in the real world because it is impossible to define the search space for $d(\mathbf{x}, \mathbf{x}') = 1$ without knowing $f(\mathbf{x}|\theta)$.

In practice, the asymptotic value G_0 in Eq. (5) (Theorem 2) can be used as an approximation for finite n cases as long as n is sufficiently large. Since G_0 depends on the Fisher information, which is a function of unknown parameters, it is technically not calculable. There are two ways to circumvent this problem – 1) replace the unknown parameters with their PP estimate or 2) derive an upper bound $\overline{G_0}$ for G_0 . Though the second approach is more conservative from a privacy perspective, it can save users’ privacy budget by eliminating the need to sanitize additional statistics. It also reduces the extra effort involved in obtaining estimates and developing and applying a randomized mechanism. The upper bound is often informed by prior knowledge of the parameter range (L, U) , combined with the global bounds $(L_{\mathbf{x}}, U_{\mathbf{x}})$ for data \mathbf{x} . For the simulation studies, we adopted the second approach. The hyperparameters used in determining $\overline{G_0}$ are provided in Table 2; the proofs are provided in Appendix A.1.2.

Table 2: Hyperparameters for $\overline{G_0}$ calculation in the simulation studies

	G_0 from Eq. (5)	(L, U)	$(L_{\mathbf{x}}, U_{\mathbf{x}})^\dagger$	$\overline{G_0}$
Bern(p)	$\frac{ x'_n - x_n }{\sqrt{2e\pi p(1-p)}}$	(0.03, 0.97)	(0, 1)	$\frac{1}{\sqrt{2e\pi} \min\{L(1-L), U(1-U)\}}$
Poisson(λ)	$\frac{ x'_n - x_n e^{-\frac{1}{2}}}{\sqrt{2e\pi\lambda}}$	(3, 35)	(0, 35)	$\frac{(U_{\mathbf{x}} - L_{\mathbf{x}})}{\sqrt{2e\pi L}}$
μ in $\mathcal{N}(\mu, \sigma^2)$	$\frac{ x'_n - x_n }{\sqrt{2e\pi\sigma^2}}$	$(\mu - k\sigma, \mu + k\sigma)$	$(\mu - k\sigma, \mu + k\sigma)$	$\frac{\sqrt{2}k}{\sqrt{e\pi}\sigma} \leq \frac{\sqrt{2}k}{\sqrt{e\pi}L_\sigma}^\ddagger$
σ^2 in $\mathcal{N}(\mu, \sigma^2)$	$\frac{ (x_n - \bar{x}_{n-1})^2 - (x'_n - \bar{x}_{n-1})^2 }{\sqrt{2e\pi \cdot 2\sigma^4}}$	(0.25, 25)	$(\mu - k\sigma, \mu + k\sigma)$	$\frac{k^2}{2\sqrt{2e\pi}\sigma^2} \leq \frac{k^2}{2\sqrt{2e\pi}L}$

[†] conservatively set to satisfy $\Pr(\mathbf{x} \notin (L_{\mathbf{x}}, U_{\mathbf{x}})) < 10^{-5}$; [‡]: $k = 5, L_\sigma = 0.25$.

We compare the numerical approximation of $G(n)$ at different n for various true parameter values against its analytical approximation G_0 and the corresponding upper bound $\overline{G_0}$ in Figure 5. The results show that the numerical $G(n)$ converges rapidly to the asymptotic G_0 as n increases; the two values are actually similar even for small n in most cases. These findings provide reassuring evidence that G_0 can be reliably used in place of $G(n)$ (with $\overline{G_0}$ serving as a conservative alternative) for calculating m and the sensitivity of a posterior

histogram in practical application of PRECISE.

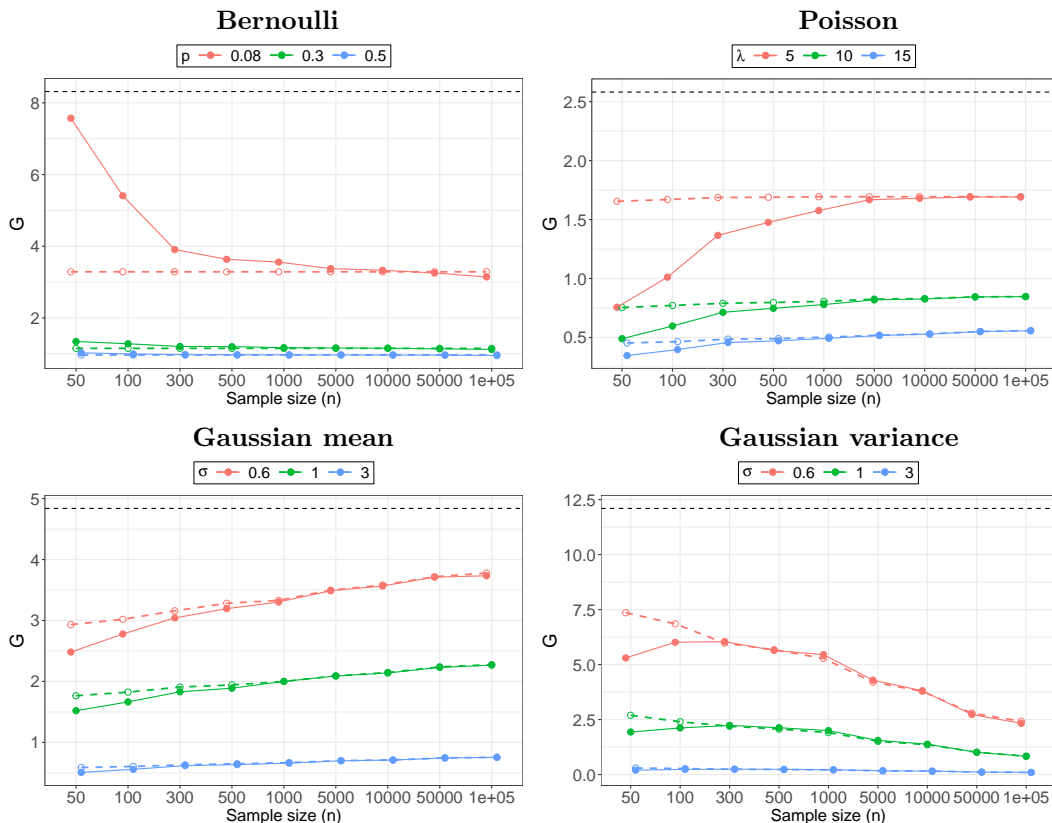


Figure 5: Comparison of numerical approximation to $G(n)$ (colored solid lines; averaged over 100 repetitions) vs asymptotic G_0 (colored dashed lines) in Theorem 2 and upper bound $\overline{G_0}$ (black dashed lines) for different true parameter values and sample sizes n .

4.1.4 Computational cost

We summarize the computational time for each method to generate PPIE for Gaussian mean in one repeat in Table 3. PRECISE and MS are very fast. The computation time for repro and BLBquant increases substantially as n grows, whereas the time for PRECISE, MS, and

Table 3: Computational time \ddagger in one repeat for Gaussian mean PPIE ($\varepsilon = 8$).

Sample size n	PRECISE	MS	PB	deconv †	repro †	BLBquant
100	0.03 sec	0.01 sec	0.10 sec	4.75 sec	8.50 sec	0.04 sec
5000	0.05 sec	0.01 sec	0.31 sec	10.22 sec	1.44 min	14.19 sec
50000	0.05 sec	0.01 sec	2.02 sec	1.26 min	17.41 min	8.11 min

† converted to μ -GDP from $(\varepsilon, \delta=1/n)$ -DP; $\mu=2.45, 1.91, 1.71$ for $n=100, 5k, 50k$ respectively.

‡ On a MacBook Pro with an Apple M3 Mac chip (16-core CPU, 40-core GPU) and 64GB of unified memory. All computations were performed on a single CPU thread without GPU acceleration.

PB remains roughly stable with n . Additionally, deconv shows a notable increase in time with n , though this increase is less pronounced compared to repro and BLBquant.

4.2 Real-world case studies

We applied PRECISE to two real-world data applications. The first case study obtains PPIE for the proportion p of an individual’s annual income over 50K in a randomly selected subset of $n = 500$ from the UCI adult dataset (Becker and Kohavi, 1996). The second study uses the UCI Cardiocography dataset (Campos and Bernardes, 2000), which consists of three fetal state classes (Normal p_1 , Suspect p_2 , and Pathologic p_3) with a sample size of $n = 2126$. we aim to obtain the PPIE for each fo the three proportions.

For the adult data, $f(p) = \text{Beta}(1, 1)$, $\overline{G}_0 = e^{-\frac{1}{2}}/(\sqrt{2\pi}L(1 - L))$ with $L = 0.03$, $h = 2.2 \times 10^{-3}$, resulting in $m = 269$. For the Cardiocography data, we used $\mathbf{p} = (p_1, p_2, p_3) \sim \text{Dirichlet}(1, 1, 1)$ and leveraged domain knowledge to choose $L = (0.5, 0.05, 0.02)$ for p_1, p_2, p_3 respectively; $\overline{G}_0 = e^{-\frac{1}{2}}/(\sqrt{2\pi}L(1 - L))$ as we examine each proportion marginally. By setting $h = (5, 0.95, 0.39) \times 10^{-4}$ for p_1, p_2, p_3 respectively, leading to $m = 1033$ sets of posterior samples on \mathbf{p} drawn from posterior distribution $\text{Dirichlet}(1 + n_1, 1 + n_2, 1 + n_3)$, where $n_1, x_2, x_3 = (1655, 295, 176)$ are the observed counts for the 3 classes. The privacy budget of $\varepsilon/3$ is allocated for sanitizing posterior samples for each element in \mathbf{p} .

We run both case studies with ε -DP guarantees at $\varepsilon = 0.1, 0.5$ and repeat 100 times to measure the stability of the methods, The results are presented in Table 4. For the adult data, PRECISE $+m^*$ yields tighter and more stable PPIE at $\varepsilon = 0.1$, while $-m^*$ is the best performer at $\varepsilon = 0.5$. For the Cardiocography data, the ranking among the PRECISE versions is $+m^* > -m^* \approx -m > +m$ in performance and $+m^*$ produces PPIE closest to the original results with the smallest SD, highlighting its stability.⁵

⁵We also run MS, PB, BLBQuant in the adult data. Consistent with the observations in the simulation studies, PRECISE outperforms MS and PB, with narrower PPIE widths, more stable intervals, and more accurate point estimates. BLBQuant produces invalid narrow intervals leading to under-coverage.

Table 4: Average PPIE width (SD) over 100 repeats in two real datasets and an example on private point estimation (95% PPIE) from a randomly selected single repeat

(a) Adult dataset						
ϵ	original	PRECISE				
		$+m^*$	$-m^*$	$+m$	$-m$	
average 95% PPIE widths (SD) over 100 repeats ($\times 10^{-2}$)						
0.1	7.21	9.87 (1.02)	10.41 (12.50)	25.04 (18.95)	9.58 (10.58)	
0.5	7.21	9.82 (1.06)	7.54 (2.02)	10.85 (3.73)	7.76 (2.03)	
an example on posterior median (95% PPIE) from one repeat ($\times 10^{-2}$)						
0.1	21.60 (17.99, 25.21)	22.32 (17.87, 27.37)	21.34 (19.98, 25.37)	18.28 (13.72, 27.66)	22.23 (19.33, 25.74)	
0.5	21.60 (17.99, 25.21)	21.60 (17.93, 26.33)	21.10 (18.04, 23.31)	20.41 (18.02, 26.77)	21.46 (17.99, 26.82)	
(b) Cardiotocography dataset						
ϵ	original	PRECISE				
		$+m^*$	$-m^*$	$+m$	$-m$	
average 95% PPIE widths (SD) over 100 repeats ($\times 10^{-2}$)						
0.1	Normal	3.5	11.1 (9.7)	6.1 (6.8)	20.3 (11.5)	7.5 (8.4)
	Suspect	2.9	4.6 (0.4)	5.5 (12.0)	18.0 (23.0)	7.3 (16.0)
	Pathologic	2.3	3.7 (0.3)	5.9 (14.4)	12.9 (19.8)	5.0 (9.6)
0.5	Normal	3.5	5.2 (0.5)	4.8 (4.3)	5.6 (2.1)	4.1 (1.2)
	Suspect	2.9	4.6 (0.3)	3.3 (0.8)	5.2 (3.2)	3.5 (0.9)
	Pathologic	2.3	3.6 (0.3)	2.7 (0.7)	3.9 (0.7)	2.8 (0.7)
example posterior median (95% PPIE) from one repeat ($\times 10^{-2}$)						
0.1	Normal	77.8 (76.1, 79.6)	77.4 (74.9, 80.8)	77.2 (75.8, 80.9)	80.4 (50.0, 80.6)	78.7 (75.1, 79.1)
	Suspect	13.9 (12.4, 15.3)	14.0 (11.6, 16.2)	14.5 (11.6, 16.2)	12.4 (5.3, 16.2)	14.0 (11.6, 16.2)
	Pathologic	8.3 (7.1, 9.4)	8.6 (6.8, 10.5)	8.3 (7.2, 10.5)	7.2 (6.5, 10.6)	7.3 (6.8, 10.0)
0.5	Normal	77.8 (76.1, 79.6)	77.8 (75.1, 80.5)	77.4 (75.7, 79.7)	79.6 (75.4, 80.9)	77.5 (75.6, 80.1)
	Suspect	13.9 (12.4, 15.3)	13.9 (11.5, 16.2)	14.2 (12.9, 16.3)	13.2 (11.3, 16.4)	14.2 (11.9, 14.7)
	Pathologic	8.3 (7.1, 9.4)	8.3 (6.6, 10.0)	8.4 (7.8, 9.7)	7.3 (6.5, 10.1)	8.2 (7.2, 9.9)

5 Discussion

Statistical inference with uncertainty quantification, including interval estimations, is central to accurately interpreting data and making informed decisions. In this work, we proposed the PRECISE approach for general-purpose privacy-preserving interval estimation in the Bayesian framework. We theoretically proved the MSE consistency of PRECISE PPIE. We have shown in extensive simulation studies that PRECISE outperformed all other examined PPIE methods, offering nominal coverage, significantly narrower interval estimates, and fast computation. With the theoretically proven statistical validity, guaranteed privacy, along

with demonstrated superiority in utility and computation over other PPIE methods, we believe that PRECISE provides a practically promising, useful, and effective procedure for releasing interval estimates with DP guarantees in real-world applications.

As a future direction, we plan to extend PRECISE for PPIE in high-dimensional settings and tackle more complex inferential tasks, such as Bayesian regularized regressions and prediction intervals. While PRECISE is theoretically applicable to any inferential task that fits in a Bayesian framework and allows for posterior sampling, its practical performance can be influenced by factors such as the dimensionality of an estimation problem, number of posterior samples, sample size, and the PRECISE hyperparameters. Addressing these considerations will be the focus of our upcoming work.

In summary, this work provides a promising tool for practitioners who seek to release interval estimates without compromising the privacy of individuals who contribute their data, fostering trust in data collection and information sharing across data contributors, curators, and users.

Data and Code

The data and code in the simulation and case studies are available at [url] (will be open after the paper has been finalized).

References

- Abowd, J. M. (2018). The us census bureau adopts differential privacy. In *Proceedings of the 24th ACM SIGKDD international conference on knowledge discovery & data mining*, pages 2867–2867.
- Alabi, D., McMillan, A., Sarathy, J., Smith, A., and Vadhan, S. (2020). Differentially private simple linear regression. *arXiv preprint arXiv:2007.05157*.
- Alabi, D. and Vadhan, S. (2022). Hypothesis testing for differentially private linear regression. *Advances in Neural Information Processing Systems*, 35:14196–14209.
- Amin, K., Dick, T., Kulesza, A., Munoz, A., and Vassilvitskii, S. (2019). Differentially private covariance estimation. *Advances in Neural Information Processing Systems*, 32.

- Apple (2020). Apple differential privacy technical overview. https://www.apple.com/privacy/docs/Differential_Privacy_Overview.pdf.
- Asi, H. and Duchi, J. C. (2020). Near instance-optimality in differential privacy. *arXiv preprint arXiv:2005.10630*.
- Avella-Medina, M., Bradshaw, C., and Loh, P.-L. (2023). Differentially private inference via noisy optimization. *The Annals of Statistics*, 51(5):2067–2092.
- Awan, J. and Slavković, A. (2018). Differentially private uniformly most powerful tests for binomial data. *Advances in Neural Information Processing Systems*, 31.
- Awan, J. and Wang, Z. (2023). Simulation-based, finite-sample inference for privatized data. *arXiv preprint arXiv:2303.05328*.
- Becker, B. and Kohavi, R. (1996). Adult. *UCI Machine Learning Repository*, 10:C5XW20.
- Bernstein, G. and Sheldon, D. R. (2019). Differentially private bayesian linear regression. *Advances in Neural Information Processing Systems*, 32.
- Biswas, S., Dong, Y., Kamath, G., and Ullman, J. (2020). Coinpress: Practical private mean and covariance estimation. *Advances in Neural Information Processing Systems*, 33:14475–14485.
- Bojkovic, N. and Loh, P.-L. (2024). Differentially private synthetic data with private density estimation. *arXiv preprint arXiv:2405.04554*.
- Campos, D. and Bernardes, J. (2000). Cardiocography. UCI Machine Learning Repository. DOI: <https://doi.org/10.24432/C51S4N>.
- Chadha, K., Duchi, J., and Kuditipudi, R. (2024). Resampling methods for private statistical inference. *arXiv preprint arXiv:2402.07131*.
- Chaudhuri, K., Monteleoni, C., and Sarwate, A. D. (2011). Differentially private empirical risk minimization. *Journal of Machine Learning Research*, 12(3).
- Covington, C., He, X., Honaker, J., and Kamath, G. (2021). Unbiased statistical estimation and valid confidence intervals under differential privacy. *arXiv preprint arXiv:2110.14465*.
- Dong, J., Roth, A., and Su, W. J. (2022). Gaussian differential privacy. *Journal of the Royal Statistical Society Series B: Statistical Methodology*, 84(1):3–37.
- D’Orazio, V., Honaker, J., and King, G. (2015). Differential privacy for social science inference. *Sloan Foundation Economics Research Paper*, (2676160).
- Drechsler, J., Globus-Harris, I., Mcmillan, A., Sarathy, J., and Smith, A. (2022). Non-parametric differentially private confidence intervals for the median. *Journal of Survey Statistics and Methodology*, 10(3):804–829.

- Du, W., Foot, C., Moniot, M., Bray, A., and Groce, A. (2020). Differentially private confidence intervals. *arXiv preprint arXiv:2001.02285*.
- Dwork, C., Kenthapadi, K., McSherry, F., Mironov, I., and Naor, M. (2006a). Our data, ourselves: Privacy via distributed noise generation. In *Advances in Cryptology-EUROCRYPT 2006: 24th Annual International Conference on the Theory and Applications of Cryptographic Techniques, St. Petersburg, Russia, 2006. Proceedings 25*, pages 486–503. Springer.
- Dwork, C. and Lei, J. (2009). Differential privacy and robust statistics. In *Proceedings of the 41st annual ACM symposium on Theory of computing*, pages 371–380.
- Dwork, C., McSherry, F., Nissim, K., and Smith, A. (2006b). Calibrating noise to sensitivity in private data analysis. In *Theory of Cryptography: Third Theory of Cryptography Conference, TCC 2006, New York, NY, USA, 2006. Proceedings 3*, pages 265–284. Springer.
- Erlingsson, Ú., Pihur, V., and Korolova, A. (2014). Rappor: Randomized aggregatable privacy-preserving ordinal response. In *Proceedings of the 2014 ACM SIGSAC conference on computer and communications security*, pages 1054–1067.
- Evans, G., King, G., Schwenzfeier, M., and Thakurta, A. (2023). Statistically valid inferences from privacy-protected data. *American Political Science Review*, 117(4):1275–1290.
- Ferrando, C., Wang, S., and Sheldon, D. (2022). Parametric bootstrap for differentially private confidence intervals. In *International Conference on Artificial Intelligence and Statistics*, pages 1598–1618. PMLR.
- Gaboardi, M., Lim, H., Rogers, R., and Vadhan, S. (2016). Differentially private chi-squared hypothesis testing: Goodness of fit and independence testing. In *International conference on machine learning*, pages 2111–2120. PMLR.
- Gillenwater, J., Joseph, M., and Kulesza, A. (2021). Differentially private quantiles. In *International Conference on Machine Learning*, pages 3713–3722. PMLR.
- Ju, N., Awan, J., Gong, R., and Rao, V. (2022). Data augmentation mcmc for bayesian inference from privatized data. *Advances in neural information processing systems*, 35:12732–12743.
- Karwa, V. and Vadhan, S. (2017). Finite sample differentially private confidence intervals. *arXiv preprint arXiv:1711.03908*.
- Kleiner, A., Talwalkar, A., Sarkar, P., and Jordan, M. I. (2014). A scalable bootstrap for massive data. *Journal of the Royal Statistical Society Series B: Statistical Methodology*, 76(4):795–816.

- Kulkarni, T., Jälkö, J., Koskela, A., Kaski, S., and Honkela, A. (2021). Differentially private bayesian inference for generalized linear models. In *International Conference on Machine Learning*, pages 5838–5849. PMLR.
- Lin, S., Bun, M., Gaboardi, M., Kolaczyk, E. D., and Smith, A. (2024). Differentially private confidence intervals for proportions under stratified random sampling. *Electronic Journal of Statistics*, 18(1):1455–1494.
- Liu, F. (2022). Model-based differentially private data synthesis and statistical inference in multiply synthetic differentially private data. *Transactions on Data Privacy*, 15(3):141–175.
- McSherry, F. and Talwar, K. (2007). Mechanism design via differential privacy. In *48th Annual IEEE Symposium on Foundations of Computer Science*, pages 94–103. IEEE.
- Mitzenmacher, M. and Upfal, E. (2017). *Probability and computing: Randomization and probabilistic techniques in algorithms and data analysis*. Cambridge university press.
- Nagaraja, H. N., Bharath, K., and Zhang, F. (2015). Spacings around an order statistic. *Annals of the Institute of Statistical Mathematics*, 67(3):515–540.
- Räisä, O., Jälkö, J., Kaski, S., and Honkela, A. (2023). Noise-aware statistical inference with differentially private synthetic data. In *International Conference on Artificial Intelligence and Statistics*, pages 3620–3643. PMLR.
- Sheffet, O. (2017). Differentially private ordinary least squares. In *International Conference on Machine Learning*, pages 3105–3114. PMLR.
- Smirnov, N. V. (1949). Limit distributions for the terms of a variational series. *Trudy Matematicheskogo Instituta imeni VA Steklova*, 25:3–60.
- Smith, A. (2011). Privacy-preserving statistical estimation with optimal convergence rates. In *Proceedings of the 43rd ACM symposium on Theory of Computing*, pages 813–822.
- Walker, A. (1968). A note on the asymptotic distribution of sample quantiles. *Journal of the Royal Statistical Society Series B: Statistical Methodology*, 30(3):570–575.
- Wang, Y., Kifer, D., and Lee, J. (2019). Differentially private confidence intervals for empirical risk minimization. *Journal of Privacy and Confidentiality*, 9(1).
- Wang, Y.-X. (2018). Revisiting differentially private linear regression: optimal and adaptive prediction & estimation in unbounded domain. *arXiv preprint arXiv:1803.02596*.
- Wang, Z., Cheng, G., and Awan, J. (2022). Differentially private bootstrap: New privacy analysis and inference strategies. *arXiv preprint arXiv:2210.06140*.

Appendix

A Proofs	1
A.1 Proof of Theorem 2	1
A.1.1 A single parameter θ	1
A.1.2 Specific Cases	5
A.1.3 Multi-dimensional θ	7
A.2 Proof of Theorem 5	12
A.3 Proof of Theorem 6	12
A.4 Proof of Proposition 7	16
A.5 Proof of Theorem 8	17
A.6 Proof of Theorem 9	20
B Experiment details	24
B.1 Hyperparameters and code	24
B.2 Sensitivity of LS linear regression coefficients	25
C Additional experimental results	26

A Proofs

A.1 Proof of Theorem 2

A.1.1 A single parameter θ

Let $G \triangleq \sup_{\theta \in \Theta, d(\mathbf{x}, \mathbf{x}')=1} |f_{\theta|\mathbf{x}}(\theta) - f_{\theta|\mathbf{x}'}(\theta)|$, where the parameter $\theta \in \Theta$ is a scalar. By the Bernstein-von Mises theorem, as $n \rightarrow \infty$,

$$\sqrt{n} \cdot \theta|\mathbf{x} \xrightarrow{d} \mathcal{N}(\hat{\theta}_n, I_{\theta_0}^{-1}), \quad (1)$$

where $\mathbf{x} = \{x_1, x_2, \dots, x_n\}$, $\hat{\theta}_n$ is the MLE based on \mathbf{x} , and I_{θ_0} is the Fisher information matrix evaluated at the true population parameter θ_0 . Since we assume non-informative prior $f(\theta)$ relative to the amount of data, we will use MLE and MAP interchangeably in this proof as they converge to the same value asymptotically; the same applies to other proofs if applicable.

Assume the neighboring datasets \mathbf{x} and \mathbf{x}' differ by the last element, and $\hat{\theta}'_n$ denotes the

MLE based on \mathbf{x}' . Assume $\hat{\theta}'_n - \hat{\theta}_n \approx \frac{C}{n} + o(n^{-1})$ as $n \rightarrow \infty$.

Substitution neighboring relation

$$|f_{\theta|\mathbf{x}}(\theta) - f_{\theta|\mathbf{x}'}(\theta)| \rightarrow \frac{\sqrt{n}}{\sqrt{2\pi I_{\theta_0}^{-1}}} \left| \exp\left(-\frac{n(\theta - \hat{\theta}_n)^2}{2I_{\theta_0}^{-1}}\right) - \exp\left(-\frac{n(\theta - \hat{\theta}'_n)^2}{2I_{\theta_0}^{-1}}\right) \right| \quad (2)$$

$$\triangleq \frac{\sqrt{n}}{\sqrt{2\pi I_{\theta_0}^{-1}}} |g(\hat{\theta}_n) - g(\hat{\theta}'_n)|. \quad (3)$$

Per Taylor expansion of $g(x)$ around x_0 : $g(x) \approx g(x_0) + g'(x_0)(x - x_0) + \frac{g''(x_0)}{2!}(x - x_0)^2 + \dots$.

$$\begin{aligned} & g(\hat{\theta}'_n) - g(\hat{\theta}_n) \\ & \approx \exp\left(-\frac{n(\theta - \hat{\theta}_n)^2}{2I_{\theta_0}^{-1}}\right) \left[\frac{n(\theta - \hat{\theta}_n)}{I_{\theta_0}^{-1}}(\hat{\theta}'_n - \hat{\theta}_n) + \frac{(\hat{\theta}'_n - \hat{\theta}_n)^2}{2} \left(\frac{n^2(\theta - \hat{\theta}_n)^2}{I_{\theta_0}^{-2}} - \frac{n}{I_{\theta_0}^{-1}} \right) \right. \\ & \quad \left. + \frac{(\hat{\theta}'_n - \hat{\theta}_n)^3}{3!} \left(\frac{n^3(\theta - \hat{\theta}_n)^3}{I_{\theta_0}^{-3}} - \frac{3n^2(\theta - \hat{\theta}_n)}{I_{\theta_0}^{-2}} \right) \right] \quad (4) \end{aligned}$$

$$\rightarrow g(\hat{\theta}_n) \left[\frac{C(\theta - \hat{\theta}_n)}{I_{\theta_0}^{-1}} + \frac{C^2}{2} \left(\frac{(\theta - \hat{\theta}_n)^2}{I_{\theta_0}^{-2}} - \frac{1}{nI_{\theta_0}^{-1}} \right) + \frac{C^3}{3!} \left(\frac{(\theta - \hat{\theta}_n)^3}{I_{\theta_0}^{-3}} - \frac{3(\theta - \hat{\theta}_n)}{nI_{\theta_0}^{-2}} \right) \right], \quad (5)$$

$$\text{where } C = \hat{\theta}'_n - \hat{\theta}_n. \quad (6)$$

To obtain $G(n)$, we aim to solve for θ value that maximizes $|g(\hat{\theta}'_n) - g(\hat{\theta}_n)|$. Toward that end, we take the 1st-derivative of Eq. (5) with respect to θ .

$$\begin{aligned} & \frac{\partial(g(\hat{\theta}'_n) - g(\hat{\theta}_n))}{\partial\theta} \\ & = g(\hat{\theta}_n) \left(-\frac{n(\theta - \hat{\theta}_n)}{I_{\theta_0}^{-1}} \right) \left[\frac{C(\theta - \hat{\theta}_n)}{I_{\theta_0}^{-1}} + \frac{C^2}{2} \left(\frac{(\theta - \hat{\theta}_n)^2}{I_{\theta_0}^{-2}} - \frac{1}{nI_{\theta_0}^{-1}} \right) + \frac{C^3}{3!} \left(\frac{(\theta - \hat{\theta}_n)^3}{I_{\theta_0}^{-3}} - \frac{3(\theta - \hat{\theta}_n)}{nI_{\theta_0}^{-2}} \right) \right] \\ & \quad + g(\hat{\theta}_n) \left[\frac{C}{I_{\theta_0}^{-1}} + \frac{C^2(\theta - \hat{\theta}_n)}{I_{\theta_0}^{-2}} + \frac{C^3}{2} \left(\frac{(\theta - \hat{\theta}_n)^2}{I_{\theta_0}^{-3}} - \frac{1}{nI_{\theta_0}^{-2}} \right) \right]. \quad (7) \end{aligned}$$

WLOG, assume $C \geq 0$ so $\mathcal{N}(\hat{\theta}'_n, I_{\theta_0}^{-1})$ is shifted to the right of $\mathcal{N}(\hat{\theta}_n, I_{\theta_0}^{-1})$, with a single intersection point $\tilde{\theta} = \frac{\hat{\theta}_n + \hat{\theta}'_n}{2} \in (\hat{\theta}_n, \hat{\theta}'_n)$; and $g(\hat{\theta}'_n) - g(\hat{\theta}_n) \leq 0$ for $\theta \leq \tilde{\theta}$, and $g(\hat{\theta}'_n) - g(\hat{\theta}_n) \geq 0$ for $\theta \geq \tilde{\theta}$. Due to symmetry, $|g(\hat{\theta}'_n) - g(\hat{\theta}_n)|$ achieve its maximum at two θ values; that is, there exists a constant $d \geq 0$ such that $\frac{\partial(g(\hat{\theta}'_n) - g(\hat{\theta}_n))}{\partial\theta} \Big|_{\theta = \hat{\theta}_n - d} = 0$ and $\frac{\partial(g(\hat{\theta}'_n) - g(\hat{\theta}_n))}{\partial\theta} \Big|_{\theta = \hat{\theta}'_n + d} = 0$. Thus, it suffices to show that $g(\hat{\theta}'_n) - g(\hat{\theta}_n)$ is unimodal has a unique maximizer when $\theta \leq \tilde{\theta}$.

$$g(\hat{\theta}'_n) - g(\hat{\theta}_n) = g(\hat{\theta}_n) \left(\frac{g(\hat{\theta}'_n)}{g(\hat{\theta}_n)} - 1 \right) \Rightarrow \log(g(\hat{\theta}'_n) - g(\hat{\theta}_n)) = \log(g(\hat{\theta}_n)) + \log\left(\frac{g(\hat{\theta}'_n)}{g(\hat{\theta}_n)} - 1 \right).$$

If we show $\log(g(\hat{\theta}'_n) - g(\hat{\theta}_n))$ is concave and has a unique maximizer, the same maximizer applies to $g(\hat{\theta}'_n) - g(\hat{\theta}_n)$ due the monotonicity of the log transformation. First,

$$\begin{aligned} \frac{\partial^2 \log(g(\hat{\theta}_n))}{\partial \theta^2} &= \frac{\partial(-\frac{n(\theta-\hat{\theta}_n)}{I_{\theta_0}^{-1}})}{\partial \theta} = -\frac{n}{I_{\theta_0}^{-1}} < 0; \text{ then} \\ z(\theta) &= \log\left(\frac{g(\hat{\theta}'_n)}{g(\hat{\theta}_n)} - 1\right) = \log\left(\exp\left(-\frac{n(\theta-\hat{\theta}'_n)^2}{2I_{\theta_0}^{-1}} + \frac{n(\theta-\hat{\theta}_n)^2}{2I_{\theta_0}^{-1}}\right) - 1\right), \\ \frac{\partial z(\theta)}{\partial \theta} &= \frac{-\frac{n(\theta-\hat{\theta}'_n)}{I_{\theta_0}^{-1}}g(\hat{\theta}'_n)g(\hat{\theta}_n) + \frac{n(\theta-\hat{\theta}_n)}{I_{\theta_0}^{-1}}g(\hat{\theta}_n)g(\hat{\theta}'_n)}{g^2(\hat{\theta}_n)\left(\frac{g(\hat{\theta}'_n)}{g(\hat{\theta}_n)} - 1\right)} = \frac{g(\hat{\theta}'_n)}{g(\hat{\theta}'_n) - g(\hat{\theta}_n)} \cdot \frac{n(\hat{\theta}'_n - \hat{\theta}_n)}{I_{\theta_0}^{-1}} \\ \frac{\partial^2 z(\theta)}{\partial \theta^2} &= \frac{n(\hat{\theta}'_n - \hat{\theta}_n)}{I_{\theta_0}^{-1}} \cdot \frac{g(\hat{\theta}'_n)(g(\hat{\theta}'_n) - g(\hat{\theta}_n))\frac{-n(\theta-\hat{\theta}'_n)}{I_{\theta_0}^{-1}} - g(\hat{\theta}'_n)\left(-\frac{n(\theta-\hat{\theta}'_n)}{I_{\theta_0}^{-1}}\right)g(\hat{\theta}'_n) + \frac{n(\theta-\hat{\theta}_n)}{I_{\theta_0}^{-1}}g(\hat{\theta}_n)}{(g(\hat{\theta}'_n) - g(\hat{\theta}_n))^2} \\ &= \frac{n(\hat{\theta}'_n - \hat{\theta}_n)}{I_{\theta_0}^{-1}} \cdot \frac{g'(\hat{\theta}_n)\left(\frac{-n(\theta-\hat{\theta}'_n)}{I_{\theta_0}^{-1}}g(\hat{\theta}'_n) + \frac{n(\theta-\hat{\theta}_n)}{I_{\theta_0}^{-1}}g(\hat{\theta}_n)\right) + \frac{n(\theta-\hat{\theta}'_n)}{I_{\theta_0}^{-1}}g(\hat{\theta}'_n) - \frac{n(\theta-\hat{\theta}_n)}{I_{\theta_0}^{-1}}g(\hat{\theta}_n)}{(g(\hat{\theta}'_n) - g(\hat{\theta}_n))^2} \\ &= -\left(\frac{n(\hat{\theta}'_n - \hat{\theta}_n)}{I_{\theta_0}^{-1}}\right)^2 \cdot \frac{g(\hat{\theta}'_n)g(\hat{\theta}_n)}{(g(\hat{\theta}'_n) - g(\hat{\theta}_n))^2} < 0, \end{aligned}$$

Therefore, both $g(\hat{\theta}_n) > 0$ and $\frac{g(\hat{\theta}'_n)}{g(\hat{\theta}_n)} - 1 > 0$ are log-concave. Given both $g(\hat{\theta}_n) > 0$ and $\frac{g(\hat{\theta}'_n)}{g(\hat{\theta}_n)} - 1 > 0$, per the product of log-concave functions is also log-concave, $g(\hat{\theta}'_n) - g(\hat{\theta}_n) = g(\hat{\theta}_n)\left(\frac{g(\hat{\theta}'_n)}{g(\hat{\theta}_n)} - 1\right)$ is also log-concave, thus unimodal for $\theta \geq \tilde{\theta}$.

Now that we have shown $g(\hat{\theta}'_n) - g(\hat{\theta}_n)$ has a unique maximum, the next step is to derive the maximizer. Let Eq. (7) equal to 0, we have

$$\frac{n(\theta-\hat{\theta}_n)}{I_{\theta_0}^{-1}} \left[(\theta-\hat{\theta}_n) + \frac{C}{2} \left(\frac{(\theta-\hat{\theta}_n)^2}{I_{\theta_0}^{-1}} - \frac{1}{n} \right) + \frac{C^2}{3!} \left(\frac{(\theta-\hat{\theta}_n)^3}{I_{\theta_0}^{-2}} - \frac{3(\theta-\hat{\theta}_n)}{nI_{\theta_0}^{-1}} \right) \right] = 1 + \frac{C(\theta-\hat{\theta}_n)}{I_{\theta_0}^{-1}} + \frac{C^2}{2} \left(\frac{(\theta-\hat{\theta}_n)^2}{I_{\theta_0}^{-2}} - \frac{1}{nI_{\theta_0}^{-1}} \right)$$

Rearranging the terms, we have

$$1 - \frac{C^2}{2nI_{\theta_0}^{-1}} = \frac{n(\theta-\hat{\theta}_n)^2}{I_{\theta_0}^{-1}} - \frac{3(\theta-\hat{\theta}_n)C}{2I_{\theta_0}^{-1}} - \frac{C^2(\theta-\hat{\theta}_n)^2}{I_{\theta_0}^{-2}} + \frac{nC(\theta-\hat{\theta}_n)^3}{2I_{\theta_0}^{-2}} + \frac{nC^2(\theta-\hat{\theta}_n)^4}{6I_{\theta_0}^{-3}}. \quad (8)$$

Substituting $\hat{\theta}_n - d$ and $\hat{\theta}'_n + d \approx \hat{\theta}_n + \frac{C}{n} + d + o(n^{-1})$ for θ in Eq. (8), its RHS is

$$\begin{aligned} \text{RHS}|_{\theta=\hat{\theta}_n-d} &= \frac{nd^2}{I_{\theta_0}^{-1}} + \frac{3dC}{2I_{\theta_0}^{-1}} - \frac{C^2d^2}{I_{\theta_0}^{-2}} - \frac{nCd^3}{2I_{\theta_0}^{-2}} + \frac{nd^4C^2}{6I_{\theta_0}^{-3}} \\ \text{RHS}|_{\theta=\hat{\theta}'_n+d} &\approx \frac{n\left(\frac{C}{n} + d + o(n^{-1})\right)^2}{I_{\theta_0}^{-1}} - \frac{3\left(\frac{C}{n} + d + o(n^{-1})\right)C}{2I_{\theta_0}^{-1}} - \frac{C^2\left(\frac{C}{n} + d + o(n^{-1})\right)^2}{I_{\theta_0}^{-2}} \end{aligned} \quad (9)$$

$$+ \frac{nC(\frac{C}{n} + d + o(n^{-1}))^3}{2I_{\theta_0}^{-2}} + \frac{n(\frac{C}{n} + d + o(n^{-1}))^4 C^2}{6I_{\theta_0}^{-3}}, \quad (10)$$

respectively. Taking the difference between Eq. (10) and Eq. (9) leads to

$$0 = \text{RHS}|_{\theta=\hat{\theta}_n+d} - \text{RHS}|_{\theta=\hat{\theta}_n-d} = -\frac{(3\frac{C}{n} + 6d)C}{2I_{\theta_0}^{-1}} + \frac{C(2\frac{C}{n} + 4d)}{2I_{\theta_0}^{-1}} - \frac{C^2((\frac{C}{n} + d)^2 - d^2)}{I_{\theta_0}^{-2}} \\ + \frac{nC((\frac{C}{n} + d)^3 + d^3)}{2I_{\theta_0}^{-2}} + \frac{n((\frac{C}{n} + d)^4 - d^4)C^2}{6I_{\theta_0}^{-3}} \quad (11)$$

$$\Rightarrow \frac{(\frac{C}{n} + 2d)}{2} + \frac{(\frac{C}{n} + 2d)\frac{C^2}{n}}{I_{\theta_0}^{-1}} \quad (12)$$

$$= \frac{n(\frac{C}{n} + 2d)((\frac{C}{n} + d)^2 - (\frac{C}{n} + d)d + d^2)}{2I_{\theta_0}^{-1}} + \frac{((\frac{C}{n} + d)^2 + d^2)C^2(\frac{C}{n} + 2d)}{6I_{\theta_0}^{-2}} \\ \Rightarrow \frac{1}{2} + \frac{C^2}{nI_{\theta_0}^{-1}} = \frac{n((\frac{C}{n} + d)^2 - (\frac{C}{n} + d)d + d^2)}{2I_{\theta_0}^{-1}} + \frac{((\frac{C}{n} + d)^2 + d^2)C^2}{6I_{\theta_0}^{-2}} \\ = \frac{C^2}{2nI_{\theta_0}^{-1}} + \frac{Cd}{2I_{\theta_0}^{-1}} + \frac{nd^2}{2I_{\theta_0}^{-1}} + \frac{((\frac{C}{n})^2 + 2\frac{C}{n}d + 2d^2)C^2}{6I_{\theta_0}^{-2}} \quad (13)$$

$$\Rightarrow \frac{1}{2} + \frac{C^2}{2nI_{\theta_0}^{-1}} - \frac{C^4}{6n^2I_{\theta_0}^{-2}} = \frac{Cd}{2I_{\theta_0}^{-1}} + \frac{nd^2}{2I_{\theta_0}^{-1}} + \frac{(\frac{C}{n}d + d^2)C^2}{3I_{\theta_0}^{-2}} \quad (14)$$

$$\Rightarrow \frac{1}{2} + \frac{C^2}{2nI_{\theta_0}^{-1}} - \frac{C^4}{6n^2I_{\theta_0}^{-2}} = \left(\frac{C}{2I_{\theta_0}^{-1}} + \frac{C^3}{3nI_{\theta_0}^{-2}} \right) d + \left(\frac{n}{2I_{\theta_0}^{-1}} + \frac{C^2}{3I_{\theta_0}^{-2}} \right) d^2$$

$$\Rightarrow \underbrace{I_{\theta_0}^{-1} + \frac{C^2}{n} - \frac{C^4}{3n^2I_{\theta_0}^{-1}}}_{=c} = \underbrace{\left(C + \frac{2C^3}{3nI_{\theta_0}^{-1}} \right)}_{=b} d + \underbrace{\left(n + \frac{2C^2}{3I_{\theta_0}^{-1}} \right)}_{=a} d^2$$

$$\Rightarrow ad^2 + bd + c = 0. \quad (15)$$

Given the quadratic equation with respect to d , its roots can be obtained analytically

$$\Delta = b^2 - 4ac = \left(C + \frac{2C^3}{3nI_{\theta_0}^{-1}} \right)^2 + 4 \left(n + \frac{2C^2}{3I_{\theta_0}^{-1}} \right) \left(I_{\theta_0}^{-1} + \frac{C^2}{n} - \frac{C^4}{3n^2I_{\theta_0}^{-1}} \right) \\ = 4I_{\theta_0}^{-1}n + \left(1 + 4 + \frac{8}{3} \right) C^2 + \frac{C^4}{nI_{\theta_0}^{-1}} \left(\frac{4}{3} - \frac{4}{3} + \frac{8}{3} \right) + \frac{C^6}{n^2I_{\theta_0}^{-2}} \left(\frac{4}{9} - \frac{8}{9} \right) \\ = 4I_{\theta_0}^{-1}n + \frac{23}{3}C^2 + \frac{8}{3} \cdot \frac{C^4}{nI_{\theta_0}^{-1}} - \frac{4}{9} \cdot \frac{C^6}{n^2I_{\theta_0}^{-2}} \quad (16) \\ d = \frac{-b \pm \sqrt{\Delta}}{2a} = \frac{-C - \frac{2C^3}{3nI_{\theta_0}^{-1}} \pm \sqrt{4I_{\theta_0}^{-1}n + \frac{23}{3}C^2 + \frac{8}{3} \cdot \frac{C^4}{nI_{\theta_0}^{-1}} - \frac{4}{9} \cdot \frac{C^6}{n^2I_{\theta_0}^{-2}}}}{2(n + \frac{2C^2}{3I_{\theta_0}^{-1}})}$$

$$\approx \frac{-C}{2n} \pm \sqrt{\frac{I_{\theta_0}^{-1}}{n}} \asymp n^{-1/2}. \quad (17)$$

Plugging d from Eq. (17) into Eq. (5), we have

$$g(\hat{\theta}'_n) - g(\hat{\theta}_n)|_{\theta=\hat{\theta}_n-d} \approx \exp\left(-\frac{nd^2}{2I_{\theta_0}^{-1}}\right) \left[\frac{-dC}{I_{\theta_0}^{-1}} + \frac{C^2}{2} \left(\frac{d^2}{I_{\theta_0}^{-2}} - \frac{1}{nI_{\theta_0}^{-1}} \right) + \frac{C^3}{3!} \left(\frac{-d^3}{I_{\theta_0}^{-3}} + \frac{3d}{nI_{\theta_0}^{-2}} \right) \right] \quad (18)$$

$$= \exp\left(-\frac{n\left(\frac{I_{\theta_0}^{-1}}{n} + \frac{C^2}{4n^2} - \frac{C}{n}\sqrt{\frac{I_{\theta_0}^{-1}}{n}}\right)}{2I_{\theta_0}^{-1}}\right) \left[\frac{\left(\frac{C}{2n} - \sqrt{\frac{I_{\theta_0}^{-1}}{n}}\right)C}{I_{\theta_0}^{-1}} + \mathcal{O}(n^{-1}) \right] \quad (19)$$

$$= \exp\left(-\frac{1}{2} + \mathcal{O}(n^{-1/2})\right) \left[\frac{-C}{\sqrt{nI_{\theta_0}^{-1}}} + \mathcal{O}(n^{-1}) \right] \quad (20)$$

Finally, $G(n)$ can be derived by plugging Eq. (20) into Eq. (3)

$$G(n) = \frac{\sqrt{n}}{\sqrt{2\pi I_{\theta_0}^{-1}}} |g(\hat{\theta}_n) - g(\hat{\theta}'_n)|_{\theta=\hat{\theta}_n-d} \quad (21)$$

$$\approx \frac{\sqrt{n}}{\sqrt{2\pi I_{\theta_0}^{-1}}} e^{-\frac{1}{2} + \mathcal{O}(n^{-1/2})} \left[\frac{C}{\sqrt{nI_{\theta_0}^{-1}}} + \mathcal{O}(n^{-1}) \right] = \frac{C e^{-\frac{1}{2} + \mathcal{O}(n^{-1/2})}}{\sqrt{2\pi I_{\theta_0}^{-1}}} + \mathcal{O}(n^{-\frac{1}{2}}) \quad (22)$$

Removal neighboring Relation Our work so far suggested that a generic formulation on $G(n)$ is analytically challenging to derive in the case of removal neighboring relation. We will continue to investigate this problem in the future.

A.1.2 Specific Cases

In this section, we derive C for some specific cases, including the cases examined in the simulation and case studies. $G(n)$ can be obtained by plugging in C into Eq.(22). Unless mentioned otherwise, all neighboring relations are assumed to be substitution.

1. If $\hat{\theta}_n = \bar{x}$, then $C = |x'_n - x_n|$. Note that this applies to categorical data; for example, for binary data, where $\hat{\theta}_n$ is the proportion of a level, $x \in \{0, 1\}$, then $C = 1$

2. If $\hat{\theta}_n = n^{-1} \sum_{i=1}^n (x_i - \bar{x})^2$, then $\hat{\sigma}'^2 - \hat{\sigma}^2$

$$\begin{aligned} &= n^{-1} (\sum_{i=1}^n (x_i^2 - x_i'^2) - n(\bar{x}^2 - \bar{x}'^2)) \\ &= n^{-1} (x_n^2 - x_n'^2 - n^{-1}(x_n - x_n')(2 \sum_{i=1}^{n-1} x_i + x_n + x_n')) \\ &= n^{-1}(x_n - x_n')(x_n + x_n' - n^{-1}(2 \sum_{i=1}^{n-1} x_i + x_n + x_n')) \\ &= n^{-1}(x_n - x_n') \left((1 - n^{-1})x_n + (1 - n^{-1})x_n' - 2n^{-1} \sum_{i=1}^{n-1} x_i \right) \\ &= n^{-1}(1 - n^{-1})(x_n^2 - x_n'^2) - 2n^{-2}(n - 1)(x_n - x_n')\bar{x}_{n-1}, \text{ where } \bar{x}_{n-1} = (n - 1)^{-1} \sum_{i=1}^{n-1} x_i \end{aligned}$$

$$= \frac{n-1}{n^2} (x_n^2 - x_n'^2 - 2(x_n - x_n')\bar{x}_{n-1}) = \frac{n-1}{n^2} ((x_n - \bar{x}_{n-1})^2 - (x_n' - \bar{x}_{n-1})^2),$$

leading to $C = (x_n - \bar{x}_{n-1})^2 - (x_n' - \bar{x}_{n-1})^2$

3. For linear regression $\mathbf{y} = \mathbf{x}\boldsymbol{\beta} + \varepsilon$

$f(\sigma^2, \boldsymbol{\beta} | \mathbf{x}, \mathbf{y}) = f(\sigma^2 | \mathbf{x}, \mathbf{y}) f(\boldsymbol{\beta} | \sigma^2, \mathbf{x}, \mathbf{y})$, where

$$f(\sigma^2 | \mathbf{x}, \mathbf{y}) = \text{IG} \left(\frac{n - (p+1)}{2}, \frac{(\mathbf{y} - \mathbf{x}\hat{\boldsymbol{\beta}})^\top (\mathbf{y} - \mathbf{x}\hat{\boldsymbol{\beta}})}{2} \right)$$

$f(\boldsymbol{\beta} | \sigma^2, \mathbf{x}, \mathbf{y}) = \mathcal{N}_{p+1}(\hat{\boldsymbol{\beta}}, \boldsymbol{\Sigma})$, where $\hat{\boldsymbol{\beta}} = (\mathbf{x}^\top \mathbf{x})^{-1} (\mathbf{x}^\top \mathbf{y})$ and $\boldsymbol{\Sigma} = \sigma^2 (\mathbf{x}^\top \mathbf{x})^{-1}$.

In the case of simple linear regression, the marginal posterior distributions of β_0 and β_1 are

$$\beta_1 | \mathbf{x}, \mathbf{y} \sim t_{n-2} \left(\hat{\beta}_1, \frac{\hat{\sigma}^2}{\sum_{i=1}^n (x_i - \bar{x})^2} \right) \text{ where } \hat{\sigma}^2 = \frac{\sum_{i=1}^n (y_i - \hat{y}_i)^2}{n-2},$$

$$\beta_0 | \mathbf{x}, \mathbf{y} \sim t_{n-2} \left(\hat{\beta}_0, \hat{\sigma}^2 \left(\frac{1}{n} + \frac{\bar{x}^2}{\sum_{i=1}^n (x_i - \bar{x})^2} \right) \right) \text{ where } \hat{\sigma}^2 = \frac{\sum_{i=1}^n (y_i - \hat{y}_i)^2}{n-2}.$$

We first derive the constant C for β_1 . Note that $\hat{\beta}_1 = \frac{S_{xy}}{S_{xx}}$, and

$$n(\hat{\beta}'_1 - \hat{\beta}_1) = n \frac{S_{x'y'} S_{xx} - S_{xy} S_{x'x'}}{S_{x'x'} S_{xx}} = n \frac{S_{xx} (S_{x'y'} - S_{xy}) - S_{xy} (S_{x'x'} - S_{xx})}{S_{x'x'} S_{xx}}, \text{ where}$$

$$\begin{aligned} S_{x'x'} - S_{xx} &= \left(\sum_{i=1}^{n-1} x_i^2 + x_n'^2 - n\bar{x}'^2 \right) - \left(\sum_{i=1}^{n-1} x_i^2 + x_n^2 - n\bar{x}^2 \right) = x_n'^2 - x_n^2 - n(\bar{x}'^2 - \bar{x}^2) \\ &= x_n'^2 - x_n^2 - n \left(\left(\frac{n-1}{n} \bar{x}_{n-1} + \frac{x_n'}{n} \right)^2 - \left(\frac{n-1}{n} \bar{x}_{n-1} + \frac{x_n}{n} \right)^2 \right) \\ &= x_n'^2 - x_n^2 - (x_n' - x_n) \left(\frac{2(n-1)}{n} \bar{x}_{n-1} + \frac{x_n' + x_n}{n} \right) = \frac{n-1}{n} (x_n'^2 - x_n^2 - 2\bar{x}_{n-1} (x_n' - x_n)) \end{aligned}$$

$$\begin{aligned} S_{x'y'} - S_{xy} &= x_n' y_n' - n\bar{x}' \bar{y}' - x_n y_n + n\bar{x} \bar{y} \\ &= x_n' y_n' - x_n y_n - n \left[\left(\frac{n-1}{n} \bar{x}_{n-1} + \frac{x_n'}{n} \right) \left(\frac{n-1}{n} \bar{y}_{n-1} + \frac{y_n'}{n} \right) \right. \\ &\quad \left. - \left(\frac{n-1}{n} \bar{x}_{n-1} + \frac{x_n}{n} \right) \left(\frac{n-1}{n} \bar{y}_{n-1} + \frac{y_n}{n} \right) \right] \\ &= x_n' y_n' - x_n y_n - n \left(\frac{n-1}{n^2} \bar{x}_{n-1} (y_n' - y_n) + \frac{n-1}{n^2} \bar{y}_{n-1} (x_n' - x_n) + \frac{x_n' y_n' - x_n y_n}{n^2} \right) \\ &= \frac{n-1}{n} (x_n' y_n' - x_n y_n - \bar{x}_{n-1} (y_n' - y_n) - \bar{y}_{n-1} (x_n' - x_n)). \end{aligned}$$

$$\begin{aligned}
\text{Thus } n(\hat{\beta}'_1 - \hat{\beta}_1) &= n \frac{S_{x'y'}S_{xx} - S_{xy}S_{x'x'}}{S_{x'x'}S_{xx}} = n \frac{S_{xx}(S_{x'y'} - S_{xy}) - S_{xy}(S_{x'x'} - S_{xx})}{S_{x'x'}S_{xx}} \\
&= \frac{n-1}{S_{x'x'}S_{xx}} \left[S_{xx}(x'_n y'_n - x_n y_n - \bar{x}_{n-1}(y'_n - y_n) - \bar{y}_{n-1}(x'_n - x_n)) - S_{xy}(x_n'^2 - x_n^2 - 2\bar{x}_{n-1}(x'_n - x_n)) \right] \\
&= \frac{n-1}{\underbrace{S_{x'x'}}_{\rightarrow(\sigma^2)^{-1}}} \left[\underbrace{x'_n y'_n - x_n y_n - \bar{x}_{n-1}(y'_n - y_n) - (x'_n - x_n)\bar{y}_{n-1}}_{=A} - \hat{\beta}_1(x'_n - x_n)(x'_n + x_n - 2\bar{x}_{n-1}) \right] = C_1.
\end{aligned}$$

$$\text{Together with } I_{\theta} = \begin{pmatrix} \frac{1}{\sigma^2} & \frac{x_i}{\sigma^2} & 0 \\ \frac{x_i}{\sigma^2} & \frac{x_i^2}{\sigma^2} & 0 \\ 0 & 0 & \frac{1}{2\sigma^4} \end{pmatrix},$$

$$G(n) \approx \frac{|C_1|e^{-\frac{1}{2} + \mathcal{O}(n^{-\frac{1}{2}})}}{\sqrt{2\pi}I_{\theta_0}^{-1}} + \mathcal{O}(n^{-\frac{1}{2}}) \rightarrow \frac{|C_1|e^{-\frac{1}{2}}}{\sqrt{2\pi} \frac{\sum_{i=1}^n x_i^2}{n\sigma^2}} = \frac{|A - \hat{\beta}_1(x'_n - x_n)(x'_n + x_n - 2\bar{x}_{n-1})|\sigma^2 e^{-\frac{1}{2}}}{\sqrt{2\pi}(\bar{x}^2 + \frac{S_{xx}}{n})(\frac{S_{xx}}{n-1} + \frac{A}{n})}.$$

For example, in the simulation study, $\mathbf{y} = \beta_0 + \beta_1 \mathbf{x} + \mathcal{N}(0, \sigma^2 = 0.25^2)$ with $\beta_0 = 1, \beta_1 = 0.5$ and $\mathbf{x} \sim \mathcal{N}(0, 1)$. Then $\frac{\sum_{i=1}^n x_i^2}{n} = \frac{\sum_{i=1}^n x_i^2 - n\bar{x}^2 + n\bar{x}^2}{n} = \bar{x}^2 + \frac{S_{xx}}{n} \rightarrow 1$, $A \rightarrow x'_n y'_n - x_n y_n - (x'_n - x_n)\bar{y}_{n-1}$ as $n \rightarrow \infty$, and

$$\begin{aligned}
G(n) &\rightarrow \frac{|x'_n y'_n - x_n y_n - (x'_n - x_n)(\bar{y}_{n-1} + \hat{\beta}_1 x'_n + \hat{\beta}_1 x_n)|\sigma^2 e^{-\frac{1}{2}}}{\sqrt{2\pi}\sigma_x^2(\sigma_x^2 + \frac{A}{n})} \\
&\leq \frac{\sigma^2 e^{-\frac{1}{2}}}{\sqrt{2\pi}\sigma_x^4} \cdot (|x'_n y'_n| + |x_n y_n| + |(x'_n - x_n)(\bar{y}_{n-1} + \hat{\beta}_1 x'_n + \hat{\beta}_1 x_n)|)
\end{aligned}$$

In the case of $\beta_0 = \bar{y} - \bar{x}\hat{\beta}_1$,

$$\begin{aligned}
\hat{\beta}'_0 - \hat{\beta}_0 &= \frac{y'_n - y_n}{n} - \bar{x}'\hat{\beta}'_1 + \bar{x}'\hat{\beta}_1 - \bar{x}'\hat{\beta}_1 + \bar{x}\hat{\beta}_1 = \frac{(y'_n - y_n) - \hat{\beta}_1(x'_n - x_n)}{n} - \bar{x}'(\hat{\beta}'_1 - \hat{\beta}_1) \\
n(\hat{\beta}'_0 - \hat{\beta}_0) &= (y'_n - y_n) - \hat{\beta}_1(x'_n - x_n) - n\bar{x}'(\hat{\beta}'_1 - \hat{\beta}_1) \rightarrow (y'_n - y_n) - \hat{\beta}_1(x'_n - x_n) - \bar{x}'C_1 = C_0
\end{aligned}$$

A.1.3 Multi-dimensional θ

Let $\theta = (\theta_1, \theta_2, \dots, \theta_p)^\top \in \Theta$ be a p -dimensional parameter vector. Denote the dataset by $\mathbf{X} = \{\mathbf{x}_i\}_{i=1}^n$ that contain data points on n individuals, where $\mathbf{x}_i \in \mathbb{R}^q$. Per the Bernstein-von Mises theorem, as $n \rightarrow \infty$,

$$\sqrt{n} \cdot \theta | \mathbf{X} \xrightarrow{d} \mathcal{N}_p(\hat{\theta}_n, I_{\theta_0}^{-1}), \tag{23}$$

where $\hat{\theta}_n$ is the MLE based on \mathbf{X} , and I_{θ_0} is the Fisher information matrix evaluated at the true population parameter θ_0 .

For the substitution neighboring relation, WLOG, assume datasets \mathbf{X} and \mathbf{X}' differ in the last observation \mathbf{x}_n vs \mathbf{x}'_n . Let $\hat{\theta}'_n$ denote the MLE based on \mathbf{X}' . Assume $\hat{\theta}'_n - \hat{\theta}_n \approx \frac{c}{n} + o(n^{-1})$

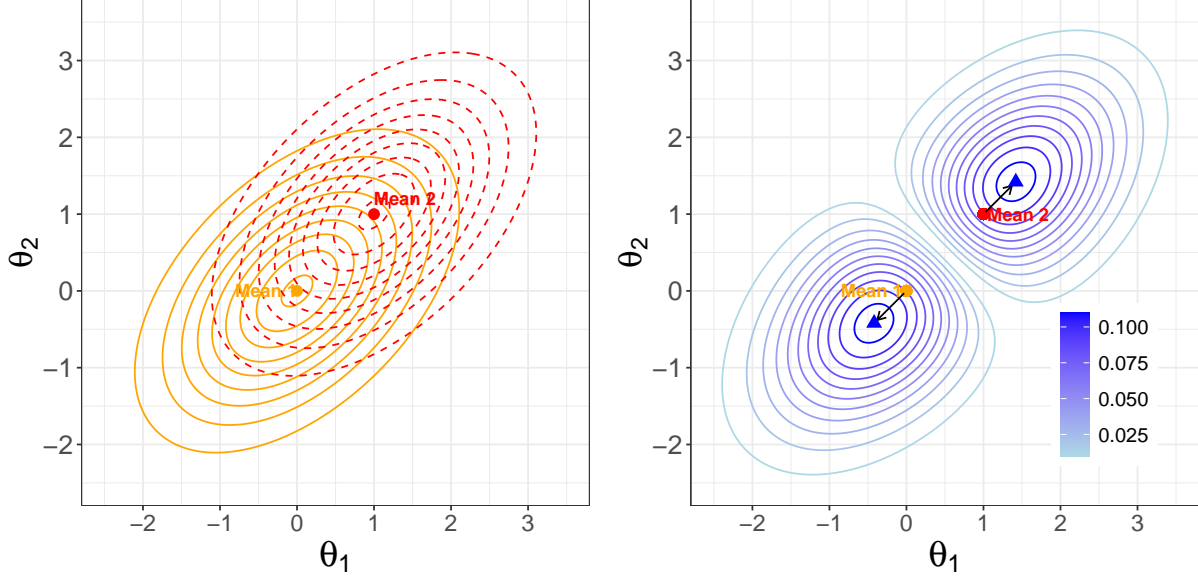


Figure S.1: Contour plots for the densities of two bivariate Gaussian distributions with $\boldsymbol{\mu}_1 = (0, 0)^\top$ and $\boldsymbol{\mu}_2 = (1, 1)^\top$ and the same covariance matrix (left) and the absolute difference between these two densities (right), where the two black vectors are identical in magnitude but in opposite directions.

as $n \rightarrow \infty$, where $\mathbf{C} \in \mathbb{R}^p$. Then

$$\begin{aligned}
& |f_{\boldsymbol{\theta}|\mathbf{X}}(\boldsymbol{\theta}) - f_{\boldsymbol{\theta}|\mathbf{X}'}(\boldsymbol{\theta})| \\
&= (2\pi)^{-\frac{p}{2}} \sqrt{\frac{1}{\det(I_{\boldsymbol{\theta}_0}^{-1}/n)}} \cdot \left| \exp\left(-\frac{n}{2}(\boldsymbol{\theta} - \hat{\boldsymbol{\theta}}_n)^\top I_{\boldsymbol{\theta}_0}(\boldsymbol{\theta} - \hat{\boldsymbol{\theta}}_n)\right) - \exp\left(-\frac{n}{2}(\boldsymbol{\theta} - \hat{\boldsymbol{\theta}}'_n)^\top I_{\boldsymbol{\theta}_0}(\boldsymbol{\theta} - \hat{\boldsymbol{\theta}}'_n)\right) \right| \\
&\triangleq (2\pi)^{-\frac{p}{2}} \sqrt{\frac{n^p}{\det(I_{\boldsymbol{\theta}_0}^{-1})}} \cdot |g(\hat{\boldsymbol{\theta}}_n) - g(\hat{\boldsymbol{\theta}}'_n)|. \tag{24}
\end{aligned}$$

Apply the Taylor expansion to $g(\mathbf{x})$ around \mathbf{x}_0 ,

$$g(\mathbf{x}) \approx g(\mathbf{x}_0) + \nabla g(\mathbf{x}_0)^\top (\mathbf{x} - \mathbf{x}_0) + \frac{1}{2}(\mathbf{x} - \mathbf{x}_0)^\top \nabla^2 g(\mathbf{x}_0) (\mathbf{x} - \mathbf{x}_0),$$

where the gradient $\nabla g(\mathbf{x})$ and Hessian matrix $\nabla^2 g(\mathbf{x})$ are

$$\nabla g(\mathbf{x}) = \frac{\partial}{\partial \mathbf{x}} \exp\left(-\frac{n}{2}(\boldsymbol{\theta} - \mathbf{x})^\top I_{\boldsymbol{\theta}_0}(\boldsymbol{\theta} - \mathbf{x})\right) = g(\mathbf{x}) \cdot (nI_{\boldsymbol{\theta}_0}(\boldsymbol{\theta} - \mathbf{x})) \tag{25}$$

$$\begin{aligned}
\nabla^2 g(\mathbf{x}) &= \frac{\partial}{\partial \mathbf{x}} g(\mathbf{x}) \cdot (nI_{\boldsymbol{\theta}_0}(\boldsymbol{\theta} - \mathbf{x})) = n^2 g(\mathbf{x}) \cdot (I_{\boldsymbol{\theta}_0}(\boldsymbol{\theta} - \mathbf{x})(\boldsymbol{\theta} - \mathbf{x})^\top I_{\boldsymbol{\theta}_0}) - g(\mathbf{x})nI_{\boldsymbol{\theta}_0} \\
&= g(\mathbf{x}) (n^2 (I_{\boldsymbol{\theta}_0}(\boldsymbol{\theta} - \mathbf{x})(\boldsymbol{\theta} - \mathbf{x})^\top I_{\boldsymbol{\theta}_0}) - nI_{\boldsymbol{\theta}_0}). \tag{26}
\end{aligned}$$

Substituting $\widehat{\boldsymbol{\theta}}_n$ and $\widehat{\boldsymbol{\theta}}'_n$ for \mathbf{x} and \mathbf{x}_0 , respectively, we have

$$\begin{aligned} g(\widehat{\boldsymbol{\theta}}_n) &\approx g(\widehat{\boldsymbol{\theta}}'_n) + g(\widehat{\boldsymbol{\theta}}'_n) \left[n(\boldsymbol{\theta} - \widehat{\boldsymbol{\theta}}'_n)^\top I_{\boldsymbol{\theta}_0} (\widehat{\boldsymbol{\theta}}_n - \widehat{\boldsymbol{\theta}}'_n) \right. \\ &\quad \left. + \frac{1}{2} (\widehat{\boldsymbol{\theta}}_n - \widehat{\boldsymbol{\theta}}'_n)^\top \left(n^2 \left(I_{\boldsymbol{\theta}_0} (\boldsymbol{\theta} - \widehat{\boldsymbol{\theta}}'_n) (\boldsymbol{\theta} - \widehat{\boldsymbol{\theta}}'_n)^\top I_{\boldsymbol{\theta}_0} \right) - n I_{\boldsymbol{\theta}_0} \right) (\widehat{\boldsymbol{\theta}}_n - \widehat{\boldsymbol{\theta}}'_n) \right] \\ &\approx g(\widehat{\boldsymbol{\theta}}'_n) \left[1 - (\boldsymbol{\theta} - \widehat{\boldsymbol{\theta}}'_n)^\top I_{\boldsymbol{\theta}_0} \mathbf{C} + \frac{1}{2n} \mathbf{C}^\top \left(n \left(I_{\boldsymbol{\theta}_0} (\boldsymbol{\theta} - \widehat{\boldsymbol{\theta}}'_n) (\boldsymbol{\theta} - \widehat{\boldsymbol{\theta}}'_n)^\top I_{\boldsymbol{\theta}_0} \right) - I_{\boldsymbol{\theta}_0} \right) \mathbf{C} \right]. \end{aligned} \quad (27)$$

WLOG, assume $C_j \geq 0$ for $\forall 1 \leq j \leq p$ so $\mathcal{N}(\widehat{\boldsymbol{\theta}}'_n, I_{\boldsymbol{\theta}_0}^{-1})$ is shifted to the right of $\mathcal{N}(\widehat{\boldsymbol{\theta}}_n, I_{\boldsymbol{\theta}_0}^{-1})$ elementwisely, with a single intersection point $\tilde{\boldsymbol{\theta}}$. For $\boldsymbol{\theta} \leq \tilde{\boldsymbol{\theta}}$, we have $g(\widehat{\boldsymbol{\theta}}'_n) - g(\widehat{\boldsymbol{\theta}}_n) \leq 0$ while for $\boldsymbol{\theta} \geq \tilde{\boldsymbol{\theta}}$, $g(\widehat{\boldsymbol{\theta}}'_n) - g(\widehat{\boldsymbol{\theta}}_n) \geq 0$. Due to symmetry (see Figure S.1 for an illustration), there are two maximizers in $\boldsymbol{\theta}$, where $|g(\widehat{\boldsymbol{\theta}}_n) - g(\widehat{\boldsymbol{\theta}}'_n)|$ achieves the maximum; that is, there exists a constant vector $\mathbf{d} = (d_1, \dots, d_p)^\top$ with $d_j \geq 0$ such that $\frac{\partial(g(\widehat{\boldsymbol{\theta}}_n) - g(\widehat{\boldsymbol{\theta}}'_n))}{\partial \boldsymbol{\theta}} \Big|_{\boldsymbol{\theta} = \widehat{\boldsymbol{\theta}}'_n + \mathbf{d}} = 0$ and $\frac{\partial(g(\widehat{\boldsymbol{\theta}}_n) - g(\widehat{\boldsymbol{\theta}}'_n))}{\partial \boldsymbol{\theta}} \Big|_{\boldsymbol{\theta} = \widehat{\boldsymbol{\theta}}_n - \mathbf{d}} = 0$.

Similar to Section A.1.1, we first prove the uniqueness of maximum for $g(\widehat{\boldsymbol{\theta}}'_n) - g(\widehat{\boldsymbol{\theta}}_n)$ when $\boldsymbol{\theta} \geq \tilde{\boldsymbol{\theta}}$. Applying the same log-transformation to $g(\widehat{\boldsymbol{\theta}}_n) \left(\frac{g(\widehat{\boldsymbol{\theta}}'_n)}{g(\widehat{\boldsymbol{\theta}}_n)} - 1 \right)$. First,

$$\nabla_{\boldsymbol{\theta}}^2 \log(g(\widehat{\boldsymbol{\theta}}_n)) = \frac{-n I_{\boldsymbol{\theta}_0} (\widehat{\boldsymbol{\theta}}'_n - \widehat{\boldsymbol{\theta}}_n)}{\partial \boldsymbol{\theta}} = -\frac{n}{I_{\boldsymbol{\theta}_0}^{-1}} < 0;$$

$$\text{Let } z(\boldsymbol{\theta}) = \log \left(\frac{g(\widehat{\boldsymbol{\theta}}'_n)}{g(\widehat{\boldsymbol{\theta}}_n)} - 1 \right) = \log \left(\exp \left(-\frac{n}{2} (\boldsymbol{\theta} - \widehat{\boldsymbol{\theta}}'_n)^\top I_{\boldsymbol{\theta}_0} (\boldsymbol{\theta} - \widehat{\boldsymbol{\theta}}'_n) + \frac{n}{2} (\boldsymbol{\theta} - \widehat{\boldsymbol{\theta}}_n)^\top I_{\boldsymbol{\theta}_0} (\boldsymbol{\theta} - \widehat{\boldsymbol{\theta}}_n) \right) - 1 \right),$$

$$\begin{aligned} \text{then } \nabla_{\boldsymbol{\theta}} z(\boldsymbol{\theta}) &= \frac{\nabla \frac{g(\widehat{\boldsymbol{\theta}}'_n)}{g(\widehat{\boldsymbol{\theta}}_n)}}{\frac{g(\widehat{\boldsymbol{\theta}}'_n)}{g(\widehat{\boldsymbol{\theta}}_n)} - 1} = \frac{g(\widehat{\boldsymbol{\theta}}_n) \nabla g(\widehat{\boldsymbol{\theta}}'_n) - g(\widehat{\boldsymbol{\theta}}'_n) \nabla g(\widehat{\boldsymbol{\theta}}_n)}{g^2(\widehat{\boldsymbol{\theta}}_n) \left(\frac{g(\widehat{\boldsymbol{\theta}}'_n)}{g(\widehat{\boldsymbol{\theta}}_n)} - 1 \right)} \\ &= \frac{-n I_{\boldsymbol{\theta}_0} (\boldsymbol{\theta} - \widehat{\boldsymbol{\theta}}'_n) g(\widehat{\boldsymbol{\theta}}'_n) + g(\widehat{\boldsymbol{\theta}}'_n) n I_{\boldsymbol{\theta}_0} (\boldsymbol{\theta} - \widehat{\boldsymbol{\theta}}_n)}{g(\widehat{\boldsymbol{\theta}}'_n) - g(\widehat{\boldsymbol{\theta}}_n)} = \frac{g(\widehat{\boldsymbol{\theta}}'_n)}{g(\widehat{\boldsymbol{\theta}}'_n) - g(\widehat{\boldsymbol{\theta}}_n)} \cdot n I_{\boldsymbol{\theta}_0} (\widehat{\boldsymbol{\theta}}'_n - \widehat{\boldsymbol{\theta}}_n) \end{aligned}$$

$$\begin{aligned} \nabla_{\boldsymbol{\theta}}^2 z(\boldsymbol{\theta}) &= n I_{\boldsymbol{\theta}_0} (\widehat{\boldsymbol{\theta}}'_n - \widehat{\boldsymbol{\theta}}_n) \cdot \nabla_{\boldsymbol{\theta}} \left(\frac{g(\widehat{\boldsymbol{\theta}}'_n)}{g(\widehat{\boldsymbol{\theta}}'_n) - g(\widehat{\boldsymbol{\theta}}_n)} \right) \\ &= n I_{\boldsymbol{\theta}_0} (\widehat{\boldsymbol{\theta}}'_n - \widehat{\boldsymbol{\theta}}_n) \frac{(g(\widehat{\boldsymbol{\theta}}'_n) - g(\widehat{\boldsymbol{\theta}}_n)) \nabla_{\boldsymbol{\theta}} g(\widehat{\boldsymbol{\theta}}'_n) - g(\widehat{\boldsymbol{\theta}}'_n) \nabla_{\boldsymbol{\theta}} (g(\widehat{\boldsymbol{\theta}}'_n) - g(\widehat{\boldsymbol{\theta}}_n))}{(g(\widehat{\boldsymbol{\theta}}'_n) - g(\widehat{\boldsymbol{\theta}}_n))^2} \\ &= \frac{-n I_{\boldsymbol{\theta}_0} (\boldsymbol{\theta} - \widehat{\boldsymbol{\theta}}'_n) (g(\widehat{\boldsymbol{\theta}}'_n) - g(\widehat{\boldsymbol{\theta}}_n)) g(\widehat{\boldsymbol{\theta}}'_n) - g(\widehat{\boldsymbol{\theta}}'_n) (-n I_{\boldsymbol{\theta}_0} (\boldsymbol{\theta} - \widehat{\boldsymbol{\theta}}'_n) g(\widehat{\boldsymbol{\theta}}'_n) + n I_{\boldsymbol{\theta}_0} (\boldsymbol{\theta} - \widehat{\boldsymbol{\theta}}_n) g(\widehat{\boldsymbol{\theta}}_n))}{(g(\widehat{\boldsymbol{\theta}}'_n) - g(\widehat{\boldsymbol{\theta}}_n))^2} \\ &\quad \cdot n I_{\boldsymbol{\theta}_0} (\widehat{\boldsymbol{\theta}}'_n - \widehat{\boldsymbol{\theta}}_n) \\ &= -n I_{\boldsymbol{\theta}_0} (\widehat{\boldsymbol{\theta}}'_n - \widehat{\boldsymbol{\theta}}_n)^2 \frac{g(\widehat{\boldsymbol{\theta}}_n) g(\widehat{\boldsymbol{\theta}}'_n)}{(g(\widehat{\boldsymbol{\theta}}'_n) - g(\widehat{\boldsymbol{\theta}}_n))^2} < 0 \end{aligned}$$

Similarly to the argument in the single-parameter case in Section A.1.1, $g(\widehat{\boldsymbol{\theta}}'_n) - g(\widehat{\boldsymbol{\theta}}_n) = g(\widehat{\boldsymbol{\theta}}_n)\left(\frac{g(\widehat{\boldsymbol{\theta}}'_n)}{g(\widehat{\boldsymbol{\theta}}_n)} - 1\right)$ is log-concave and has a unique maximum.

To solve for $\boldsymbol{\theta}$ that leads to the maximum difference, we take the 1st derivative of Eq. (27) with respect to $\boldsymbol{\theta}$.

$$\begin{aligned} \frac{\partial(g(\widehat{\boldsymbol{\theta}}_n) - g(\widehat{\boldsymbol{\theta}}'_n))}{\partial\boldsymbol{\theta}} &\approx \frac{\partial g(\widehat{\boldsymbol{\theta}}'_n)}{\partial\boldsymbol{\theta}} \left[-(\boldsymbol{\theta} - \widehat{\boldsymbol{\theta}}'_n)^\top I_{\boldsymbol{\theta}_0} \mathbf{C} + \frac{1}{2n} \mathbf{C}^\top \left(n \left(I_{\boldsymbol{\theta}_0} (\boldsymbol{\theta} - \widehat{\boldsymbol{\theta}}'_n) (\boldsymbol{\theta} - \widehat{\boldsymbol{\theta}}'_n)^\top I_{\boldsymbol{\theta}_0} \right) - I_{\boldsymbol{\theta}_0} \right) \mathbf{C} \right] \\ &+ g(\widehat{\boldsymbol{\theta}}'_n) \left[-I_{\boldsymbol{\theta}_0} \mathbf{C} + \frac{1}{2} \underbrace{\frac{\partial \mathbf{C}^\top I_{\boldsymbol{\theta}_0} (\boldsymbol{\theta} - \widehat{\boldsymbol{\theta}}'_n) (\boldsymbol{\theta} - \widehat{\boldsymbol{\theta}}'_n)^\top I_{\boldsymbol{\theta}_0} \mathbf{C}}{\partial(\boldsymbol{\theta} - \widehat{\boldsymbol{\theta}}'_n) (\boldsymbol{\theta} - \widehat{\boldsymbol{\theta}}'_n)^\top}}_{=I_{\boldsymbol{\theta}_0}^\top \mathbf{C} \mathbf{C}^\top I_{\boldsymbol{\theta}_0}} \cdot \underbrace{\frac{\partial(\boldsymbol{\theta} - \widehat{\boldsymbol{\theta}}'_n) (\boldsymbol{\theta} - \widehat{\boldsymbol{\theta}}'_n)^\top}{\partial\boldsymbol{\theta}}}_{=2(\boldsymbol{\theta} - \widehat{\boldsymbol{\theta}}'_n)} \right] \end{aligned} \quad (28)$$

$$\begin{aligned} &= g(\widehat{\boldsymbol{\theta}}'_n) (-n I_{\boldsymbol{\theta}_0} (\boldsymbol{\theta} - \widehat{\boldsymbol{\theta}}'_n)) \left[-(\boldsymbol{\theta} - \widehat{\boldsymbol{\theta}}'_n)^\top I_{\boldsymbol{\theta}_0} \mathbf{C} + \frac{1}{2n} \mathbf{C}^\top \left(n \left(I_{\boldsymbol{\theta}_0} (\boldsymbol{\theta} - \widehat{\boldsymbol{\theta}}'_n) (\boldsymbol{\theta} - \widehat{\boldsymbol{\theta}}'_n)^\top I_{\boldsymbol{\theta}_0} \right) - I_{\boldsymbol{\theta}_0} \right) \mathbf{C} \right] \\ &+ g(\widehat{\boldsymbol{\theta}}'_n) \left[-I_{\boldsymbol{\theta}_0} \mathbf{C} + I_{\boldsymbol{\theta}_0} \mathbf{C} \mathbf{C}^\top I_{\boldsymbol{\theta}_0} (\boldsymbol{\theta} - \widehat{\boldsymbol{\theta}}'_n) \right]. \end{aligned} \quad (29)$$

Set Eq. (29) equal to 0, then

$$\begin{aligned} 0 &= n I_{\boldsymbol{\theta}_0} (\boldsymbol{\theta} - \widehat{\boldsymbol{\theta}}'_n) (\boldsymbol{\theta} - \widehat{\boldsymbol{\theta}}'_n)^\top I_{\boldsymbol{\theta}_0} \mathbf{C} + \frac{1}{2} I_{\boldsymbol{\theta}_0} (\boldsymbol{\theta} - \widehat{\boldsymbol{\theta}}'_n) \mathbf{C}^\top I_{\boldsymbol{\theta}_0} \mathbf{C} \\ &- \frac{n}{2} I_{\boldsymbol{\theta}_0} (\boldsymbol{\theta} - \widehat{\boldsymbol{\theta}}'_n) \mathbf{C}^\top I_{\boldsymbol{\theta}_0} (\boldsymbol{\theta} - \widehat{\boldsymbol{\theta}}'_n) (\boldsymbol{\theta} - \widehat{\boldsymbol{\theta}}'_n)^\top I_{\boldsymbol{\theta}_0} \mathbf{C} - I_{\boldsymbol{\theta}_0} \mathbf{C} + I_{\boldsymbol{\theta}_0} \mathbf{C} \underbrace{\mathbf{C}^\top I_{\boldsymbol{\theta}_0} (\boldsymbol{\theta} - \widehat{\boldsymbol{\theta}}'_n)}_{=c} \end{aligned} \quad (30)$$

$$\begin{aligned} &= nc I_{\boldsymbol{\theta}_0} (\boldsymbol{\theta} - \widehat{\boldsymbol{\theta}}'_n) + \frac{1}{2} I_{\boldsymbol{\theta}_0} (\boldsymbol{\theta} - \widehat{\boldsymbol{\theta}}'_n) \mathbf{C}^\top I_{\boldsymbol{\theta}_0} \mathbf{C} - \frac{nc^2}{2} I_{\boldsymbol{\theta}_0} (\boldsymbol{\theta} - \widehat{\boldsymbol{\theta}}'_n) + (c-1) I_{\boldsymbol{\theta}_0} \mathbf{C} \\ &= \left(nc - \frac{nc^2}{2} + \frac{\mathbf{C}^\top I_{\boldsymbol{\theta}_0} \mathbf{C}}{2} \right) I_{\boldsymbol{\theta}_0} (\boldsymbol{\theta} - \widehat{\boldsymbol{\theta}}'_n) + (c-1) I_{\boldsymbol{\theta}_0} \mathbf{C}. \end{aligned} \quad (31)$$

Plug in $\boldsymbol{\theta} - \widehat{\boldsymbol{\theta}}'_n = \mathbf{d}$ and $\boldsymbol{\theta} - \widehat{\boldsymbol{\theta}}'_n \approx \boldsymbol{\theta} - (\widehat{\boldsymbol{\theta}}_n + \frac{\mathbf{c}}{n} + o(n^{-1})) = -\frac{\mathbf{c}}{n} - \mathbf{d} + o(n^{-1})$ and define two constants,

$$c_1 = \mathbf{C}^\top I_{\boldsymbol{\theta}_0} \mathbf{d} \quad (32)$$

$$c_2 \approx -\mathbf{C}^\top I_{\boldsymbol{\theta}_0} \left(\frac{\mathbf{C}}{n} + \mathbf{d} + o(n^{-1}) \right) = -\frac{1}{n} \underbrace{\mathbf{C}^\top I_{\boldsymbol{\theta}_0} \mathbf{C}}_{=a} - c_1. \quad (33)$$

and plug Eqs (32) and (33) into Eq. (31), we have

$$\left(nc_1 - \frac{nc_1^2}{2} + \frac{\mathbf{C}^\top I_{\boldsymbol{\theta}_0} \mathbf{C}}{2} \right) I_{\boldsymbol{\theta}_0} \mathbf{d} = (1 - c_1) I_{\boldsymbol{\theta}_0} \mathbf{C} \quad (34)$$

$$\left(nc_2 - \frac{nc_2^2}{2} + \frac{\mathbf{C}^\top I_{\boldsymbol{\theta}_0} \mathbf{C}}{2} \right) I_{\boldsymbol{\theta}_0} \left(\frac{\mathbf{C}}{n} + \mathbf{d} \right) = (1 - c_2) I_{\boldsymbol{\theta}_0} \mathbf{C}. \quad (35)$$

Taking the difference between Eq. (34) and Eq. (35), we have

$$\begin{aligned} (c_2 - c_1)I_{\theta_0}\mathbf{C} &= \left(n(c_1 - c_2) + \frac{n(c_2 - c_1)(c_2 + c_1)}{2} \right) I_{\theta_0}\mathbf{d} - \left(c_2 - \frac{c_2^2}{2} + \frac{\mathbf{C}^\top I_{\theta_0}\mathbf{C}}{2n} \right) I_{\theta_0}\mathbf{C} \\ &\triangleq n(c_2 - c_1) \left(-1 + \frac{(c_2 + c_1)}{2} \right) I_{\theta_0}\mathbf{d} - \left(c_2 - \frac{c_2^2}{2} + \frac{a}{2n} \right) I_{\theta_0}\mathbf{C}, \text{ where } a \triangleq \mathbf{C}^\top I_{\theta_0}\mathbf{C} \end{aligned} \quad (36)$$

$$\Rightarrow -\left(\frac{a}{n} + 2c_1\right)I_{\theta_0}\mathbf{C} = -n\left(\frac{a}{n} + 2c_1\right) \left(-1 - \frac{a}{2n}\right) I_{\theta_0}\mathbf{d} - \left(c_2 - \frac{c_2^2}{2} + \frac{a}{2n}\right) I_{\theta_0}\mathbf{C} \quad (37)$$

$$\Rightarrow (2c_1 - \frac{a}{2n})a = n\left(\frac{a}{n} + 2c_1\right) \left(-1 - \frac{a}{2n}\right) c_1 + \left(-\frac{a}{n} - c_1 - \frac{(-\frac{a}{n} - c_1)^2}{2}\right) a \quad (38)$$

$$\Rightarrow \left(\frac{3a}{2} + 2n\right) c_1^2 - \left(2a + \frac{3a^2}{2n}\right) c_1 + \frac{a^3}{2n^2} - 2a - \frac{a^2}{2n} = 0. \quad (39)$$

c_1 can be solved analytically from Eq. (39)

$$\begin{aligned} \Delta &= \left(2a + \frac{3a^2}{2n}\right)^2 - 4\left(\frac{3a}{2} + 2n\right) \left(\frac{a^3}{2n^2} - 2a - \frac{a^2}{2n}\right) \\ &= 4a^2 + \frac{9a^4}{4n^2} + \frac{6a^3}{n} - 4\left(\frac{3a^4}{4n^2} - 3a^2 - \frac{3a^3}{4n} + \frac{a^3}{n} - 4an - a^2\right) \\ &= 4a^2 + \frac{9a^4}{4n^2} + \frac{6a^3}{n} + 16a^2 + 16an - \frac{a^3}{n} + \frac{3a^4}{n^2} \\ &= 16an + 20a^2 + \frac{21a^4}{4n^2} - \frac{5a^3}{n} \end{aligned} \quad (40)$$

$$\begin{aligned} c_1 &= -(\mathbf{x}'_n - \mathbf{x}_n)^\top I_{\theta_0}\mathbf{d} \\ &= \frac{\left(2a + \frac{3a^2}{2n}\right) \pm \sqrt{\Delta}}{4n + 3a} = \frac{\left(2a + \frac{3a^2}{2n}\right) \pm \sqrt{16an + 20a^2 + \frac{21a^4}{4n^2} - \frac{5a^3}{n}}}{4n + 3a} \approx \frac{a}{2n} \pm \sqrt{\frac{a}{n}}. \end{aligned} \quad (41)$$

Plug Eq. (41) into Eq. (24), we can have

$$\begin{aligned} G(n) &= (2\pi)^{-\frac{p}{2}} \sqrt{\frac{n^p}{\det(I_{\theta_0}^{-1})}} \left| g(\hat{\boldsymbol{\theta}}_n) - g(\hat{\boldsymbol{\theta}}'_n) \right|_{\boldsymbol{\theta} = \hat{\boldsymbol{\theta}}'_n = \mathbf{d}} \\ &\approx (2\pi)^{-\frac{p}{2}} \sqrt{\frac{n^p}{\det(I_{\theta_0}^{-1})}} \exp\left(-\frac{n}{2}\mathbf{d}^\top I_{\theta_0}\mathbf{d}\right) \cdot \left| -\mathbf{d}^\top I_{\theta_0}\mathbf{C} + \frac{1}{2n}\mathbf{C}^\top (nI_{\theta_0}\mathbf{d}\mathbf{d}^\top I_{\theta_0} - I_{\theta_0})\mathbf{C} \right| \\ &= (2\pi)^{-\frac{p}{2}} \sqrt{\frac{n^p}{\det(I_{\theta_0}^{-1})}} \exp\left(-\frac{n}{2}\mathbf{d}^\top I_{\theta_0}\mathbf{d}\right) \left| -c_1 + \frac{c_1^2}{2} - \frac{a}{2n} \right| \\ &= (2\pi)^{-\frac{p}{2}} \sqrt{\frac{n^p}{\det(I_{\theta_0}^{-1})}} \exp\left(-\frac{nc_1^2}{2} ([\mathbf{C}^\top I_{\theta_0}]^{-1})^\top I_{\theta_0} [\mathbf{C}^\top I_{\theta_0}]^{-1}\right) \left| -c_1 + \frac{c_1^2}{2} - \frac{a}{2n} \right| \end{aligned}$$

$$\begin{aligned}
&= (2\pi)^{-\frac{p}{2}} \sqrt{\frac{n^p}{\det(I_{\theta_0}^{-1})}} \exp\left(-\frac{nc_1^2}{2} \underbrace{[I_{\theta_0} \mathbf{C}]^{-1} [\mathbf{C}^\top]^{-1}}_{=a^{-1}}\right) \left| -c_1 + \frac{c_1^2}{2} - \frac{a}{2n} \right| \\
&= (2\pi)^{-\frac{p}{2}} \sqrt{\frac{n^p}{\det(I_{\theta_0}^{-1})}} \exp\left(-\frac{nc_1^2}{2a}\right) \left| -c_1 + \frac{c_1^2}{2} - \frac{a}{2n} \right| \tag{42}
\end{aligned}$$

$$\approx (2\pi)^{-\frac{p}{2}} \sqrt{\frac{n^p}{\det(I_{\theta_0}^{-1})}} \exp\left(-\frac{1}{2} + \mathcal{O}(n^{-1/2})\right) \left| \sqrt{\frac{a}{n}} + \mathcal{O}(n^{-1}) \right| \tag{43}$$

$$= n^{\frac{p-1}{2}} (2\pi)^{-\frac{p}{2}} \sqrt{\frac{\mathbf{C}^\top I_{\theta_0} \mathbf{C}}{\det(I_{\theta_0}^{-1})}} \exp\left(-\frac{1}{2} + \mathcal{O}(n^{-1/2})\right) + \mathcal{O}(n^{-1/2}) \tag{44}$$

A.2 Proof of Theorem 5

Proof. H_p and H'_p , the histograms with bin width h represented in probability based on m samples of θ , are discretized probability distribution estimates for $f_{\theta|\mathbf{x}}$ and $f_{\theta|\mathbf{x}'}$, respectively. The ℓ_1 distance between H_p and H'_p is $\|H_p - H'_p\|_1 = 2\text{TVD}_{H_p, H'_p} = 2 \sup_{b \in \{1, \dots, B\}} |p_b - p'_b|$, where TVD stands for total variation distance, $p_b = \Pr(\theta \in \text{bin } b \text{ in } H_p)$, and $p'_b = \Pr(\theta \in \text{bin } b \text{ in } H'_p)$. The ℓ_1 global sensitivity of the histogram with one-record change in \mathbf{x} is given by $\Delta_H = \max_{d(\mathbf{x}, \mathbf{x}')=1} \|H_p - H'_p\|_1 = 2 \max_{d(\mathbf{x}, \mathbf{x}')=1} \sup_{b \in \{1, \dots, B\}} |p_b - p'_b| \leq 2 \sup_{d(\mathbf{x}, \mathbf{x}')=1, b \in \{1, \dots, B\}} |p_b - p'_b|$. Since $p_b = f_{\theta|\mathbf{x}}(\xi_b)h$ and $p'_b = f_{\theta|\mathbf{x}'}(\xi'_b)h$ per the mean value theorem, where $\xi'_b \approx \xi_b \in \Lambda_b$ if h is small enough, $|p_b - p'_b| = |f_{\theta|\mathbf{x}}(\xi_b) - f_{\theta|\mathbf{x}'}(\xi_b)|h$, which is $\leq Gh$. Thus $\Delta_{H_p} = 2Gh$ and $\Delta_H = 2mGh$, where H is the histogram represented in frequencies/counts. \square

A.3 Proof of Theorem 6

Proof. Let \mathcal{M} denote the PRECISE procedure in Alg. 2; and we use $\theta_{(q)}^*$ and $\theta_{([qm])}^*$ interchangeably to denote the PP q^{th} sample quantile in this section.

First, we can expand the Mean Squared Error (MSE) between the sanitized q^{th} posterior sample quantile $\theta_{([qm])}^*$ and the population posterior quantile $F_{\theta|\mathbf{x}}^{-1}(q)$ as

$$\begin{aligned}
&\mathbb{E}_{\theta} \mathbb{E}_{\mathcal{M}|\theta} \left(\theta_{([qm])}^* - F_{\theta|\mathbf{x}}^{-1}(q) \right)^2 = \mathbb{E}_{\theta} \mathbb{E}_{\mathcal{M}|\theta} \left(\theta_{([qm])}^* - \theta_{([qm])} + \theta_{([qm])} - F_{\theta|\mathbf{x}}^{-1}(q) \right)^2 \\
&= \mathbb{E}_{\theta} \mathbb{E}_{\mathcal{M}|\theta} \left(\theta_{([qm])}^* - \theta_{([qm])} \right)^2 + \mathbb{E}_{\theta} \mathbb{E}_{\mathcal{M}|\theta} \left(\theta_{([qm])} - F_{\theta|\mathbf{x}}^{-1}(q) \right)^2 \\
&\quad + 2\mathbb{E}_{\theta} \mathbb{E}_{\mathcal{M}|\theta} \left(\theta_{([qm])}^* - \theta_{([qm])} \right) \left(\theta_{([qm])} - F_{\theta|\mathbf{x}}^{-1}(q) \right) \\
&\leq \mathbb{E}_{\theta} \mathbb{E}_{\mathcal{M}|\theta} \left(\theta_{([qm])}^* - \theta_{([qm])} \right)^2 + \mathbb{E}_{\theta} \mathbb{E}_{\mathcal{M}|\theta} \left(\theta_{([qm])} - F_{\theta|\mathbf{x}}^{-1}(q) \right)^2 \\
&\quad + 2\sqrt{\mathbb{E}_{\theta} \mathbb{E}_{\mathcal{M}|\theta} \left(\theta_{([qm])}^* - \theta_{([qm])} \right)^2 \mathbb{E}_{\theta} \mathbb{E}_{\mathcal{M}|\theta} \left(\theta_{([qm])} - F_{\theta|\mathbf{x}}^{-1}(q) \right)^2}. \tag{45}
\end{aligned}$$

The last inequality in Eq. (45) holds per the Cauchy-Schwarz inequality. Per Theorem 1 in

Walker (1968), sample quantiles are asymptotically Gaussian, that is

$$\sqrt{m} \left(\theta_{([qm])} - F_{\theta|\mathbf{x}}^{-1}(q) \right) \xrightarrow{d} \mathcal{N} \left(0, q(1-q) \cdot \left(f_{\theta|\mathbf{x}} \left(F_{\theta|\mathbf{x}}^{-1}(q) \right) \right)^{-2} \right), \quad (46)$$

based on which, we obtain the following result for the second square term in Eq. (45),

$$\mathbb{E}_{\theta} \mathbb{E}_{\mathcal{M}|\theta} \left(\theta_{([qm])} - F_{\theta|\mathbf{x}}^{-1}(q) \right)^2 = \mathbb{E}_{\theta} \left(\theta_{([qm])} - F_{\theta|\mathbf{x}}^{-1}(q) \right)^2 \rightarrow \frac{q(1-q)}{m} \cdot \left(f_{\theta|\mathbf{x}} \left(F_{\theta|\mathbf{x}}^{-1}(q) \right) \right)^{-2}. \quad (47)$$

Next we upper bound the term $\mathbb{E}_{\theta} \mathbb{E}_{\mathcal{M}|\theta} \left(\theta_{([qm])}^* - \theta_{([qm])} \right)^2$ in Eq. (45). We first show the bias introduced by the truncation at 0 (step 8 Alg. 2) decays exponentially as $\varepsilon \rightarrow \infty$. For $\forall b \in \{0, \dots, B' + 1\}$,

$$\begin{aligned} \mathbb{E}_{\mathcal{M}|\theta} (c_b^*) &= \int_{-\infty}^{\infty} \max\{0, c_b + x\} \frac{\varepsilon}{2} e^{-\varepsilon|x|} dx = 0 + \int_{-c_b}^{\infty} (c_b + x) \frac{\varepsilon}{2} e^{-\varepsilon|x|} dx \\ &= \int_{-c_b}^0 (c_b + x) \frac{\varepsilon}{2} e^{\varepsilon x} dx + \int_0^{\infty} (c_b + x) \frac{\varepsilon}{2} e^{-\varepsilon x} dx \\ &= \frac{\varepsilon c_b}{2} \int_{-c_b}^0 e^{\varepsilon x} dx + \frac{\varepsilon}{2} \int_{-c_b}^0 x e^{\varepsilon x} dx + \frac{\varepsilon c_b}{2} \int_0^{\infty} e^{-\varepsilon x} dx + \frac{\varepsilon}{2} \int_0^{\infty} x e^{-\varepsilon x} dx \\ &= \frac{c_b}{2} (1 - e^{-\varepsilon c_b}) + \frac{1}{2} \left(c_b e^{-\varepsilon c_b} - \frac{1}{\varepsilon} (1 - e^{-\varepsilon c_b}) \right) + \frac{c_b}{2} + \frac{1}{2\varepsilon} \\ &= c_b + \frac{e^{-\varepsilon c_b}}{2\varepsilon}. \end{aligned} \quad (48)$$

Then, we calculate the second moment for c_b^* in a similar manner

$$\begin{aligned} \mathbb{E}_{\mathcal{M}|\theta} (c_b^{*2}) &= \int_{-\infty}^{\infty} (\max\{0, c_b + x\})^2 \frac{\varepsilon}{2} e^{-\varepsilon|x|} dx = 0 + \int_{-c_b}^{\infty} (c_b + x)^2 \frac{\varepsilon}{2} e^{-\varepsilon|x|} dx \\ &= \int_{-c_b}^0 (c_b^2 + x^2 + 2c_b x) \frac{\varepsilon}{2} e^{\varepsilon x} dx + \int_0^{\infty} (c_b^2 + x^2 + 2c_b x) \frac{\varepsilon}{2} e^{-\varepsilon x} dx \\ &= \frac{\varepsilon c_b^2}{2} \int_{-c_b}^0 e^{\varepsilon x} dx + \frac{\varepsilon}{2} \int_{-c_b}^0 x^2 e^{\varepsilon x} dx + \varepsilon c_b \int_{-c_b}^0 x e^{\varepsilon x} dx \\ &\quad + \frac{\varepsilon c_b^2}{2} \int_0^{\infty} e^{-\varepsilon x} dx + \frac{\varepsilon}{2} \int_0^{\infty} x^2 e^{-\varepsilon x} dx + \varepsilon c_b \int_0^{\infty} x e^{-\varepsilon x} dx \\ &= \frac{c_b^2}{2} (1 - e^{-\varepsilon c_b}) - \frac{c_b^2}{2} e^{-\varepsilon c_b} - \left(\frac{c_b}{\varepsilon} e^{-\varepsilon c_b} - \frac{1}{\varepsilon^2} (1 - e^{-\varepsilon c_b}) \right) + \frac{c_b^2}{2} + \frac{1}{\varepsilon^2} + \frac{c_b}{\varepsilon} \\ &\quad + c_b \left(c_b e^{-\varepsilon c_b} - \frac{1}{\varepsilon} (1 - e^{-\varepsilon c_b}) \right) \\ &= c_b^2 + \frac{2}{\varepsilon^2} - \frac{e^{-\varepsilon c_b}}{\varepsilon^2}. \end{aligned} \quad (49)$$

Given Eqs (48) and (49), we are ready to show the MSE consistency of c_b^* for c_b over sanit-

zation, that is, $\mathbb{E}_{\mathcal{M}|\theta}(c_b^* - c_b)^2 \rightarrow 0$. For $\forall b \in \{0, \dots, B' + 1\}$,

$$\begin{aligned}\mathbb{E}_{\mathcal{M}|\theta}((c_b^* - c_b)^2) &= \mathbb{E}_{\mathcal{M}|\theta}(c_b^{*2}) - 2c_b\mathbb{E}_{\mathcal{M}|\theta}(c_b^*) + c_b^2 \\ &= c_b^2 + \frac{2}{\varepsilon^2} - \frac{e^{-\varepsilon c_b}}{\varepsilon^2} - 2c_b\left(c_b + \frac{e^{-\varepsilon c_b}}{2\varepsilon}\right) + c_b^2 \\ &= \frac{2}{\varepsilon^2} - \frac{e^{-\varepsilon c_b}}{\varepsilon^2} - \frac{c_b e^{-\varepsilon c_b}}{\varepsilon} = \mathcal{O}(\varepsilon^{-2}).\end{aligned}\quad (50)$$

In addition, we derive the variance for c_b^* for later use,

$$\begin{aligned}\mathbb{V}_{\mathcal{M}|\theta}(c_b^*) &= \mathbb{E}_{\mathcal{M}|\theta}(c_b^{*2}) - (\mathbb{E}_{\mathcal{M}|\theta}(c_b^*))^2 = c_b^2 + \frac{2}{\varepsilon^2} - \frac{e^{-\varepsilon c_b}}{\varepsilon^2} - \left(c_b + \frac{e^{-\varepsilon c_b}}{2\varepsilon}\right)^2 \\ &= \frac{2 - e^{-\varepsilon c_b} - e^{-2\varepsilon c_b}/4}{\varepsilon^2} - \frac{c_b e^{-\varepsilon c_b}}{\varepsilon}.\end{aligned}\quad (51)$$

Let $g(b) = |\sum_{i \leq b} c_i - qm|$ and $g^*(b) = |\sum_{i \leq b} c_i^* - qm^*|$, where $m^* = \sum_{b=0}^{B'+1} c_b^*$ in step 1 of Alg. 2. Let \hat{b} be the true index of bin for $\theta_{(qm)}$, i.e., $\theta_{(qm)} \in I_{\hat{b}}$, where $\hat{b} = \min\{\arg \min_{b \in \{0, \dots, B'+1\}} g(b)\}$. We prove $\mathbb{E}_{\mathcal{M}|\theta}(b^* - b)^2 \rightarrow 0$, where $b^* = \min\{\arg \min_{b \in \{0, \dots, B'+1\}} g^*(b)\}$, by first showing the squared error between the functions, from which b and b^* are solved, converges to 0 as $\varepsilon \rightarrow \infty$; that is

$$\mathbb{E}_{\mathcal{M}|\theta}(g^*(b) - g(b))^2 = \mathbb{E}_{\mathcal{M}|\theta}\left(\left|\sum_{i \leq b} c_i^* - qm^*\right| - \left|\sum_{i \leq b} c_i - qm\right|\right)^2 \rightarrow 0. \quad (52)$$

Per definition of m^* , $m^* = \sum_{i \leq b} c_i^* + \sum_{i \geq b+1} c_i^*$ for $\forall b \in \{0, \dots, B' + 1\}$, then

$$\begin{aligned}\mathbb{E}_{\mathcal{M}|\theta}\left(\sum_{i \leq b} c_i^* - qm^*\right)^2 &= \mathbb{E}_{\mathcal{M}|\theta}\left((1-q)\sum_{i \leq b} c_i^* - q\sum_{i \geq b+1} c_i^*\right)^2 \\ &= (1-q)^2\mathbb{E}_{\mathcal{M}|\theta}\left(\sum_{i \leq b} c_i^*\right)^2 + q^2\mathbb{E}_{\mathcal{M}|\theta}\left(\sum_{i \geq b+1} c_i^*\right)^2 - 2q(1-q)\mathbb{E}_{\mathcal{M}|\theta}\left(\sum_{i \leq b} c_i^*\right)\mathbb{E}_{\mathcal{M}|\theta}\left(\sum_{i \geq b+1} c_i^*\right) \quad (53) \\ &= (1-q)^2\left(\mathbb{V}_{\mathcal{M}|\theta}\left(\sum_{i \leq b} c_i^*\right) + \left(\sum_{i \leq b} \mathbb{E}_{\mathcal{M}|\theta}(c_i^*)\right)^2\right) + q^2\left(\mathbb{V}_{\mathcal{M}|\theta}\left(\sum_{i \geq b+1} c_i^*\right) + \left(\sum_{i \geq b+1} \mathbb{E}_{\mathcal{M}|\theta}(c_i^*)\right)^2\right) \\ &\quad - 2q(1-q)\left(\sum_{i \leq b} \left(c_i + \frac{e^{-\varepsilon c_i}}{2\varepsilon}\right)\right)\left(\sum_{i \geq b+1} \left(c_i + \frac{e^{-\varepsilon c_i}}{2\varepsilon}\right)\right) \quad (54) \\ &= (1-q)^2\left(\sum_{i \leq b} \left(\frac{2 - e^{-\varepsilon c_i} - e^{-2\varepsilon c_i}/4}{\varepsilon^2} - \frac{c_i e^{-\varepsilon c_i}}{\varepsilon}\right) + \left(\sum_{i \leq b} \left(c_i + \frac{e^{-\varepsilon c_i}}{2\varepsilon}\right)\right)^2\right) \\ &\quad + q^2\left(\sum_{i \geq b+1} \left(\frac{2 - e^{-\varepsilon c_i} - e^{-2\varepsilon c_i}/4}{\varepsilon^2} - \frac{c_i e^{-\varepsilon c_i}}{\varepsilon}\right) + \left(\sum_{i \geq b+1} \left(c_i + \frac{e^{-\varepsilon c_i}}{2\varepsilon}\right)\right)^2\right)\end{aligned}$$

$$-2q(1-q) \left(\sum_{i \leq b} \left(c_i + \frac{e^{-\varepsilon c_i}}{2\varepsilon} \right) \right) \left(\sum_{i \geq b+1} \left(c_i + \frac{e^{-\varepsilon c_i}}{2\varepsilon} \right) \right) \quad (55)$$

$$= \left((1-q) \sum_{i \leq b} c_i - q \sum_{i \geq b+1} c_i \right)^2 + \mathcal{O}(\varepsilon^{-2}) = \left(\sum_{i \leq b} c_i - qm \right)^2 + \mathcal{O}(\varepsilon^{-2}). \quad (56)$$

Eq. (53) holds since noises are drawn independently from the DP mechanism for sanitizing each bin count in the histogram (e.g. Lap(1/ε)); and Eqs (54) and (55) follow after plugging in Eqs (48) and (51).

Based on Eq. (56), expanding the LHS of Eq. (52) and leveraging the fact that $|X| \geq X$, and $\mathbb{E}(|X|) \geq \mathbb{E}(X)$, we have

$$\begin{aligned} & \mathbb{E}_{\mathcal{M}|\theta} \left(\left| \sum_{i \leq b} c_i^* - qm^* \right| - \left| \sum_{i \leq b} c_i - qm \right| \right)^2 \\ &= \mathbb{E}_{\mathcal{M}|\theta} \left(\sum_{i \leq b} c_i^* - qm^* \right)^2 + \left(\sum_{i \leq b} c_i - qm \right)^2 - 2 \underbrace{\left| \sum_{i \leq b} c_i - qm \right|}_{\geq (\sum_{i \leq b} c_i - qm)} \cdot \underbrace{\mathbb{E}_{\mathcal{M}|\theta} \left(\left| \sum_{i \leq b} c_i^* - qm^* \right| \right)}_{\geq \mathbb{E}_{\mathcal{M}|\theta} (\sum_{i \leq b} c_i^* - qm^*)} \\ &\leq 2 \left(\sum_{i \leq b} c_i - qm \right)^2 + \mathcal{O}(\varepsilon^{-2}) - 2 \left(\sum_{i \leq b} c_i - qm \right) \cdot \mathbb{E}_{\mathcal{M}|\theta} \left((1-q) \sum_{i \leq b} c_i^* - q \sum_{i \geq b+1} c_i^* \right) \\ &= 2 \left(\sum_{i \leq b} c_i - qm \right)^2 - 2 \left(\sum_{i \leq b} c_i - qm \right) \cdot \left((1-q) \left(\sum_{i \leq b} \left(c_i + \frac{e^{-\varepsilon c_i}}{2\varepsilon} \right) \right) - q \left(\sum_{i \geq b+1} \left(c_i + \frac{e^{-\varepsilon c_i}}{2\varepsilon} \right) \right) \right) + \mathcal{O}(\varepsilon^{-2}) \\ &= 2 \left(\sum_{i \leq b} c_i - qm \right)^2 - 2 \left(\sum_{i \leq b} c_i - qm \right) \cdot \left(\sum_{i \leq b} c_i - qm + \mathcal{O} \left(\frac{B' e^{-m\varepsilon/B'}}{\varepsilon} \right) \right) + \mathcal{O}(\varepsilon^{-2}) \\ &= \mathcal{O} \left(\varepsilon^{-2} + \frac{e^{-\sqrt{n}\varepsilon}}{h\sqrt{n}\varepsilon} \right). \end{aligned} \quad (57)$$

The last equality in Eq. (57) holds because of the following: given h , we require $m = (2G(n)h)^{-1}$ for DP guarantees in Eq. (7) by setting $\Delta_H = 1$. Denote the “local” bounds for the histogram H after bin collapsing by (l, u) , we can conclude that $B' = (u - l)/h = 2Gm(u - l)$. Per the Bernstein-von Mises theorem, as $n \rightarrow \infty$,

$$\sqrt{n} \cdot \theta | X \xrightarrow{d} \mathcal{N}(\hat{\theta}_n, I_{\theta_0}^{-1}),$$

where $\hat{\theta}_n$ is the MLE and I_{θ_0} is the Fisher information. Therefore, $u - l \asymp n^{-1/2}$, and $m/B' \asymp \sqrt{n}$.

All taken together, it is proved that the MSE consistency of $|\sum_{i \leq b} c_i^* - qm^*|$ for $|\sum_{i \leq b} c_i - qm|$ for $\forall b \in \{1, \dots, B'\}$ at the rate of $O(\varepsilon^{-2} + e^{-\sqrt{n}\varepsilon}/(h\sqrt{n}\varepsilon))$. Per the assumption of $h =$

$\Omega(e^{-\sqrt{n}\varepsilon}/\sqrt{n})$, the rate can be further simplified,

$$\mathcal{O}\left(\varepsilon^{-2} + \frac{e^{-\sqrt{n}\varepsilon}}{h\sqrt{n}\varepsilon}\right) = \mathcal{O}(\varepsilon^{-1}). \quad (58)$$

Additionally, we show that $g(b)$ is Lipschitz continuous as following. $\forall b, b' \in \{0, \dots, B' + 1\}$, without loss of generality, assume $b > b'$

$$\begin{aligned} |g(b') - g(b)| &= \left| \left| \sum_{i \leq b} c_i - qm \right| - \left| \sum_{i \leq b'} c_i - qm \right| \right| \\ &\leq \left| \left(\sum_{i \leq b} c_i - qm \right) - \left(\sum_{i \leq b'} c_i - qm \right) \right| = \left| \sum_{i=b'+1}^b c_i \right| \leq (b - b') \max_i |c_i| \leq |b - b'| \cdot m. \end{aligned} \quad (59)$$

Combined with the uniqueness of b^* and \hat{b} , we can conclude $\mathbb{E}_{\mathcal{M}|\theta} (b^* - \hat{b})^2 \rightarrow 0$ at the rate of at least $\mathcal{O}(\varepsilon^{-1})$. Per step 3 of Alg. 2, $\theta_{([qm])}^* \sim \text{Unif}(I_{b^*})$, where $I_{b^*} = [L + (b^* - 1)h, L + b^*h]$ and $h = [2G(n)m]^{-1}$, then

$$\begin{aligned} \theta_{([qm])}^* - (L + (b^* - 1)h) &\sim \text{Unif}[0, h]; \quad \theta_{([qm])} - (L + (\hat{b} - 1)h) \sim \text{Unif}[0, h]. \\ \text{Let } V_1, V_2 &\sim \text{Unif}[0, h], \text{ independent of } b^* \text{ and } \hat{b} \Rightarrow \begin{cases} \theta_{([qm])}^* = (L + (b^* - 1)h) + V_1 \\ \theta_{([qm])} = (L + (\hat{b} - 1)h) + V_2 \end{cases}; \\ \mathbb{E}_{\mathcal{M}|\theta} (\theta_{([qm])}^* - \theta_{([qm])})^2 &= \mathbb{E}_{\mathcal{M}|\theta} \left((b^* - \hat{b})h + (V_1 - V_2) \right)^2 \\ &= h^2 \mathbb{E}_{\mathcal{M}|\theta} (b^* - \hat{b})^2 + \mathbb{E}_{\mathcal{M}|\theta} (V_1 - V_2)^2 + 2h \mathbb{E}_{\mathcal{M}|\theta} \left((b^* - \hat{b})(V_1 - V_2) \right) \\ &= h^2 \mathbb{E}_{\mathcal{M}|\theta} (b^* - \hat{b})^2 + \frac{2h^2}{3} - 2 \cdot \frac{h}{2} \cdot \frac{h}{2} \\ &= h^2 \mathbb{E}_{\mathcal{M}|\theta} (b^* - \hat{b})^2 + \frac{h^2}{6} = \mathcal{O}(m^{-2}) + \mathcal{O}(m^{-2}\varepsilon^{-1}). \end{aligned} \quad (60)$$

Plugging Eqs (47) and (60) into Eq. (45), we have

$$\begin{aligned} \mathbb{E}_{\theta} \mathbb{E}_{\mathcal{M}|\theta} (\theta_{(q)}^* - F_{\theta|\mathbf{x}}^{-1}(q))^2 &= \mathbb{E}_{\theta} \mathbb{E}_{\mathcal{M}|\theta} \left(\theta_{([qm])}^* - F_{\theta|\mathbf{x}}^{-1}(q) \right)^2 \\ &\leq \mathcal{O}(m^{-1} + m^{-2} + m^{-1/2}m^{-1}) = \mathcal{O}(m^{-1}) = \mathcal{O}(h). \end{aligned} \quad (61)$$

□

A.4 Proof of Proposition 7

Proof. Data $\mathbf{x} \sim f(X|\theta_0)$. Per the definition of $F_{\theta|\mathbf{x}}^{-1}(q) = \inf\{\theta: F(\theta|\mathbf{x}) \geq q\}$, where $0 < q < 1$,

$$\Pr \left(F_{\theta|\mathbf{x}}^{-1} \left(\frac{\alpha}{2} \right) \leq \theta_0 \leq F_{\theta|\mathbf{x}}^{-1} \left(1 - \frac{\alpha}{2} \right) \mid \mathbf{x} \right)$$

$$\begin{aligned}
&= \Pr\left(\theta_0 \leq F_{\theta|\mathbf{x}}^{-1}\left(1 - \frac{\alpha}{2}\right) \mid \mathbf{x}\right) - \Pr\left(\theta_0 \leq F_{\theta|\mathbf{x}}^{-1}\left(\frac{\alpha}{2}\right) \mid \mathbf{x}\right) \\
&= F_{\theta|\mathbf{x}}\left(F_{\theta|\mathbf{x}}^{-1}\left(1 - \frac{\alpha}{2}\right)\right) - F_{\theta|\mathbf{x}}\left(F_{\theta|\mathbf{x}}^{-1}\left(\frac{\alpha}{2}\right)\right) = 1 - \alpha.
\end{aligned} \tag{62}$$

Following Eq. (61), as $n \rightarrow \infty$ or $\varepsilon \rightarrow \infty$

$$\Pr\left(\theta_{\left(\lfloor \frac{\alpha}{2} m \rfloor\right)}^* \leq \theta_0 \leq \theta_{\left(\lfloor (1 - \frac{\alpha}{2}) m \rfloor\right)}^* \mid \mathbf{x}\right) \rightarrow \Pr\left(F_{\theta|\mathbf{x}}^{-1}\left(\frac{\alpha}{2}\right) \leq \theta_0 \leq F_{\theta|\mathbf{x}}^{-1}\left(1 - \frac{\alpha}{2}\right) \mid \mathbf{x}\right) = 1 - \alpha. \tag{63}$$

□

A.5 Proof of Theorem 8

Algorithm S.1: PrivateQuantile of ε -DP (Smith, 2011)

input : data $\mathbf{x} = \{x_i\}_{i=1}^n$, privacy loss parameter ε , quantile $q \in (0, 1)$, global bounds $(L_{\mathbf{x}}, U_{\mathbf{x}})$ for \mathbf{x} .

output: PP q^{th} quantile estimate $x_{\lfloor qn \rfloor}^*$ of ε -DP.

- 1 Sort \mathbf{x} in ascending order $x_{(1)}, \dots, x_{(n)}$;
 - 2 Replace $x_i < L_{\mathbf{x}}$ with L and $x_i > U_{\mathbf{x}}$ with $U_{\mathbf{x}}$;
 - 3 For $i = 0, \dots, n$, define $y_i \triangleq (x_{(i+1)} - x_{(i)}) \exp(-\varepsilon|i - qn|/2)$;
 - 4 Sample an integer $i^* \in \{0, \dots, n\}$ with probability $y_i / (\sum_{i=0}^n y_i)$;
 - 5 Draw $x_{\lfloor qn \rfloor}^*$ from $\text{Unif}(x_{(i^*)}, x_{(i^*+1)})$.
-

Assumption S.1. Let $x_{(1)} \leq x_{(2)} \leq \dots \leq x_{(n)}$ be the order statistics of a random sample x_1, \dots, x_n from a continuous distribution $f_{\mathbf{x}}$, and $F_{\mathbf{x}}^{-1}(q) = \inf\{x : F_{\mathbf{x}}(x) \geq q\}$ be the unique quantile at q , where $0 < q < 1$ and $F_{\mathbf{x}}$ is the CDF. Assume $f_{\mathbf{x}}$ is positive, finite, and continuous at $F_{\mathbf{x}}^{-1}(q)$.

Lemma S.2 (Asymptotic distribution of the spacing between two consecutive order statistics). Let $\mathbf{x} = (x_1, \dots, x_n)$ be a sample from a continuous distribution $f_{\mathbf{x}}$, and $x_{\lfloor qn \rfloor}$ be the sample quantile at q and $x_{\lfloor qn \rfloor + 1}$ be the value immediately succeeding $x_{\lfloor qn \rfloor}$. Given the regularity conditions in Assumption S.1,

$$n \cdot (x_{\lfloor qn \rfloor + 1} - x_{\lfloor qn \rfloor}) \cdot f_{\mathbf{x}}(F_{\mathbf{x}}^{-1}(q)) \xrightarrow{d} \exp(1) \text{ as } n \rightarrow \infty. \tag{64}$$

Proof. Given a sample $X = (x_1, \dots, x_n)$, since $\lim_{n \rightarrow \infty} \lfloor qn \rfloor / n = q \in (0, 1)$, per Thm. 3 in (Smirnov, 1949),

$$x_{\lfloor qn \rfloor} \xrightarrow{a.s.} F_{\mathbf{x}}^{-1}(q) \text{ as } n \rightarrow \infty \tag{65}$$

at rate $n^{-1/2}$. Let $y_{\lfloor qn \rfloor}$ be the $\lfloor qn \rfloor^{\text{th}}$ order statistic in a random sample of size n from $\text{Uni}(0, 1)$. From Eq. (65), it follows that $y_{\lfloor qn \rfloor + 1} - y_{\lfloor qn \rfloor} \xrightarrow{a.s.} 0$ as $n \rightarrow \infty$. Then, per Lemma 1 in (Nagaraja et al., 2015),

$$n \cdot (y_{\lfloor qn \rfloor + 1} - y_{\lfloor qn \rfloor}) \xrightarrow{d} \exp(1), \tag{66}$$

where $\exp(1)$ represents an exponential random variable with rate parameter 1.

In addition, $\forall 1 \leq i \leq n$, $x_{(i)} \stackrel{d}{=} F_{\mathbf{x}}^{-1}(y_{(i)})$. Then

$$\begin{aligned} (x_{([qn]+1)} - x_{([qn])}) &\stackrel{d}{=} F_{\mathbf{x}}^{-1}(y_{([qn]+1)}) - F_{\mathbf{x}}^{-1}(y_{([qn])}), \\ n \cdot (x_{([qn]+1)} - x_{([qn])}) &\stackrel{d}{=} \frac{F_{\mathbf{x}}^{-1}(y_{([qn]+1)}) - F_{\mathbf{x}}^{-1}(y_{([qn])})}{(y_{([qn]+1)} - y_{([qn])})} \cdot n \cdot (y_{([qn]+1)} - y_{([qn])}), \end{aligned} \quad (67)$$

where $\stackrel{d}{=}$ stands for “equal in distribution”, meaning two random variables have the same distribution. Per the definition of pdf and the assumptions around $f_{\mathbf{x}}$,

$$\frac{F_{\mathbf{x}}^{-1}(y_{([qn]+1)}) - F_{\mathbf{x}}^{-1}(y_{([qn])})}{(y_{([qn]+1)} - y_{([qn])})} \xrightarrow{a.s.} \frac{1}{f_{\mathbf{x}}(F_{\mathbf{x}}^{-1}(q))}. \quad (68)$$

Plugging Eqns (66) and (68) into Eq. (67), along with Slutsky’s Theorem, we have

$$\begin{aligned} n \cdot (x_{([qn]+1)} - x_{([qn])}) &\xrightarrow{d} (f_{\mathbf{x}}(F_{\mathbf{x}}^{-1}(q)))^{-1} \exp(1), \\ \mathbb{E}[n(x_{([qn]+1)} - x_{([qn])})] &\longrightarrow (f_{\mathbf{x}}(F_{\mathbf{x}}^{-1}(q)))^{-1}, \\ \mathbb{E}[n(x_{([qn]+1)} - x_{([qn])})]^2 &\longrightarrow 2(f_{\mathbf{x}}(F_{\mathbf{x}}^{-1}(q)))^{-2}. \end{aligned} \quad (69)$$

□

Theorem S.3 (MSE consistency of PrivateQuantile in Alg. S.1). *Denote the sample data of size n by \mathbf{x} and let $x_{([qn])}^*$ be the sanitized q^{th} sample quantile of X from \mathcal{M} : PrivateQuantile of ε -DP in Alg. S.1. Under the regularity conditions in Assumption S.1, and assume that \exists constant $C \geq 0$ such that the user-provided global bounds $(L_{\mathbf{x}}, U_{\mathbf{x}})$ for \mathbf{x} satisfy $\lim_{n \rightarrow \infty} (U_{\mathbf{x}} - x_{(n)}) = \lim_{n \rightarrow \infty} (x_{(1)} - L_{\mathbf{x}}) = C$, then*

$$\mathbb{E}_{\mathbf{x}} \mathbb{E}_{\mathcal{M}|\mathbf{x}} (x_{([qn])}^* - F_{\mathbf{x}}^{-1}(q))^2 = \mathcal{O}(n^{-1}) + \mathcal{O}\left(\frac{e^{-\mathcal{O}(n\varepsilon)}}{n^{3/2}}\right) = \begin{cases} \mathcal{O}(n^{-1}) & \text{for constant } \varepsilon \\ \mathcal{O}(e^{-\mathcal{O}(\varepsilon)}) & \text{for constant } n \end{cases}. \quad (70)$$

If the PrivateQuantile procedure \mathcal{M} of ρ -zCDP is used, then

$$\mathbb{E}_{\mathbf{x}} \mathbb{E}_{\mathcal{M}|\mathbf{x}} (x_{([qn])}^* - F_{\mathbf{x}}^{-1}(q))^2 = \mathcal{O}(n^{-1}) + \mathcal{O}\left(\frac{e^{-\mathcal{O}(n\sqrt{\rho})}}{n^{3/2}}\right) = \begin{cases} \mathcal{O}(n^{-1}) & \text{for constant } \rho \\ \mathcal{O}(e^{-\mathcal{O}(\sqrt{\rho})}) & \text{for constant } n \end{cases}. \quad (71)$$

Proof. Let \mathcal{M} standards for the PrivateQuantile procedure in Alg. 2 through this section and $x_{([qn])}$ be the original sample quantile at q . Similar to proof in Appendix A.3, we first expand the MSE between the sanitized q^{th} sample quantile $x_{([qn])}^*$ and the population quantile $F_{\mathbf{x}}^{-1}(q)$ as

$$\begin{aligned} \mathbb{E}_{\mathbf{x}} \mathbb{E}_{\mathcal{M}|\mathbf{x}} (x_{([qn])}^* - F_{\mathbf{x}}^{-1}(q))^2 &= \mathbb{E}_{\mathbf{x}} \mathbb{E}_{\mathcal{M}|\mathbf{x}} (x_{([qn])}^* - x_{([qn])} + x_{([qn])} - F_{\mathbf{x}}^{-1}(q))^2 \\ &= \mathbb{E}_{\mathbf{x}} \mathbb{E}_{\mathcal{M}|\mathbf{x}} (x_{([qn])}^* - x_{([qn])})^2 + \mathbb{E}_{\mathbf{x}} \mathbb{E}_{\mathcal{M}|\mathbf{x}} (x_{([qn])} - F_{\mathbf{x}}^{-1}(q))^2 \\ &\quad + 2\mathbb{E}_{\mathbf{x}} \mathbb{E}_{\mathcal{M}|\mathbf{x}} (x_{([qn])}^* - x_{([qn])}) (x_{([qn])} - F_{\mathbf{x}}^{-1}(q)) \\ &\leq \mathbb{E}_{\mathbf{x}} \mathbb{E}_{\mathcal{M}|\mathbf{x}} (x_{([qn])}^* - x_{([qn]P}))^2 + \mathbb{E}_{\mathbf{x}} (x_{([qn])} - F_{\mathbf{x}}^{-1}(q))^2 \end{aligned}$$

$$+ 2\sqrt{\mathbb{E}_{\mathbf{x}}\mathbb{E}_{\mathcal{M}|\mathbf{x}}\left(x_{([qP])}^* - x_{([qn])}\right)^2} \mathbb{E}_{\mathbf{x}}\left(x_{([qn])} - F_{\mathbf{x}}^{-1}(q)\right)^2. \quad (72)$$

The last inequality in Eq. (72) holds per the Cauchy-Schwarz inequality. Similarly based on Thm. 1 in (Walker, 1968), we have asymptotic normality for sample quantile

$$\begin{aligned} \sqrt{n}\left(x_{([qn])} - F_{\mathbf{x}}^{-1}(q)\right) &\xrightarrow{d} \mathcal{N}\left(0, \frac{q(1-q)}{\{f_{\mathbf{x}}(F_{\mathbf{x}}^{-1}(q))\}^2}\right), \\ \Rightarrow \mathbb{E}_{\mathbf{x}}\mathbb{E}_{\mathcal{M}|\mathbf{x}}\left(x_{([qn])} - F_{\mathbf{x}}^{-1}(q)\right)^2 &= \mathbb{E}_{\mathbf{x}}\left(x_{([qn])} - F_{\mathbf{x}}^{-1}(q)\right)^2 \rightarrow \frac{n^{-1}q(1-q)}{\{f_{\mathbf{x}}(F_{\mathbf{x}}^{-1}(q))\}^2}. \end{aligned} \quad (73)$$

An intermediate step of the PrivateQuantile procedure is the sampling of index i^* via the exponential mechanism with privacy loss ε (step 4 in Alg. S.1),

$$\Pr(i^*) = \frac{(x_{(i^*+1)} - x_{(i^*)}) \exp(-\varepsilon|i^* - [qn]|/2)}{\sum_{i=0}^n (x_{(i+1)} - x_{(i)}) \exp(-\varepsilon|i - [qn]|/2)} \quad (74)$$

$$\text{where } \sum_{i=0}^n (x_{(i+1)} - x_{(i)}) \exp(-\varepsilon|i - [qn]|/2) \quad (75)$$

$$= (x_{(1)} - L_{\mathbf{x}}) \exp\left(-\frac{\varepsilon \cdot [qn]}{2}\right) + (U_{\mathbf{x}} - x_{(n)}) \exp\left(-\frac{\varepsilon|n - [qn]|}{2}\right) \quad (76)$$

$$+ \sum_{i \notin \{0, n, [qn]\}} (x_{(i+1)} - x_{(i)}) \exp(-\varepsilon|i - [qn]|/2) + (x_{([qn]+1)} - x_{([qn])}). \quad (77)$$

For $i \notin \{0, n, [qn]\}$, per Lemma S.2, $(x_{(i+1)} - x_{(i)}) \rightarrow 0$ at the rate of n^{-1} as $n \rightarrow \infty$, so the first term in Eq. (77) converges to 0 at the rate of $\mathcal{O}(n^{-1}e^{-\mathcal{O}(n\varepsilon)})$, while the second term in Eq. (77) converges to 0 at the rate of $\mathcal{O}(n^{-1})$.

Also, per the assumption that \exists constant $C \geq 0$ such that the user-provided global bounds $(L_{\mathbf{x}}, U_{\mathbf{x}})$ for \mathbf{x} satisfy $\lim_{n \rightarrow \infty} (U_{\mathbf{x}} - x_{(n)}) = \lim_{n \rightarrow \infty} (x_{(1)} - L_{\mathbf{x}}) = C$. The two terms in Eq. (76) $\approx C \cdot e^{-\mathcal{O}(n\varepsilon)}$. Therefore, as $n \rightarrow \infty$ or $\varepsilon \rightarrow \infty$,

$$\Pr(i^* = [qn]) = \frac{\mathcal{O}(n^{-1})}{\mathcal{O}(n^{-1} + n^{-1}e^{-\mathcal{O}(n\varepsilon)}) + C \cdot e^{-\mathcal{O}(n\varepsilon)}} \rightarrow 1. \quad (78)$$

$$\Rightarrow \Pr(x_{([qn])}^* \sim \text{Unif}(x_{([qn])}, x_{([qn]+1)})) \rightarrow 1. \quad (79)$$

Eqns (78) and (79) imply the limiting distribution of $x_{([qn])}^*$ is a uniform distribution from $x_{([qn])}$ to $x_{([qn]+1)}$, achieved at the rate of $e^{\mathcal{O}(n\varepsilon)}$. Define $h \triangleq x_{([qn])}^* - x_{([qn])}$, then

$$e^{\mathcal{O}(n\varepsilon)}h \xrightarrow{d} \text{Unif}(0, x_{([qn]+1)} - x_{([qn])}). \quad (80)$$

Therefore, as $n \rightarrow \infty$ or $\varepsilon \rightarrow \infty$

$$\mathbb{E}_{\mathbf{x}}\mathbb{E}_{\mathcal{M}|\mathbf{x}}\left(x_{([qn])}^* - x_{([qn])}\right)^2 = \mathbb{E}_{\mathbf{x}}\mathbb{E}_{\mathcal{M}|\mathbf{x}}(h^2) = \mathbb{E}_{\mathbf{x}}\{\mathbb{V}_{\mathcal{M}|\mathbf{x}}(h) + (\mathbb{E}_{\mathcal{M}|\mathbf{x}}(h))^2\}$$

$$\begin{aligned}
& \rightarrow e^{-\mathcal{O}(n\varepsilon)} \mathbb{E}_{\mathbf{x}} \left[\frac{(x_{([qn]+1)} - x_{([qn])})^2}{12} + \frac{(x_{([qn]+1)} - x_{([qn])})^2}{4} \right] \\
& = e^{-\mathcal{O}(n\varepsilon)} \mathbb{E}_{\mathbf{x}} \left[\frac{(x_{([qn]+1)} - x_{([qn])})^2}{3} \right] \rightarrow \frac{2 \cdot n^{-2} e^{-\mathcal{O}(n\varepsilon)}}{3(f_{\mathbf{x}}(F_{\mathbf{x}}^{-1}(q)))^2} \text{ per Eq. (69) in Lemma (S.2).} \quad (81)
\end{aligned}$$

Plugging Eqns (81) and (73) into the right-hand side of Eq. (72), we have

$$\begin{aligned}
& \mathbb{E}_{\mathbf{x}} \mathbb{E}_{\mathcal{M}|\mathbf{x}} (x_{([qn])}^* - F_{\mathbf{x}}^{-1}(q))^2 \\
& \leq \frac{2 \cdot n^{-2} e^{-\mathcal{O}(n\varepsilon)}}{3(f_{\mathbf{x}}(F_{\mathbf{x}}^{-1}(q)))^2} + \frac{n^{-1}q(1-q)}{\{f_{\mathbf{x}}(F_{\mathbf{x}}^{-1}(q))\}^2} + 2\sqrt{\frac{2 \cdot n^{-2} e^{-\mathcal{O}(n\varepsilon)}}{3(f_{\mathbf{x}}(F_{\mathbf{x}}^{-1}(q)))^2} \cdot \frac{n^{-1}q(1-q)}{\{f_{\mathbf{x}}(F_{\mathbf{x}}^{-1}(q))\}^2}} \\
& = \mathcal{O}(e^{-\mathcal{O}(n\varepsilon)} n^{-2} + n^{-1} + e^{-\mathcal{O}(n\varepsilon)} n^{-3/2}) \\
& = \mathcal{O}(n^{-1}) + \mathcal{O}\left(\frac{e^{-\mathcal{O}(n\varepsilon)}}{n^{3/2}}\right) = \begin{cases} \mathcal{O}(n^{-1}) & \text{for constant } \varepsilon \\ \mathcal{O}(e^{-\mathcal{O}(\varepsilon)}) & \text{for constant } n \end{cases}.
\end{aligned} \quad (82)$$

□

A.6 Proof of Theorem 9

We first present Lemmas S.4 and S.5 that will be used in proving Theorem 9.

Lemma S.4 (Chernoff bounds (Mitzenmacher and Upfal, 2017)). *Let $Z_i \stackrel{iid}{\sim}$ Bernoulli(p) and $Z = \sum_{i=1}^n Z_i$, then for $\delta \in [0, 1]$,*

$$\begin{aligned}
\mathbb{P}(Z \geq (1 + \delta)np) & \leq e^{-np\delta^2/3}; \\
\mathbb{P}(Z \leq (1 - \delta)np) & \leq e^{-np\delta^2/2}.
\end{aligned}$$

Lemma S.5 (sample quantile is concentrated around the population quantile). *Let $\boldsymbol{\theta} = (\theta_1, \dots, \theta_m)$ be a set of samples from posterior distribution with CDF $f_{\boldsymbol{\theta}|\mathbf{x}}$, and $F_{\boldsymbol{\theta}|\mathbf{x}}^{-1}(q) = \inf\{\theta : f_{\boldsymbol{\theta}|\mathbf{x}} \geq q\}$ where $0 < q < 1$. Assume the posterior density $f_{\boldsymbol{\theta}|\mathbf{x}}$ is continuous at $F_{\boldsymbol{\theta}|\mathbf{x}}^{-1}(q)$. Let $\eta > 0$ and $0 \leq u \leq \eta$ and $p_{\min} = \inf_{|\tau - F_{\boldsymbol{\theta}|\mathbf{x}}^{-1}(q)| \leq 2\eta} f_{\boldsymbol{\theta}|\mathbf{x}}(\tau)$, then*

$$\mathbb{P}\left(\left|\theta_{([qm])} - F_{\boldsymbol{\theta}|\mathbf{x}}^{-1}(q)\right| > u\right) \leq \begin{cases} 2 \exp(-mu^2 p_{\min}^2 / 2q) & \text{if } \frac{3}{5} < q < 1; \\ 2 \exp(-mu^2 p_{\min}^2 / 3(1-q)) & \text{if } 0 < q < \frac{3}{5}. \end{cases}$$

Proof. Let $Z_j = 1\{\theta_{(j)} > F_{\boldsymbol{\theta}|\mathbf{x}}^{-1}(q) + u\}$ and $Z = \sum_{j=1}^m Z_j$ denote the number of posterior samples larger than $F_{\boldsymbol{\theta}|\mathbf{x}}^{-1}(q) + u$. Then

$$\hat{p} = \mathbb{P}(Z_j = 1) \leq 1 - q - up_{\min}.$$

If $\theta_{(\lfloor qm \rfloor)} > F_{\theta|\mathbf{x}}^{-1}(q) + u$, then $Z \geq (1 - q)m$, therefore per Chernoff bound in Lemma S.4,

$$\begin{aligned} \mathbb{P}\left(\theta_{(\lfloor qm \rfloor)} > F_{\theta|\mathbf{x}}^{-1}(q) + u\right) &\leq \mathbb{P}(Z \geq (1 - q)m) = \mathbb{P}\left(Z \geq \left(1 + \frac{1 - q}{\hat{p}} - 1\right) m\hat{p}\right) \\ &\leq \exp\left(-\frac{m\hat{p}}{3} \left(\frac{1 - q}{\hat{p}} - 1\right)^2\right) = \exp\left(-\frac{m}{3\hat{p}} \underbrace{\left(\frac{1 - q - \hat{p}}{\hat{p}}\right)^2}_{\geq up_{\min}}\right) \\ &\leq \exp\left(-\frac{mu^2 p_{\min}^2}{3\hat{p}}\right) \leq \exp\left(-\frac{mu^2 p_{\min}^2}{3(1 - q)}\right). \end{aligned} \quad (83)$$

Similarly, let $Z'_j = 1\{\theta_j < F_{\theta|\mathbf{x}}^{-1}(q) - u\}$ and $Z' = \sum_{j=1}^m Z'_j$ denote the number of posterior samples smaller than $F_{\theta|\mathbf{x}}^{-1}(q) - u$. Then $\hat{p}' = \mathbb{P}(Z'_j = 1) \leq q - up_{\min}$. If $\theta_{(\lfloor qm \rfloor)} < F_{\theta|\mathbf{x}}^{-1}(q) - u$, then $Z' \geq qm$; therefore, per the Chernoff bound in Lemma S.4,

$$\begin{aligned} \mathbb{P}\left(\theta_{(\lfloor qm \rfloor)} < F_{\theta|\mathbf{x}}^{-1}(q) - u\right) &\leq \mathbb{P}(Z' \geq qm) = \mathbb{P}\left(Z' \leq \left(1 + \frac{q}{\hat{p}'} - 1\right) m\hat{p}'\right) \leq \exp\left(-\frac{m\hat{p}'}{2} \left(\frac{q}{\hat{p}'} - 1\right)^2\right) \\ &= \exp\left(-\frac{m}{2\hat{p}'} \underbrace{\left(\frac{q - \hat{p}'}{\hat{p}'}\right)^2}_{\geq up_{\min}}\right) \leq \exp\left(-\frac{mu^2 p_{\min}^2}{2\hat{p}'}\right) \leq \exp\left(-\frac{mu^2 p_{\min}^2}{2q}\right). \end{aligned} \quad (84)$$

If $3(1 - q) < 2q \Leftrightarrow \frac{3}{5} < q < 1$, then

$$\mathbb{P}\left(|\theta_{(\lfloor qm \rfloor)} - F_{\theta|\mathbf{x}}^{-1}(q)| > u\right) \leq 2 \exp\left(-\frac{mu^2 p_{\min}^2}{2q}\right) \leq 2 \exp\left(-\frac{mu^2 p_{\min}^2}{3(1 - q)}\right);$$

otherwise, if $0 < q < \frac{3}{5}$,

$$\mathbb{P}\left(|\theta_{(\lfloor qm \rfloor)} - F_{\theta|\mathbf{x}}^{-1}(q)| > u\right) \leq 2 \exp\left(-\frac{mu^2 p_{\min}^2}{3(1 - q)}\right) \leq 2 \exp\left(-\frac{mu^2 p_{\min}^2}{2q}\right).$$

□

We now can move onto the proof of Theorem 9.

Proof. Since $\theta_{(q)} = \theta_{(\lfloor qm \rfloor)}$ and $\theta_{(q)}^* = \theta_{(\lfloor qm \rfloor)}^*$, we use the notations interchangeably for the non-private and PP q^{th} sample quantiles. The proof is inspired by Asi and Duchi (2020), with substantial extensions to address our specific problem.

First, we divide the interval $[\theta_{(k)} - \eta, \theta_{(k)} + \eta]$ into blocks of size u : $I_1, I_2, \dots, I_{2\eta/u}$. Let N_i denote the number of elements in I_i . We also define the following three events:

$$\begin{aligned} A &= \{\forall i, N_i \geq (m + 1)up_{\min}/2\}; \\ B &= \{|\theta_{(k)} - F_{\theta|\mathbf{x}}^{-1}(q)| \leq \eta/2\}; \\ D &= \{|\theta_{(\lfloor qm \rfloor)} - F_{\theta|\mathbf{x}}^{-1}(q)| \leq \eta/2\}. \end{aligned}$$

Recall that $k = \arg \min_{j \in \{0, 1, \dots, m+1\}} |\theta_{(j)} - F_{\theta|\mathbf{x}}^{-1}(q)|$ as defined in Alg. 3, thus $|\theta_{(k)} - F_{\theta|\mathbf{x}}^{-1}(q)| \leq |\theta_{(\lfloor qm \rfloor)} - F_{\theta|\mathbf{x}}^{-1}(q)| \Rightarrow D \subset B \Rightarrow \mathbb{P}(D) \leq \mathbb{P}(B) \Rightarrow \mathbb{P}(D^c) \geq \mathbb{P}(B^c)$.

Next, we derive a lower bound for $\mathbb{P}(A|B)$:

$$\mathbb{P}(A|B) \geq \mathbb{P}(A|B)\mathbb{P}(B) = \mathbb{P}(A) - \mathbb{P}(A|B^c)\mathbb{P}(B^c) \geq \mathbb{P}(A) - \mathbb{P}(B^c) \geq \mathbb{P}(A) - \mathbb{P}(D^c). \quad (85)$$

For $\mathbb{P}(D^c)$, per Lemma S.5,

$$\mathbb{P}(D^c) \leq 2 \exp\left(-\frac{m\eta^2 p_{\min}^2}{12(1-q)}\right). \quad (86)$$

For $\mathbb{P}(A)$, we first let $Z_j = 1\{\theta_{(j)} \in I_i\}$, then $N_i = \sum_{j=0}^m Z_j$. As $\hat{p} = \mathbb{P}(Z_j = 1) \geq up_{\min}$, per the Chernoff bound in Lemma S.4,

$$\begin{aligned} \mathbb{P}\left(N_i < \frac{(m+1)up_{\min}}{2}\right) &= \mathbb{P}\left(N_i < (m+1)\hat{p}\left(1 - \left(1 - \frac{up_{\min}}{2\hat{p}}\right)\right)\right) \\ &\leq \exp\left(-\frac{(m+1)\hat{p}}{2}\left(\underbrace{1 - \frac{up_{\min}}{2\hat{p}}}_{\geq 1/2}\right)^2\right) \leq \exp\left(-\frac{(m+1)up_{\min}}{8}\right). \end{aligned} \quad (87)$$

By taking a union bound across all blocks,

$$\mathbb{P}(A^c) \leq \frac{2\eta}{u} \exp\left(-\frac{(m+1)up_{\min}}{8}\right), \quad (88)$$

and thus

$$\mathbb{P}(A) \geq 1 - \frac{2\eta}{u} \exp\left(-\frac{(m+1)up_{\min}}{8}\right). \quad (89)$$

Plug Eqs. (86) and (89) into the RHS of Eq. (85),

$$\begin{aligned} \mathbb{P}(A|B) &\geq 1 - \frac{2\eta}{u} \exp\left(-\frac{(m+1)up_{\min}}{8}\right) - 2 \exp\left(-\frac{m\eta^2 p_{\min}^2}{12(1-q)}\right), \\ \Rightarrow \mathbb{P}(A^c|B) &\leq \frac{2\eta}{u} \exp\left(-\frac{(m+1)up_{\min}}{8}\right) + 2 \exp\left(-\frac{m\eta^2 p_{\min}^2}{12(1-q)}\right). \end{aligned} \quad (90)$$

Next, we establish the following inequality for later use. For any event E ,

$$\begin{aligned} \mathbb{P}(E) &= \mathbb{P}(E|A \cap B)\mathbb{P}(A \cap B) + \mathbb{P}(E|(A \cap B)^c)\mathbb{P}((A \cap B)^c) \\ &\leq \mathbb{P}(E|A \cap B) + \mathbb{P}((A \cap B)^c) \\ &= \mathbb{P}(E|A \cap B) + \mathbb{P}(A^c \cup B^c) \\ &= \mathbb{P}(E|A \cap B) + \mathbb{P}(B^c) + \mathbb{P}(A^c) - \mathbb{P}(A^c \cap B^c) \\ &= \mathbb{P}(E|A \cap B) + \mathbb{P}(B^c) + \mathbb{P}(A^c \cap B) \\ &\leq \mathbb{P}(E|A \cap B) + \mathbb{P}(B^c) + \mathbb{P}(A^c|B) \end{aligned}$$

$$\leq \mathbb{P}(E|A \cap B) + \mathbb{P}(D^c) + \mathbb{P}(A^c|B). \quad (91)$$

If both events A and B occur, then for any $\theta_{(j^*)}$ such that $|\theta_{(j^*)} - \theta_{(k)}| > 2u$, there are at least $(m+1)up_{\min}/2$ elements between $\theta_{(k)}$ and $\theta_{(j^*)}$. This implies that $|j^* - k| \geq (m+1)up_{\min}/2$. Therefore, if $C(m, \varepsilon) \triangleq \sum_{i=0}^m (\theta_{(i+1)} - \theta_{(i)}) \cdot \exp(-\frac{\varepsilon}{2(m+1)}|i - k|)$,

$$\exp\left(-\frac{\varepsilon}{2(m+1)}|j^* - k|\right) \leq \exp\left(-\frac{\varepsilon(m+1)up_{\min}}{4(m+1)}\right) = \exp\left(-\frac{\varepsilon up_{\min}}{4}\right) \quad (92)$$

$$\Rightarrow \mathbb{P}(j^*|A, B) \leq \frac{\theta_{(j^*+1)} - \theta_{(j^*)}}{C(m, \varepsilon)} \exp\left(-\frac{\varepsilon up_{\min}}{4}\right). \quad (93)$$

Let $j_{\max}^* \triangleq \arg \min_j \{\theta_{(j)} - \theta_{(k)} > 2u\}$ and $j_{\min}^* \triangleq \arg \max_j \{\theta_{(j)} - \theta_{(k)} < -2u\}$. Then,

$$\sum_{|\theta_{(j^*)} - \theta_{(k)}| > 2u} \mathbb{P}(j^*|A, B) \leq \frac{e^{-\varepsilon up_{\min}/4}}{C(m, \varepsilon)} (U - \theta_{(j_{\max}^*)} + \theta_{(j_{\min}^*)} - L).$$

WLOG, assume $2k \leq m+1$, let $s = \min_{i \in \{0, 1, \dots, m\}} (\theta_{(i+1)} - \theta_{(i)})$ and $\xi = \exp(-\frac{\varepsilon}{2(m+1)})$,

$$\begin{aligned} C(m, \varepsilon) &= \sum_{i=0}^m (\theta_{(i+1)} - \theta_{(i)}) \cdot \exp\left(-\frac{\varepsilon}{2(m+1)}|i - k|\right) \\ &\geq s (1 + 2\xi + 2\xi^2 + 2\xi^3 + \dots + 2\xi^{k-1} + 2\xi^k + \xi^{k+1} + \dots + \xi^{m-k}) \\ &\geq s \left(1 + 2\frac{\xi(1 - \xi^k)}{1 - \xi} + \frac{\xi^{k+1}(1 - \xi^{m-2k})}{1 - \xi}\right) \\ &= s \frac{1 + \xi - \xi^{k+1} - \xi^{m-k+1}}{1 - \xi}. \end{aligned} \quad (94)$$

Since $\theta_{(j_{\max}^*)} - \theta_{(j_{\min}^*)} = \theta_{(j_{\max}^*)} - \theta_{(k)} + \theta_{(k)} - \theta_{(j_{\min}^*)} > 4u$,

$$\begin{aligned} \sum_{|\theta_{(j^*)} - \theta_{(k)}| > 2u} \mathbb{P}(j^*|A, B) &\leq \frac{e^{-\varepsilon up_{\min}/4}}{C(m, \varepsilon)} (U - \theta_{(j_{\max}^*)} + \theta_{(j_{\min}^*)} - L) \\ &\leq \frac{U - L - 4u}{s} \cdot \frac{1 - \xi}{1 + \xi - \xi^{k+1} - \xi^{m-k+1}} \cdot \exp\left(-\frac{\varepsilon up_{\min}}{4}\right). \end{aligned} \quad (95)$$

Using the inequality in Eq. (91),

$$\Pr\left(\left|\theta_{(q)}^* - \theta_{(k)}\right| > 2u\right) = \Pr\left(\left|\theta_{([qm])}^* - \theta_{(k)}\right| > 2u\right) \leq \sum_{|\theta_{(j^*)} - \theta_{(k)}| > 2u} \mathbb{P}(j^*|A, B) + \mathbb{P}(D^c) + \mathbb{P}(A^c|B),$$

and plugging in Eqns (86), (90), and (95) to the RHS of the above inequality, we have

$$\Pr\left(\left|\theta_{(q)}^* - \theta_{(k)}\right| > 2u\right) \leq \frac{U - L - 4u}{s} \cdot \frac{1 - \xi}{1 + \xi - \xi^{k+1} - \xi^{m-k+1}} \cdot \exp\left(-\frac{\varepsilon up_{\min}}{4}\right) \quad (96)$$

$$+ \frac{2\eta}{u} \exp\left(-\frac{(m+1)up_{\min}}{8}\right) + 2 \exp\left(-\frac{m\eta^2 p_{\min}^2}{12(1-q)}\right). \quad (97)$$

□

Proposition S.6. *Under the conditions of Theorem 9, the probability of PPquantile in Alg. 3 selecting the correct index $[qm]$ is*

$$\Pr(j^* = [qm]) \leq \left(1 + \frac{(U - \theta_{(m)} + \theta_{(1)} - L) + s \cdot (m - 2)}{\theta_{([qm]+1)} - \theta_{([qm])}} \cdot e^{-\varepsilon}\right)^{-1}. \quad (98)$$

Proof. The probability of selecting the correct index $[qm]$ in Alg. 3 is $\Pr(j^* = [qm]) = (\theta_{([qm]+1)} - \theta_{([qm])})/C(m, \varepsilon)$, where

$$C(m, \varepsilon) = (\theta_{(1)} - L) \exp\left(-\frac{\varepsilon \cdot [qm]}{2(m+1)}\right) + (U - \theta_{(m)}) \exp\left(-\frac{\varepsilon |m - [qm]|}{2(m+1)}\right) \quad (99)$$

$$+ \sum_{i \notin \{0, m, [qm]\}} (\theta_{(j+1)} - \theta_{(j)}) \exp(-\varepsilon |j - [qm]|/2(m+1)) + (\theta_{([qm]+1)} - \theta_{([qm])}) \quad (100)$$

$$\geq (U - \theta_{(m)} + \theta_{(1)} - L) \cdot e^{-c_1 \cdot \varepsilon} + s \cdot (m - 2) \cdot e^{-c_2 \cdot \varepsilon} + (\theta_{([qm]+1)} - \theta_{([qm])}) \quad (101)$$

for $c_1, c_2 \in (0, 1)$. Therefore,

$$\Pr(j^* = [qm]) \leq \left(1 + \frac{(U - \theta_{(m)} + \theta_{(1)} - L)}{\theta_{([qm]+1)} - \theta_{([qm])}} \cdot e^{-c_1 \cdot \varepsilon} + \frac{s \cdot (m - 2)}{\theta_{([qm]+1)} - \theta_{([qm])}} \cdot e^{-c_2 \cdot \varepsilon}\right)^{-1} \quad (102)$$

$$\leq \left(1 + \frac{(U - \theta_{(m)} + \theta_{(1)} - L) + s \cdot (m - 2)}{\theta_{([qm]+1)} - \theta_{([qm])}} \cdot e^{-\varepsilon}\right)^{-1} \quad (103)$$

(L, U) need to be chosen carefully in practice. First, (L, U) should cover the spread of the posterior samples so as not to bias the posterior distribution or clip the true posterior quantiles. On the other hand, Loose (L, U) leads to large $U - \theta_{(m)} + \theta_{(1)} - L$ and small $\Pr(j^* = [qm])$, resulting in inaccurate estimation of j^* . Given the randomness of posterior sampling, especially when m is not large, $\theta_{(m)}, \theta_{(1)}, s$, and $\theta_{([qm]+1)} - \theta_{([qm])}$ can vary significantly across different sets of posterior samples, making a precise calibration of (L, U) even more important, without compromising privacy.

□

B Experiment details

B.1 Hyperparameters and code

All the PPIE methods require specification of the global bounds $(L_{\mathbf{x}}, U_{\mathbf{x}})$ for data \mathbf{x} for the population mean & variance case. We set $(L_{\mathbf{x}} = -4, U_{\mathbf{x}} = 4)$ for $\mathbf{x} \sim \mathcal{N}(0, 1)$ and $(L_{\mathbf{x}} = 0, U_{\mathbf{x}} = 25)$ for $X \sim \text{Pois}(10)$ so that $\Pr(L_{\mathbf{x}} \leq x_i \leq U_{\mathbf{x}}) \geq 99.99\%$. For the Bernoulli

case, \mathbf{x} is 0 or 1 and thus naturally bounded. The hyperparameters for the method to be compared with PRECISE in the simulation studies are listed below.

- **SYMQ**: The code is located [here](#). We set the number of parametric bootstrap sample sets at 500.
- **PB**: The code is located [here](#). We set the number of parametric bootstraps sample sets at 500. We also identified and corrected a bug in the original code of OLS, where ε is supposed to be split into 3 portions – that is, `np.random.laplace(0, Delta_w/eps/3, 1)` in the original code should be replaced by `np.random.laplace(0, Delta_w/(eps/3), 1)`.
- **repro**: The code is located [here](#). We set the number of repro samples $R = 200$.
- **deconv**: The code is located [here](#): we used $B = \max\{2000\mu^2, 2000\}$, where B is the number of bootstrap samples and μ is the privacy loss in μ -GDP.
- **Aug.MCMC**: The code is located [here](#). The prior for β is $\mathcal{N}_{p+1}(\mu, \tau^2 I_{p+1})$, where $\mu = 0.5, \tau = 1$ for $n = 100$ and $\mu = 1, \tau = 0.25$ for $n = 1000$. We run 10,000 iterations per MCMC chain and with a 5,000 burn-in period.
- **MS**: We set the number of multiple syntheses at 3.
- **BLBquant**: BLBquant involve multiple hyperparameters. Readers may refer to the original paper on what each hyperparameter is. In terms of their values in our experiments, we set the multipliers $c = 3, K = 14$ to be more risk averse as suggested by authors. The other hyperparameters follow the settings in the original paper, specifically $R = 50$, the number of Monte Carlo iterations for each little bootstrap $m_{\text{boot}} = \min\{10000, \max\{100, n^{1.5}/(s \log(n))\}\}$, the number of partitions of the dataset $s = \lfloor K \log(n)/\varepsilon_{(q)} \rfloor$, where $\varepsilon_{(q)} = 0.5\varepsilon$, where ε is the total privacy loss, and the sequence of sets $I_t = [-tc/\sqrt{n}, tc/\sqrt{n}]$ for $t = 1, 2, \dots$

B.2 Sensitivity of LS linear regression coefficients

The MS implementation in the linear regression simulation study is based on sanitized $\hat{\beta} = (\mathbf{X}'\mathbf{X})^{-1}(\mathbf{X}'\mathbf{y})$. To that end, we sanitize $(\mathbf{X}'\mathbf{X})$ and $(\mathbf{X}'\mathbf{y})$, respectively, the sensitivities of which are provided below. Let $\|\mathbf{x}_i\|_2 = (\sum_{j=1}^{p-1} x_j^2)^{1/2} \leq 1$ (no intercept) for any $p \geq 1$ and $|y_i| \leq C_Y$ for every $i = 1, \dots, n$. In the simulation study, $C_Y = 4$. For the substitution neighboring relationship between datasets D_1 and D_2 , WLOG, assuming the last data points $(\mathbf{x}'_{1n}, y_{1n})$ and $(\mathbf{x}'_{2n}, y_{2n})$ differ between D_1 and D_2 , then

$$\begin{aligned} \Delta(\mathbf{X}'\mathbf{y}) &= \sup \left\| \sum_i \mathbf{x}'_{1i} y_{1i} - \sum_i \mathbf{x}'_{2i} y_{2i} \right\|_2 = \sup \|\mathbf{x}'_{1n} y_{1n} - \mathbf{x}'_{2n} y_{2n}\|_2 \\ &\leq 2 \sup_{\mathbf{x}', y} \|\mathbf{x}' y\|_2 \leq 2 \sup_{\mathbf{x}', y} \|\mathbf{x}'\|_2 \cdot \|y\|_2 = 2C_Y, \end{aligned}$$

where the first inequality holds due to triangle inequality and second is built upon Cauchy-Schwarz inequality; and

$$\begin{aligned}
\Delta(\mathbf{X}'\mathbf{X}) &= \sup_{\mathbf{x}', \mathbf{x}} \left\| \sum_i \mathbf{x}'_{1i} \mathbf{x}_{1i} - \sum_i \mathbf{x}'_{2i} \mathbf{x}_{2i} \right\|_F = \sup_{\mathbf{x}', \mathbf{x}} \left\| \mathbf{x}'_{1n} \mathbf{x}_{1n} - \mathbf{x}'_{2n} \mathbf{x}_{2n} \right\|_F \\
&\leq 2 \sup_{\mathbf{x}', \mathbf{x}} \left\| \mathbf{x}' \mathbf{x} \right\|_F = 2 \sup_{\mathbf{x}', \mathbf{x}} \left(1 + 2 \sum_{j=1}^{p-1} x_j^2 + 2 \sum_{j=1}^{p-1} x_j^2 x_{j'}^2 + \sum_{j=1}^{p-1} x_j^4 \right) \\
&\text{since } \left\| \mathbf{x}_i \right\|_2^4 = \left(\sum_{j=1}^{p-1} x_j^2 \right)^2 \leq 2 \sum_{j=1}^{p-1} x_j^2 x_{j'}^2 + \sum_{j=1}^{p-1} x_j^4 \leq 1, \text{ then} \\
\Delta(\mathbf{X}'\mathbf{X}) &= 2 \left(1 + 2 \sup_{\mathbf{x}', \mathbf{x}} \left(\sum_{j=1}^{p-1} x_j^2 \right) + \sup_{\mathbf{x}', \mathbf{x}} \left(2 \sum_{j=1}^{p-1} x_j^2 x_{j'}^2 + \sum_{j=1}^{p-1} x_j^4 \right) \right) \leq 2(1 + 2 + 1) = 8.
\end{aligned}$$

After the sensitivities are derived, $\hat{\beta}$ can be sanitized as in $(\mathbf{x}'\mathbf{x} + \mathbf{e}_x)$ and $(\mathbf{x}'\mathbf{y} + \mathbf{e}_y)$, where \mathbf{e}_x and \mathbf{e}_y are samples drawn independently from either a Laplace distribution or a Gaussian distribution, depending on the DP mechanism.

C Additional experimental results

This section presents results for μ -GDP as a supplement to the ε -DP results shown in Figures 2 to S.6 in Section 4.1.2, the trends and the performances of methods are similar to those observed under ε -DP.

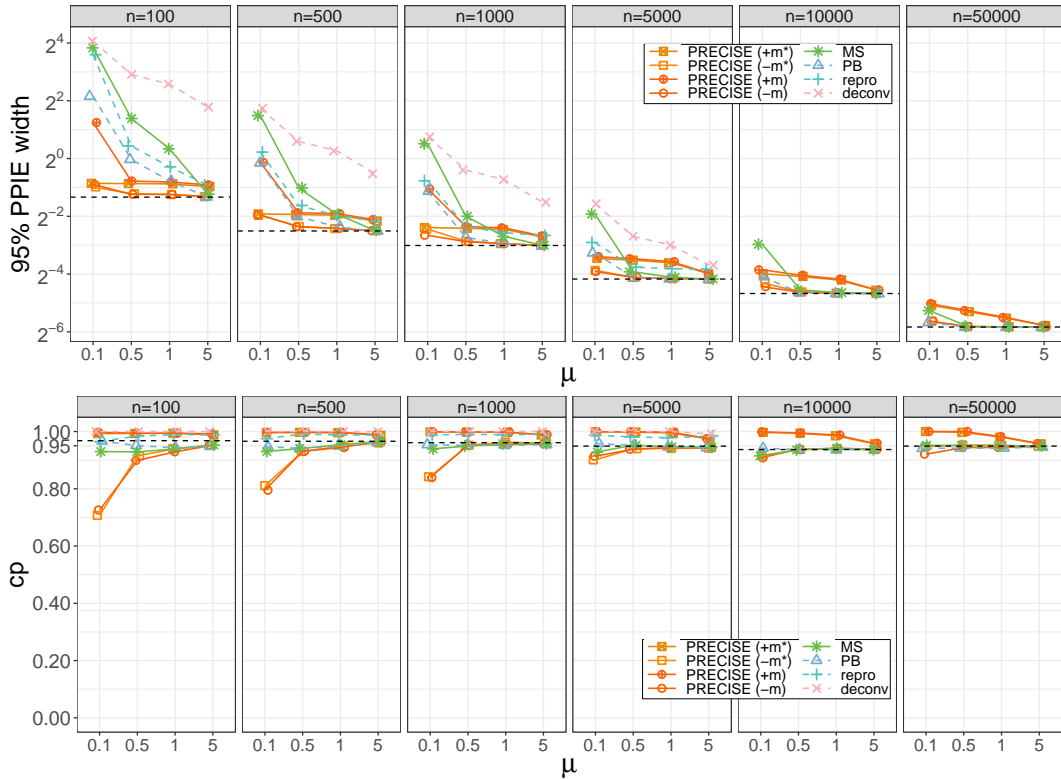


Figure S.2: PPIE width and CP for Gaussian mean (μ -GDP).

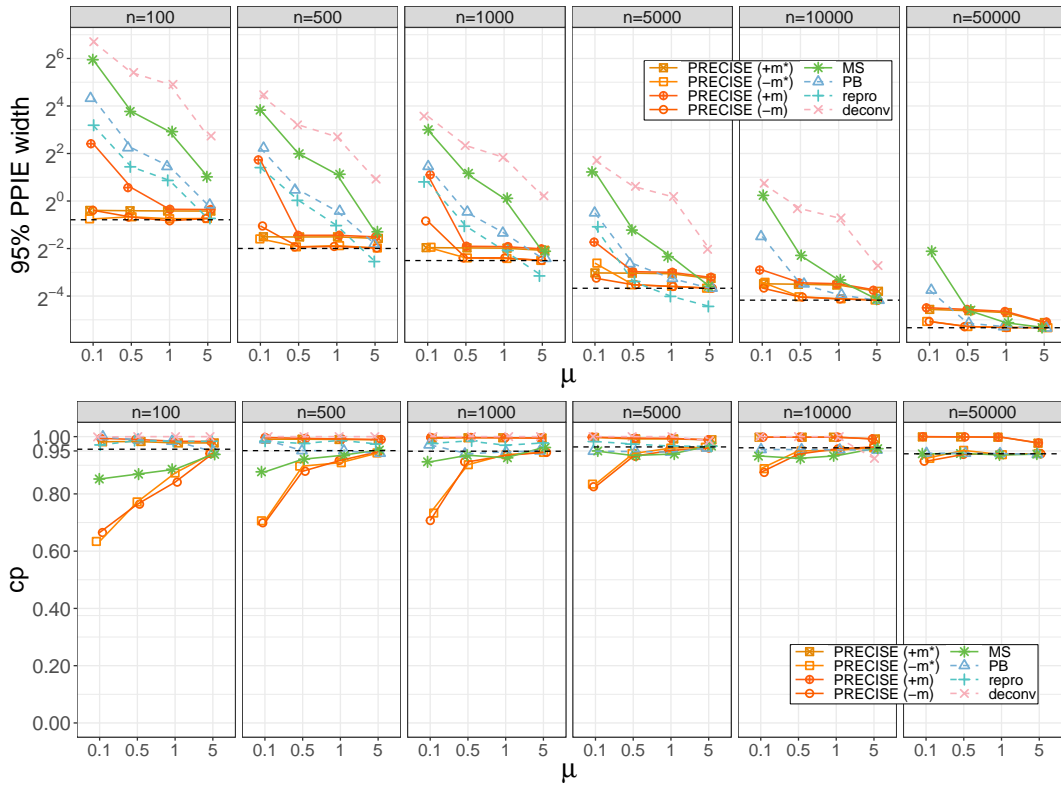


Figure S.3: PPIE width and CP for Gaussian variance (μ -GDP).

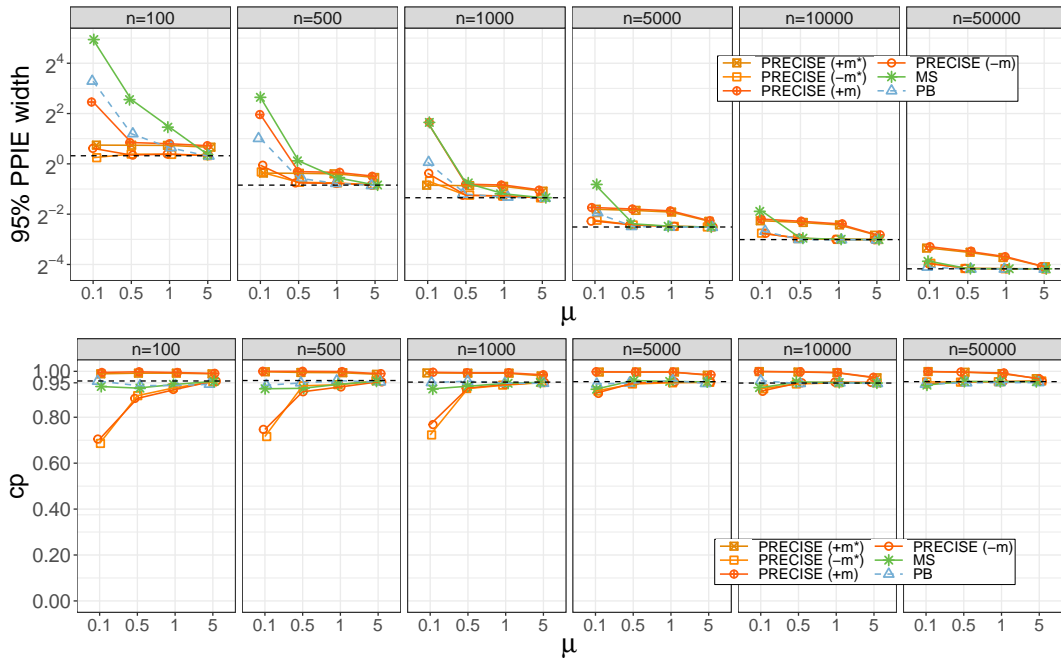


Figure S.4: PPIE width and CP for Poisson mean (μ -GDP).

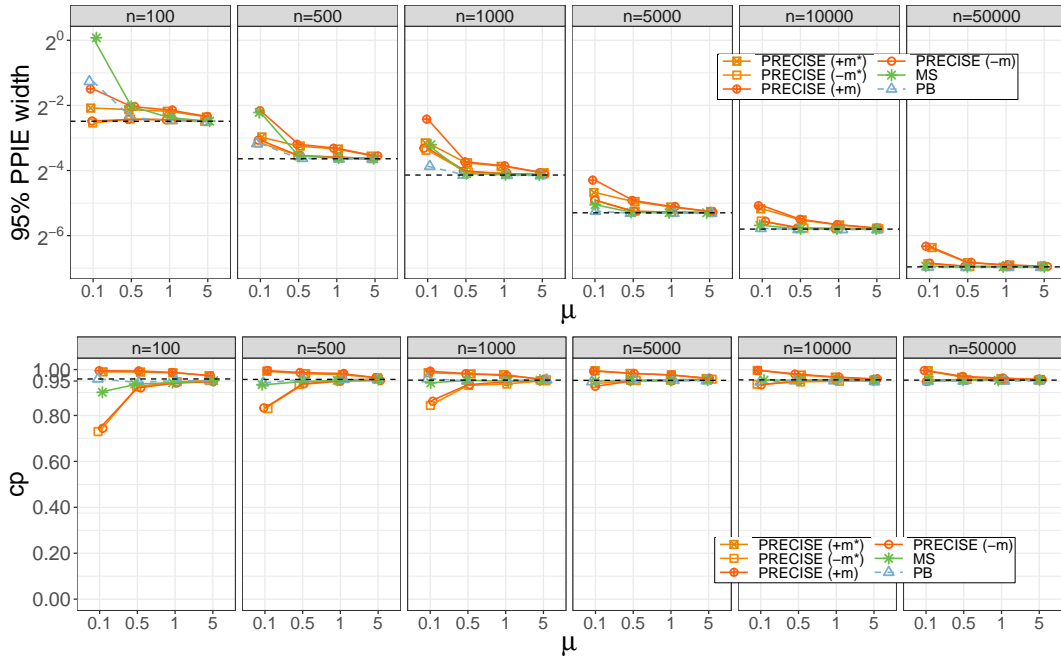


Figure S.5: PPIE width and CP for Bernoulli proportion (μ -GDP).

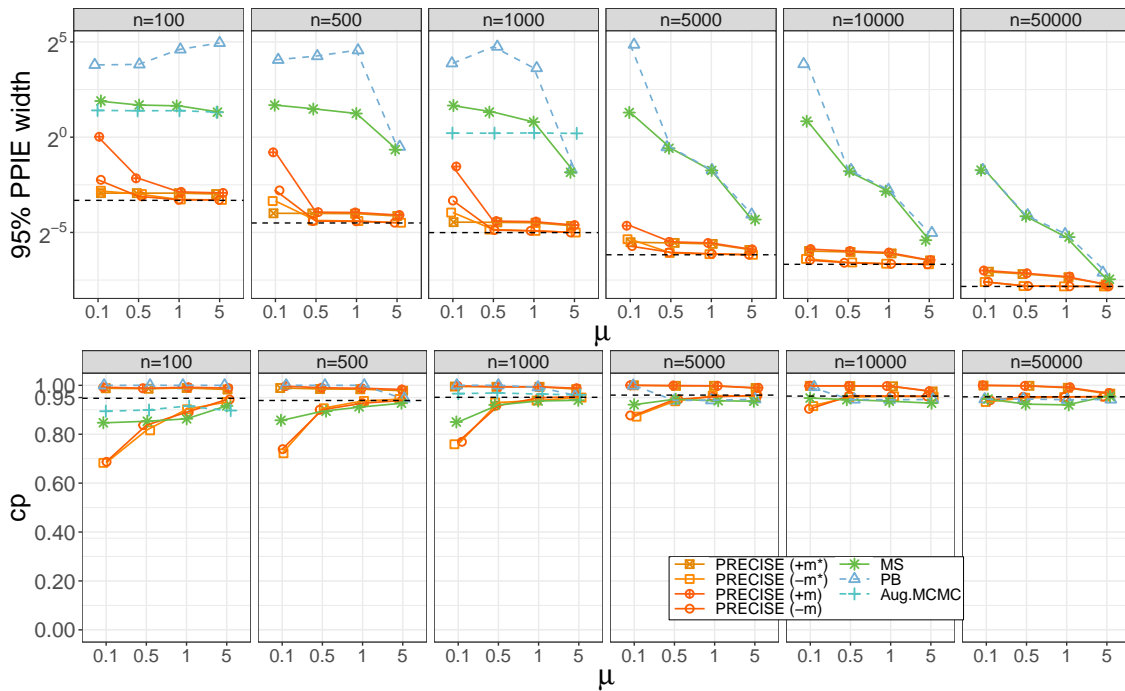


Figure S.6: PPIE width and CP for the slope in linear regression (μ -GDP).